ELECTROPHYSIOLOGY OF THE RAT MEDIAL PREFRONTAL CORTEX AND AMYGDALA DURING BEHAVIOUR

BY

ANDOR D. MAGONY

A THESIS SUBMITTED TO THE
UNIVERSITY OF BIRMINGHAM
FOR THE DEGREE OF
DOCTOR OF PHILOSOPHY

DEPARTMENT OF NEUROPHYSIOLOGY
SCHOOL OF CLINICAL AND EXPERIMENTAL MEDICINE
COLLEGE OF MEDICAL AND DENTAL SCIENCES
UNIVERSITY OF BIRMINGHAM
DECEMBER 2014

UNIVERSITY OF
BIRMINGHAM

University of Birmingham Research Archive

e-theses repository

This unpublished thesis/dissertation is copyright of the author and/or third parties. The intellectual property rights of the author or third parties in respect of this work are as defined by The Copyright Designs and Patents Act 1988 or as modified by any successor legislation.

Any use made of information contained in this thesis/dissertation must be in accordance with that legislation and must be properly acknowledged. Further distribution or reproduction in any format is prohibited without the permission of the copyright holder.

Abstract

Classical Pavlovian conditioning is a relatively simple behavioural experiment where a conditioned stimulus signals the occurrence of a reward. The repeated presentation of the stimulus and the reward leads to the evolution of a conditioned response. However, the electrophysiological correlates of participating brain structures, including the medial prefrontal cortex, that plays a role in decision making, and the central nucleus of the amygdala, that is responsible for reward learning and motivation, have not yet been fully explored. This study explores the electrophysiological properties of the prefrontal cortex and the amygdala in rats during Pavlovian conditioning, extinction and reacquisition. Multisite multichannel recordings showed a significant desynchronization in response to the conditioned stimulus. Additionally, the complex nature and role of a 4Hz activity and theta oscillation in both brain structures in reward conditioning was revealed. We found a consistent power and phase regulatory mechanism coordinating the 4Hz activity, while not affecting the theta oscillation, thus rendering these two distinct oscillations, with complementary roles, to fall out of synchrony. These findings might lay the foundations for further behavioural studies, mostly in the direction of social interaction and social behaviour.

Acknowledgements

I would like to thank my supervisors Professor Attila Sík and Professor John Jefferys for their tireless guidance and support, and professional leadership.

I would like to thank Professor Joff Lee for helping me with the experimental design.

I would like to thank dr. Premysl Jiruska for training me in surgical procedures.

I would like to thank all members of the Neuronal Networks Group for their helpful support.

I would like to thank my Wife and my Family for their never-ending care and support.

Table of Contents

Introduction 8
Behaviour 8
Parts of the brain affecting behaviour 9
Reductionist approach 9
Brain structures involved in Pavlovian conditioning 11
Medial prefrontal cortex 11
Amygdala 12
EEG oscillations and their role in regulating behaviour 16
Aim of this study 17
Materials and Methods 18
New microdrive design 18
Electrode fabrication 18
Chronic implantation surgeries 19
Pavlovian experiments 20
Recordings and experiment control 23
Data analyses and statistics 25
Results 28
Histology 29
LFP epochs 30
Correlation analysis of LFP epochs 34
Spectral characteristics of LFP epochs 44
Distribution of 4 Hz and theta peaks 59
Phase relationship between 4Hz activity and theta oscillation 64
Cross power spectral density analysis 80
Discussion 93
Correlation of wideband pre- and peri-stimulus epochs 93
Frequencies constituting the signal 95
Distribution characteristics of 4Hz and theta oscillations 97
Phasic characteristics of the 4Hz activity and the theta oscillation 97
Cross power spectral characteristics 99
Conclusion 100
Appendices 101
A2. WaveSolution: A novel analytical toolbox for electrophysiological signal processing and analysis 106
References 110

List of illustrations

Figure 1: Inputs to some specific amygdala nuclei 13
Figure 2: Outputs of central amygdalaoid nucleus 14
Figure 3: Block diagram illustrating the parameters of the conditioning phase 22
Figure 4: Block diagram illustrating the parameters of the extinction phase 22
Figure 5: Block diagram illustrating the parameters of the reacquisition phase 23
Figure 6: Example of histological study with DAPI staining 29
Figure 7: LFP epochs compared for TONE (CS) and CLICK (NS) stimuli 31
Figure 8: LFP epochs compared for TONE (CS) and CLICK (NS) stimuli 32
Figure 9: LFP epochs compared for TONE (CS) and CLICK (NS) stimuli 33
Figure 10: Comparison of correlations 35
Figure 11: Comparison of correlations 35
Figure 12: Cross-animal correlation averages in tone (CS) conditioning 37
Figure 13: Cross-animal correlation averages in click (NS) conditioning 37
Figure 14: Cross-animal cumulated correlation averages 38
Figure 15: Cross-animal correlation averages in tone (CS) extinction 39
Figure 16: Cross-animal correlation averages in click (NS) extinction 39
Figure 17: Cross-animal cumulated correlation averages 40
Figure 18: Cross-animal correlation averages in tone (PS) reacquisition 42
Figure 19: Cross-animal correlation averages in click (Fuster) reacquisition 42
Figure 20: Cross-animal cumulated correlation averages 43
Figure 21: LFP epoch STFT-spectrograms 45
Figure 22: LFP epoch STFT-spectrograms 46
Figure 23: LFP epoch STFT-spectrograms 47
Figure 24: LFP epoch STFT-spectrograms 48
Figure 25: LFP epoch STFT-spectrograms 49
Figure 26: Rat2 example of LFP epoch spectral properties 50
Figure 27: LFP epoch FFT graphs 52
Figure 28: LFP epoch FFT graphs 53
Figure 29: LFP epoch FFT graphs 54
Figure 30: LFP epoch FFT graphs 55
Figure 31: LFP epoch FFT graphs 56
Figure 32: Cross-animal integrated power of 4Hz activity 57
Figure 33: Cross-animal integrated power of Theta activity 58
Figure 34: Cross-animal distribution of 4Hz peaks 59
Figure 35: Cross-animal comparison of inter-peak intervals 60
Figure 36: Cross-animal distribution of 4Hz first peak occurrence latencies 61
Figure 37: Cross-animal distribution of 4Hz peaks 62
Figure 38: Cross-animal comparison of inter-peak intervals 63
Figure 39: Cross-animal distribution of theta first peak occurrence latencies 64
Figure 40: Phase histograms of 4Hz activity 65-67
Figure 41: Cross-animal angular relationship 68
Figure 42: Phase histograms of theta activity 69-71
Figure 43: Cross-animal angular relationship 72
Figure 44: Phase histograms of 4Hz vs theta activity 74-75

Figure 45: Phase histograms of 4Hz vs theta activity 76-77
Figure 46: Phase histograms of 4Hz vs theta activity 78-79
Figure 47: Cross power spectral density maps comparing all area-pairs 81-82
Figure 48: Cross power spectral density maps comparing all area-pairs 83-84
Figure 49: Cross power spectral density maps comparing all area-pairs 85-86
Figure 50: Cross power spectral density maps comparing all area-pairs 87-88
Figure 51: Cross power spectral density maps comparing all area-pairs 89-90
Figure 52: Cross-animal integrated power of 4Hz cross power spectral density 91
Figure 53: The main window of WaveSolution 108

List of definitions and abbreviations

AMY	amygdala
AMY-L	left amygdala
AMY-R	right amygdala
ANOVA	analysis of variance
AP	action potential
[redacted]	[redacted]
C1,C2,C3,C4,C5	Conditioning Day #
CA1	Cornu Ammonis 1 region of hippocampus
CeN	amygdala central nucleus
CPSD	cross power spectral density
CR	conditioned response
CS	conditioned stimulus
DAPI	4',6-diamidino-2-phenylindole staining
DC	direct current
E1,E2,E3,E4	Extinction Day #
EEG	electroencephalography
EP	evoked potential
FFT	fast Fourier transform
LFP	local field potential
mPFC	medial prefrontal cortex
NS	neutral stimulus
PFC-L	left prefrontal cortex
PFC-R	right prefrontal cortex
PSP	postsynaptic potential
R1	Reacquisition Day 1
STFT	short-time Fourier transform
TDT	Tucker-Davis Technologies
VTA	ventral tegmental area

Introduction

Behaviour

Behavioural science is made up of a set of complex, methodical analyses and examination techniques that attempt to investigate animal and human behaviour through controlled and systematic observation. The crucial process of decision making – either conscious or through automatic mechanisms – in a living organism is affected by multiple factors of the internal and external environment, whether they are of physical, chemical, emotional or social nature or origin (Weiskrantz 1964, Lupien, McEwen et al. 2009). Both internal functional needs and external constraints, as well as social interaction can modulate the underlying mechanisms of behaviour (Naiman 2008), leading to different outcomes with special respect to communication strategies and decision processes (Whishaw and Kolb 2004). The number of variations in internal and external stimuli, as well as the measurable physiological effects is virtually infinite, therefore the only possible way to carry out reliable and consistent behavioural studies is by having good and comprehensive control over as many variables as possible (Wiley 2003, Bennett-Levy J, Butler G et al. 2004), and following standard procedures including the (a) observation of environmental effects and stimuli, (b) studying their nature and influence on the population, (c) examination of ongoing processes that control and determine reactions, (d) intervention if the outcome is undesired (Bennett-Levy J, Butler G et al. 2004).

Although multiple brain regions influence behaviour to some extent, we concentrate our effort only on a few designated areas, which (a) play important roles in forming behaviour during well described and widely used behavioural paradigms, and (b) are connected with each other, so that communication patterns and driving mechanisms can be examined with common analytical techniques for a better understanding of how external and internal circumstances lead to specific outcomes after neural processing. Connected regions are more likely to work together in the functions they deliver, thus assessing the nature of connections is fundamental to starting to understand network function.

Parts of the brain affecting behaviour

Various brain areas have been identified to contribute to the mechanisms that control behaviour, from sensory input regions (including structures collecting auditory, tactile, olfactory and visual stimuli), to relay areas (thalamus, a switchboard of information between different subcortical areas and the cerebral cortex), to modulatory regions (limbic system, the centre of emotion and memory), and structures responsible for cognitive control and decision making (prefrontal cortex)(Hyman, Zilli Ea Fau - Paley et al. 2005, Bouton 2007, Fujisawa and Buzsáki 2011, Glascher, Adolphs et al. 2012). Also important roles are assigned to the ventral tegmental area, a group of dopamine expressing neurons sending dopaminergic projections to the cerebral cortex, thus, playing an important role in the natural reward circuitry of the brain (Kita, Kile et al. 2009), and it has been shown that the dopamine input arising from this region regulates the hippocampal-prefrontal synaptic plasticity (Adams, Kusljic et al. 2008).

The median raphe nucleus sends serotonergic axons to other brain regions including prefrontal cortical areas and the hippocampus. It is reciprocally connected to the prefrontal cortex, thus cortical activity regulates serotonin release. Serotonergic systems have been implicated in diverse behavioural processes including motor function, motivation, behavioural inhibition and response to stress. Abnormal level of serotonin level is implicated in mood disorders, depression and sexual dysfunction among others (Lechin, van der Dijs et al. 2006).

It is easy to see, that even the above incomplete list of affected structures carries a high level of complexity, therefore a rational and reductionist approach needs to be used through the recording and characterising of behavioural aspects.

Reductionist approach

Designing the adequate experiment is the most important key factor while trying to interpret behaviour. A good design can take into account the majority of possible freedom values and define parameters by which variance can be minimised while controllability can be maximized. A poor design has minimal control over internal or external factors and not only can it end with no results at all, but can also produce false outcome, which is always a serious setback for all fields of science. Design is therefore crucial (Bennett-Levy J, Butler G et al. 2004, Whishaw and Kolb 2004).

Classical Pavlovian conditioning is a relatively simple form of learning where a conditioned stimulus (CS) signals the occurrence of a reward or a punishment (Pavlov and Anrep 1927, Mackintosh 1975, Bouton 2007). Through excitatory conditioning the acquisition of a conditioned response (CR) can be observed that is elicited by a conditioned stimulus. The magnitude and occurrence of conditioned response shows a gradual increase through the conditioning process (Pavlov and Anrep 1927). There are various possibilities for the realization of classical reward conditioning, with different stages of the experiment and numerous parameters (Pearce and Hall 1980), but in order not to increase complexity we proceed along the lines determined by Pavlov and Gallagher (Pavlov and Anrep 1927, Gallagher, Graham et al. 1990) with the experiment design. Therefore this study is to explore the realization of the classical Pavlovian reward conditioning with three stages: 1) Conditioning, 2) Extinction, 3) Reacquisition.

In the conditioning phase according to Gallagher (Gallagher, Graham et al. 1990) rats are presented with an external sound stimulus as a precursor of a food reward, and gradually, the animal will form a relation between the stimulus and food pellet. In order to assess this phenomenon and the attributes of this relation there has got to be a control situation as well, in which there is a neutral stimulus, different from the CS, the presentation of which is not followed by a food reward. This enables the comparison of effects and reactions given to corresponding stimuli and increases controllability of the experiment.
However, it is also essential to explore what happens if the learning curve is interrupted by the extinction of the conditioned response, through which the reversal of the conditioning is performed and conditioned responses disappear (Pavlov and Anrep 1927, Quirk and Mueller 2008). With this phase of the experiment, where neither of the stimuli is rewarded in any way, it is possible to see how animals react when they are forced to return to the original state by the extinction of the previously conditioned response.

And, eventually, the ultimate evidence can be obtained if the animals participating in the experiment have to return to stage one in a reacquisition phase which has the same conditions they were presented with in the conditioning phase: the conditioned stimulus (CS) is followed by a food reward again, thus the conditioned response is expected to reappear (Rescorla,

Wagner et al. 1972). According to Pavlov (1927) the reappearance of the food reward after the conditioned stimulus following the extinction may result in faster reacquisition.

Brain structures involved in Pavlovian conditioning

Appetitive, positive Pavlovian conditioning has long been linked with the amygdala, the centre for reward learning and motivation; while implications have been made, that the prefrontal cortex, the structure responsible for cognitive control and decision making, is also involved in the reward conditioning (Gallagher, Graham et al. 1990, Morris and Dolan 2001, Baxter and Murray 2002, Everitt, Cardinal et al. 2003, Gottfried, O'Doherty et al. 2003, Hampton, Adolphs et al. 2007, Francois, Huxter et al. 2014). To explore the possible relationship within this behavioural paradigm, it is important to reveal their individual roles and operating mechanisms, as well as functional connections between the two regions.

Medial prefrontal cortex

The prefrontal cortex is a group of interconnected neocortical regions sending and receiving projections from nearly all cortical sensory systems, motor systems, and various subcortical structures (Miller and Cohen 2001) having a layered structure with functional connectivity between layer 2/3 serving as input and layer 5 as output (Yang, Seamans et al. 1996, Goodfellow, Benekareddy et al. 2009, Song, Opris I Fau - Chan et al. 2012). Major roles of the prefrontal cortex include the prevention of inappropriate behaviour through the regulation of social manifestation, planning complex cognitive behaviour and decision making, and it is also considered to be the centre of personality expression (Miller and Cohen 2001, Miller, Freedman et al. 2002, Satoru, Mitsuyasu et al. 2004, Fuster 2008). It is also responsible for the comparison of qualities (good and bad, same and different) as well as the prediction of future consequences based on current circumstances (Miller and Cohen 2001, Miller, Freedman et al. 2002). This cortical region is a gateway for the input of the cholinergic and monoaminergic systems to the rest of the cerebral cortex. Prefrontal cortex is reciprocally connected to the basal

forebrain, locus coeruleus and raphe nuclei and is therefore able to control the noradrenalin, serotonin and dopamine level in the brain (Otani 2004, Seamans and Yang 2004). Recognition of the importance of emotional motivation and the ongoing processes during decision is an essential component in order to understand how the regulation and cooperation of connected areas are orchestrated (Holland and Gallagher 2004). Current views of associative learning recognize that Pavlovian conditioning often establishes associations between stimulus or response events and internal memorial representations (Rescorla 1987). It is also acknowledged that the prefrontal cortex is essential for cognitive flexibility and it appears to be involved every time a novel strategy has to be adopted or a switch from old to new tactics is necessary (Otani 2004). This feature can supposedly be quite important during Pavlovian conditioning. Pyramidal neurons of the medial prefrontal cortex are associated with extensive cognitive ability. Since the prefrontal cortex receives inputs from various areas of the brain that are implicated in processing all the sensory modalities, neurons in the prefrontal cortex process many different types of inputs (Elston 2003). Discharges of these neurons are facilitated through the delay period of a delayed-response task when information must be retained temporarily and used subsequently to coordinate adequate responses (Yang, Seamans et al. 1996).

Amygdala

The rat amygdala is a complex structure composed of 13 nuclei and their subdivisions. Studies demonstrated that each nucleus is uniquely interconnected with other brain regions. According to one theory, the amygdala is built up of a primitive and an advanced group, the former associated with the olfactory system (cortical, medial and central nuclei), while the latter relates with cortical structures (lateral, basal nuclei). But the borderlines of these regions are not set in stone, there has been a rekindled enthusiasm in a number of attempts to reclassify the amygdala and its relation with other areas. Some have argued that central and medial subdivisions make continuous structures with divisions of the stria terminalis (Heimer 2003). Others believe that the use of the term amygdala is not correct as it does not exist as a coherent unit (Swanson and Petrovich 1998). The majority of the inputs to the amygdala involve excitatory pathways that use glutamate as a transmitter, forming synaptic connections on the dendrites of excitatory principal neurons that transport signals to other regions of the amygdala or to external regions.

Principal neurons are therefore also called projection neurons. At the same time, axons of principal neurons also establish local connections to inhibitory interneurons which provide feedback inhibition to the principal neurons (Aggleton 2000).

The central amygdaloid nucleus (CeN) is deeply involved in reward learning, motivation, attention and perception (Aggleton 2000, Tye and Janak 2007). It has four divisions: capsular, lateral, intermediate and medial. It is located at the dorsomedial aspect of the rostral half of the amygdala. In vitro recordings from the central nucleus revealed the cell types found in the nuclei of the amygdala. While the basolateral nucleus contains spiny pyramidal neurons and spine-sparse non-pyramidal neurons, principal neurons of the central nucleus include multipolar, bitufted and bipolar neurons which are varieties of non-pyramidal cells (Schiess, Callahan et al. 1999, Aggleton 2000). This nucleus receives projections from the medial and lateral prefrontal cortex (Dumont, Martina et al. 2002, Holland and Gallagher 2004, Vertes 2004) and although it does not project to sensory related cortical regions (frontal cortex, hippocampal formation or the olfactory system) the central nucleus provides substantial inputs to many other areas including modulatory systems, periaqueductal gray, thalamus and hypothalamus (figure 1 and 2).

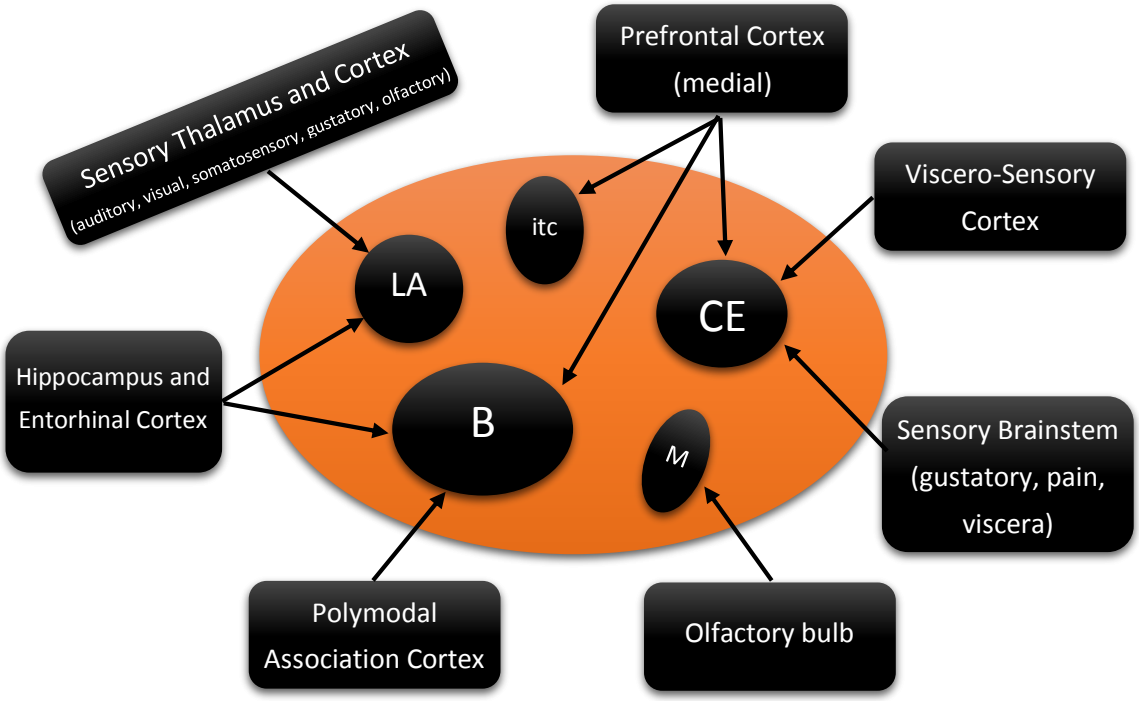

Figure 1: Inputs to some specific amygdala nuclei (B: basal, CE: central, itc: intercalated cells, LA: lateral nucleus, M: medial nucleus).

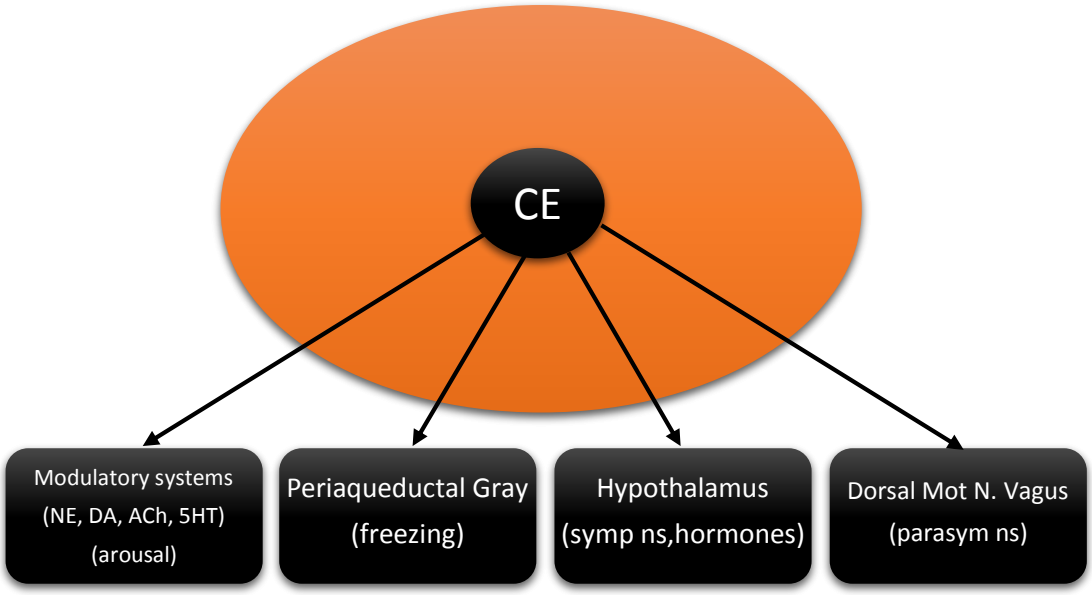

Figure 2: Outputs of central amygdalaoid nucleus (CE: central nucleus, NE: norepinephrine, DA: dopamine, ACh: acetylcholine 5HT: serotonin, parasym ns: parasympathetic nervous system, symp ns: sympathetic nervous system).

It has been found in rats, that neurotoxic lesions in the central amygdala lead to impairments in the acquisition of conditioned responses generated by conditioned stimuli during Pavlovian reward conditioning, compared to unaffected control animals (Gallagher, Graham et al. 1990). It has also been revealed, that targeted microinjections of d-amphetamine (a dopamine receptor agonist) to the amygdala enhance appetitive Pavlovian conditioning (Hitchcott, Bonardi et al. 1997). On the other hand, studies showed that Pavlovian drug (morphine) conditioned stimuli increase dopamine release in the medial prefrontal cortex (Bassareo, De Luca et al. 2007).

In a recent study by Buzsáki's group (Fujisawa and Buzsáki 2011), it has also been found that there exists a special 4 Hz oscillation which synchronizes prefrontal, hippocampal and ventral tegmental area activities in a working-memory task. They demonstrated, that this (2-5 Hz band) oscillation dominates in PFC-VTA communication, and that it is also phase locked to hippocampal theta oscillations, while jointly modulating gamma waves and action potentials in the triangle of the aforementioned structures. These findings indicate the presence of a mechanism that coordinates the functioning of distinct brain areas during a behavioural paradigm, which involved the association of a cue with the spatial position of a reward.

However, reward-related behavioural experiments usually reference the involvement of the amygdala, a similarly important region that is associated as the primary brain centre of reward

learning and motivation. The role of amygdala central nucleus (CeN) in classical Pavlovian conditioning and in the brain reward circuitry has been well described (Gallagher, Graham et al. 1990, Wise 2000, Baxter and Murray 2002, Cardinal, Parkinson et al. 2002, Wise 2002, Everitt, Cardinal et al. 2003, Ikemoto 2010), as well as its involvement in motivation, attention and perception (Swanson and Petrovich 1998, Shinnick-Gallagher 2003).
It has also been described, how a rhythmically synchronized theta activity between the amygdala and CA1 region of the hippocampus can occur, that is thought to improve communication during Pavlovian fear memory retrieval (Seidenbecher, Laxmi et al. 2003).

In a recent study, Lesting et al. explored the presence of theta coupling in the amygdala (basolateral nucleus) – hippocampus (CA1) – medial prefrontal cortex circuit during fear conditioning (Lesting, Narayanan et al. 2011). Their aim was to look beyond individual functions and clarify how these areas interact and function as a system. In their paradigm, the animal associates a conditioned auditory stimulus with an aversive unconditioned stimulus, leading to a state where the conditioned stimulus elicits a conditioned fear response. The experiments consisted of three sessions: fear conditioning, fear extinction (presentation of conditioned stimulus on its own) and recall of fear extinction. Through multisite electrophysiological recordings they found, that during Pavlovian fear conditioning theta oscillations may connect these structures functionally. Cross correlations of theta increased between all regions during retrieval of fear memory characterized by freezing behaviour while exposed to the conditioned stimulus. Theta correlation decreased significantly during extinction, and somewhat increased again through the recall phase, but showing locational specificity (increased between the hippocampal-prefrontal and amygdala-prefrontal pairs, but remained low between the hippocampus and the amygdala). These findings suggest that certain underlying mechanisms efficiently coordinate the functioning of the amygdala-prefrontal cortex-hippocampus circuitry during aversive conditioning, and therefore raise the question how it compares to reward conditioning.

EEG oscillations and their role in regulating behaviour

An approach to assessing the real-time performance of an area or cell population is the registration of local bioelectrical activity generated by interacting neurons. Electrophysiology is a widely used methodology for measuring the electrical properties of biological cells and tissues as it reveals voltage changes on a wide range of scales from single cells (single unit activity) to whole brain regions, depending on the recording site (Buzsaki, Anastassiou et al. 2012). Its importance springs from the fact that each and every neuron is excitable, produces responses to electrical, chemical and other stimuli (Kandel E. R., Schwartz J. H. et al. 2000, Niedermeyer 2004). According to classical theories the constitution of EEG signals is carried out by the cumulative activity on widely-spread dendrites of numerous neurons. These cooperative connections belonging to multiple neurons are called synaptic functional units. However, action potentials are also integral part of the cerebral bioelectrical activity, but due to the nature of these activities, their magnitude in the total mass is significantly smaller (Kandel E. R., Schwartz J. H. et al. 2000).

Brain neural network oscillations play a vital role in the orchestration of communication between distinct cerebral regions. Historically five major types of continuous rhythmic sinusoidal EEG activity are recognized (delta 0.5-4 Hz, theta 4-8 Hz, alpha 8-12 Hz, beta 12-30 Hz and gamma 30-100 Hz), although there is no precise agreement on the frequency ranges for each type, and additionally, the band limits can shift across species (Corsi-Cabrera, Perez-Garci et al. 2001).

These basic and fundamental components of the classical EEG signals can be crucially important while trying to analyse behaviour and its underlying mechanisms. As they all are cursors of recognized and actively discussed phenomena of both sleeping and awake states, it is a good starting point to extract most of the features and characteristics of these classical frequency bands and waveforms, and study their contextual importance.

Aim of this study

The role of a 4 Hz oscillation in the synchronization across the PFC-VTA-hippocampus axis has been described previously, as well as the theta-rhythm synchronization between the amygdala and the hippocampus during memory retrieval. Also, the presence and role of theta coupling in the prefrontal-hippocampal-amygdalar circuit have been addressed in fear conditioning, extinction and reacquisition. Based on these findings and on the known interconnections between the medial prefrontal cortex and the amygdala, we hypothesize an oscillatory phenomena, presumably related to the prefrontal 2-4 Hz band activity and/or the hippocampal theta oscillation, that has regulatory/modulatory effects on the co-functioning of these structures in a reward based behavioural paradigm. Reward learning and motivation (key features in classical conditioning) are thus covered by the amygdala. The other key factor related to motivation is decision making through which the animal reacts to the conditioned stimulus in a certain manner. Decision making is linked with the prefrontal cortex, a brain region that has also been implicated in personality expression, planning complex cognitive behaviour and regulating social behaviour (Miller and Cohen 2001, Miller, Freedman et al. 2002, Fuster 2008). Since the medial prefrontal cortex is connected with the amygdala central nucleus (Holland and Gallagher 2004, Lopez de Armentia and Sah 2004), these areas are candidates for a detailed and joint neurophysiological examination.

To summarize the goals, we intended to address these issues: 1) through classical reward conditioning activate the medial prefronto-cortical – amygdalar circuitry, 2) examine the electrophysiological characteristics of reward conditioning in this circuit, 3) measure the correlation and elucidate the synchronization patterns across the affected regions to show the level of cooperation during reward-related behaviour, 4) identify any oscillatory activity that can account for the orchestration of synchrony across these structures and eventually answer: does the 4 Hz or theta oscillation play a role in this process, and if it does, how.

Materials and Methods

New microdrive design

Although not used in the current study, a significant amount of time was spent on the development of a new, extra small microdrive. As multisite implantations are limited by available space in small animals, the need for a miniature, yet reliable microdrive that allows for increased implantation counts in a single animal is of utmost importance. Based on a previously used design, but by substituting parts with miniature modelling components, we managed to build a reduced size microdrive which is reliable, biocompatible and customizable. The new device is fully compatible with existing solutions, but it can be implanted in increased amounts into a single animal. The theoretical number of implantable microdrives is 10 in mice, 24 in rats, and is now primarily limited by the connector size. For further details see Appendices.

Electrode fabrication

Multisite, tetrode recording electrodes were constructed manually similar to already existing descriptions in the literature (Jog, Connolly et al. 2002, Nguyen, Layton et al. 2009). Teflon coated tungsten wires with a diameter of 12 μm (California Fine Wire Company, Grover Beach, CA, USA) were cut to size, then looped twice, fixed to a holder bar and spun on a magnetic spinner with a weight keeping the wires straight until the top of the plait approached the holder bar to about 15 millimetres. Wires were then twisted backwards a couple of turns to release tension. Using a heat gun the insulation was slightly melted to fix the posture and to strengthen the structure of the tetrode. The magnetic weight was then cut down and the electrode was released from the holder bar. Not-twisted wires were cut to have four freely moving wires at the end of the tetrode. The coating was removed about 1 mm from wire tips on all four wires with a flame using a lighter. Each exposed wire was then soldered to dismantled connector pins (Omnetics) and adjoining surfaces were insulated with non-conductive paint. Contacts and conductance were tested in 0.9% saline solution with an electrical stimulator. With good contacts bubbles emerged in the solution after stimulation. Tetrodes were then stored in a box

separately for later use. Prior to usage pins were inserted carefully into the connector (NPD-18-VV-GS, Omnetics, Minneapolis, USA) and sealed with epoxy. Tetrodes were then put in a protective cannula (34Gx18mm, Cooper's Needle Works Ltd, Birmingham, UK) and cut to desired size with sharp surgical scissors. Impedance values were measured and lowered to ~300 kΩ (measured at 1 kHz) using electroplating (nanoZ, Neuralynx, Bozeman, USA) with gold solution.

Chronic implantation surgeries

Fifteen male Sprague-Dawley rats (Charles-River, Margate, UK) with weight between 300 and 350g were used for the Pavlovian conditioning and had chronic recording implants. All procedures conformed to the UK Animals (Scientific Procedures) Act 1986, implantation surgeries were performed in designated surgical theatres of the [redacted], with sterile tools and equipment. The anaesthesia of the animals was induced in an anaesthetic chamber with isoflurane vaporized in oxygen (3% isoflurane, 100% oxygen). Rats were shaved on the head and then fixed in a stereotactic frame where a decreased (1.5%) inhalational isoflurane anaesthesia was provided via a nose mask. The pinch reflex was checked regularly to assess the depth of anaesthesia. Heart rate, breathing pattern and body temperature were monitored constantly. Body temperature was controlled by a heating pad and maintained at 37°C. Eyes were covered with moisturising agent, ear canals were lubricated with EMLA cream (25 mg lidocaine and 25 mg prilocain / g) to reduce possible inconvenience caused by the ear bars. After cutting the skin and cleaning, then drying the skull surface, four holes were drilled for anchoring screws to achieve better fixation for the dental cement. Small craniotomies were drilled above the targeted regions /coordinates relative to the Bregma were obtained from the Rat Brain Atlas (Paxinos and Watson 1986) and related scientific literature (Gallagher, Graham et al. 1990)/. The dura was carefully removed and then four identical tetrodes were inserted into the craniotomies: one electrode was lowered in the prefrontal cortex each side (AP: +3.2 mm, ML: ±0.8, DV: 3 mm), and one electrode to the amygdalae on both sides (AP: -2.5 mm, ML: ±4 mm, DV: 7.8 mm). Reference and ground electrodes were connected and placed under one of the posterior anchoring screws above the

cerebellum. Cannulas, all wires and the Omnetics connector in the middle were embedded in Refobacin dental cement (providing antibiotic release). The skin was then stitched with sterile sutures, and following analgesia (Temgesic, 1 ml / kg was administered intraperitoneally) the animal was removed from the stereotactic frame and transported to the recovery room and placed in a container above a heating pad, where sucrose fluid was injected subcutaneously to compensate possible dehydration. Animals recovered and were fed ad libitum for one week before the experiment commenced. At the end of the experiments all animals were deeply anaesthetised, , starting with 0.9 percent saline solution, followed by 4 percent paraformaldehyde solution to further process the brains in histological studies. Brains were sectioned in a Vibratome at 70 μm slices in the coronal plane, then mounted on slides, DAPI stained and cover-slipped. Histological studies revealed that tetrodes reached the targeted areas successfully (figure 6).

Pavlovian experiments

In my classical appetitive Pavlovian conditioning experiments I followed the guidelines determined by the literature (Gallagher, Graham et al. 1990). Fifteen previously implanted rats were used for Pavlovian reward conditioning experiments. All procedures conformed to the UK Animals (Scientific Procedures) Act 1986. Experiments were performed in a designated room of the . Following the implantation procedure and the one week recovery period all animals were diet restricted and gradually brought down by 10% of their postoperative ad libitum bodyweights and were maintained at that level throughout the experiment. A conditioning box of 30 cm x 50 cm x 50 cm was constructed to provide undisturbed experimental conditions and to minimise external stimuli. The box with an open top was lifted onto a circular platform which had its side covered with dark curtains. The roof of the platform frame had halogen lights built in pointed downwards to illuminate the experimental box and had a video camera as well to record the experiments. The masking noise of 60 dB was provided by the ventilation fans in the room. The box had a built in speaker facing the inside of the box to provide the sound stimulus. A battery operated electronic food dispenser was also attached to the side of the box, and its output continued in a plastic tube

that led to a small glass bowl fixed with Velcro on the floor of the box in a corner. The tube ended a couple of centimetres above the bowl to allow an easy and unrestricted access to the glass container. The end of the tube also had a bottleneck in order to slow down and attenuate the fall of the sucrose pellet lest it should bounce back and hide from the animal, which could alter the conditioning and result in adverse outcome. The signal preamplifier was placed just outside the box connected to the recording cable that was held above the box by an elastic rubber band that slightly raised the cable and minimised the constraints on the animal.

Conditioning - At the beginning of each session the animal was transported from the rat room to the experimental room and placed in the box. The cable was connected to the connector on the head of the animal, and was left to explore around, for 15 minutes, in order to compensate the excitement of the transportation.

In every conditioning session the animal was presented with a conditioned sound stimulus (CS), a tone of 3000 Hz, with a duration of 5 seconds, at 80 dB, with an inter-stimulus interval of 8 minutes, 10 times in each session. At the end of the 5 second stimulus the food dispenser dropped a 45 mg sucrose pellet (Lillico Biotechnology, Hookwood, UK) through the tube to the glass bowl. At a randomized latency between 1 and 7 minutes after the onset of the tone the animal was given a neutral click stimulus (NS) which was not followed by a food reward. Each session was performed once every consecutive day, thus one animal had one conditioning session per day. An animal was declared to be conditioned if it found and ate the pellet all 10 times of the session within 10 seconds after the onset of the tone stimulus (CS). The total duration of the conditioning phase was 5 days (figure 3).

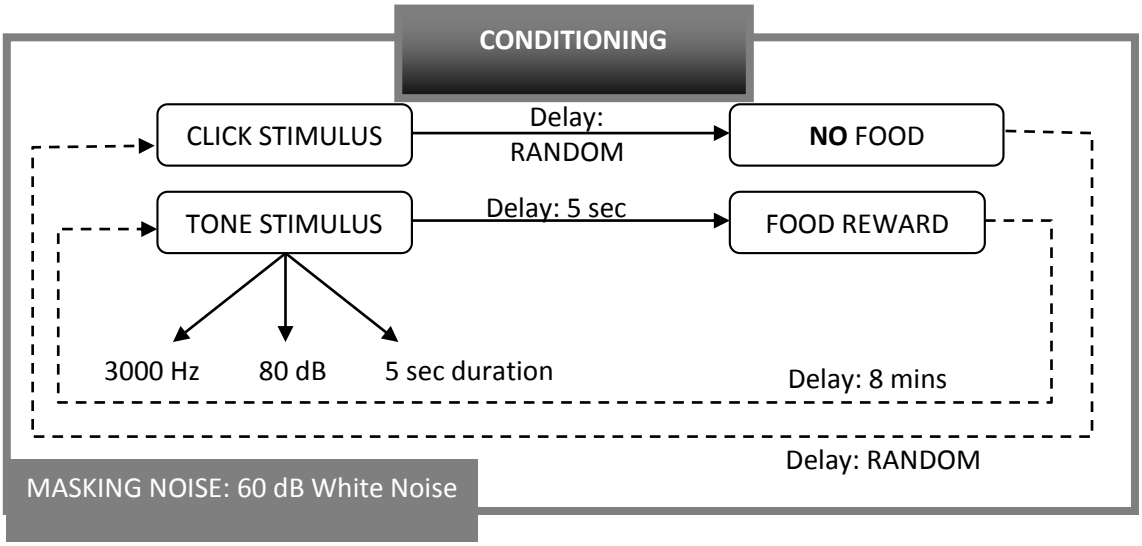

Figure 3: Block diagram illustrating the parameters of the conditioning phase

Extinction - During the extinction phase one parameter of the experiment changed in a way that was disadvantageous for the animal – both the tone (CS) and click (NS) stimuli remained the same, but neither of them was followed by a food reward anymore. Both stimuli retained their characteristics (frequency, strength, occurrence) and there were still 10 runs each day. The stimulus and its reaction were considered extinct if the animal did not respond to the tone (CS) stimulus by checking the food bowl in any of the 10 runs. The duration of the extinction phase was 4 days (figure 4).

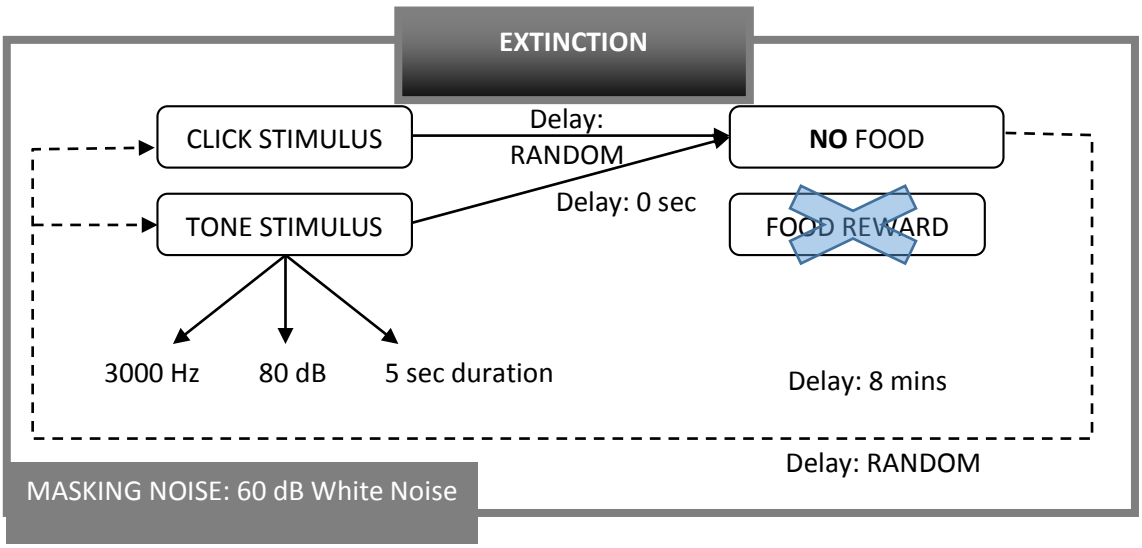

Figure 4: Block diagram illustrating the parameters of the extinction phase

Reacquisition – A favourable and advantageous change came after the extinction phase for the animals – with the same parameters of the conditioning phase (stimulus frequency, strength, occurrence) the sucrose pellets returned again and rewarded each tone (CS) stimulus after 5 seconds. The click (NS) stimulus however remained unrewarded and randomly distributed (figure 5).

Note, that during the experimental sessions no clear or objective measure of orientation could be obtained to register a distinct and direct behavioural reaction to any of the stimuli, thus, to avoid biasing and the subjective judgment of what qualifies as orientation or direct reaction, only the 10-second rule was applied.

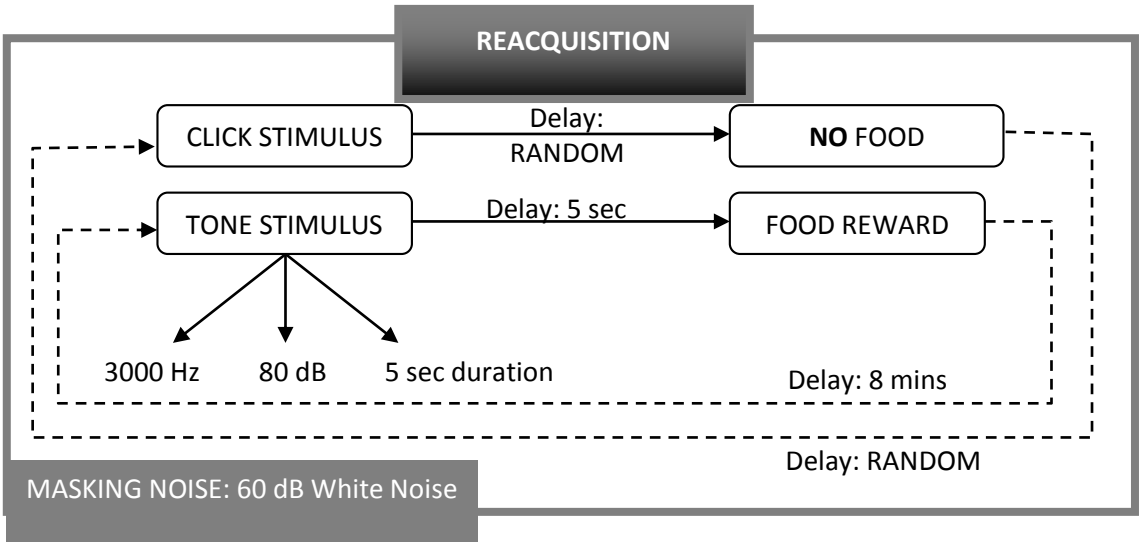

Figure 5: Block diagram illustrating the parameters of the reacquisition phase

Recordings and experiment control

All signals were recorded using TDT (Tucker-Davis Technologies, Alachua, USA) chronic shielded cables with high-impedance headstages connected to a TDT PZ2 preamplifier linked with an RZ2 base station, which then sent digitised data to a quad core Windows PC.

Recordings were made using TDT's data acquisition software tool in which the whole recording script and project was made by myself. One analogue BNC output was connected to the food dispenser, and pellet drop was triggered automatically in the software by sending a TTL signal through the output channel. Another analogue BNC output connector sent out the tone (CS) and click (NS) stimuli to the speaker attached to the conditioning box, also controlled by the software. 16 channel data were stored on the computer's hard drive at a sampling rate of 24 kHz with a 0.5 Hz – 12 kHz band-pass filter, 16-bit signal resolution. The sound output was also fed back to the recording equipment within the RZ2 base station in order to register the stimuli with the bioelectrical data. There was one more stream of data stored on the computer, which was the down-sampled version of the original raw wideband signal. Prior to down-sampling the data to 1 kHz a low-pass filter was applied to the signal (LP limit below 500 Hz) in order to avoid aliasing. Audio stimuli were also recorded to store trigger events.

Recorded files were then converted to Matlab format to process all data with the Wave Solution software toolbox (see Appendices for details). Data representation remained the same (24 kHz and 1 kHz sampled versions with 16 bit resolution) there was no loss of information during the conversion. Files were loaded in Wave Solution and event time codes were extracted for both tone (CS) and click (NS) stimuli. Data sampled at 1 kHz (considered field potential signal) were epoched around both stimuli with -5000 ms … 0 … +5000 ms limits (10 second epochs), where 0 was the occurrence of the stimulus. Thus, 10 tone-centred and 10 click-centred epochs were extracted from the continuous recordings for each day (as there were 10 runs of stimulation every day). To obtain the single-session performance as well as to minimise noise and other artefacts, all 10 epochs were regarded as evoked potentials and averaged on a daily basis, therefore only one, averaged 16 channel epoch remained for the tone (CS) stimulus, and another one for the click (NS) stimulus. To integrate the multisite performance of each electrode and to further increase robustness and improve signal quality, the activity of all four channels from each recording site was averaged, resulting in only four channels in total, 1-1 channel for each site. Eventually we obtained two very robust and low-noise epochs per day (one for CS and the other for NS), each containing four channels only. Spectral features and correlation characteristics were then computed to derive as much valuable information as possible. Any DC shift introduced by the recording equipment was corrected by signal demeaning for every epoch.

Data analyses and statistics

Correlation analysis

The inter-channel calculation of correlation and its representation in map format for ensuring better visibility and easier detection of changes in correlation coefficients, is an important tool. This way, all possible channel-pairs were used to calculate the correlation, resulting in an N x N dimensional matrix where N denotes the number of channels. In each case, pre-stimulus and peri-stimulus segments were separated and calculated separately, in order to be able to compare the correlation coefficients.

The used formula for correlation: $$R(i,j) = \frac{C(i,j)}{\sqrt{C(i,i)C(j,j)}}$$, which is the formula for the Pearson product-moment correlation coefficient, defined as the covariance /C( )/ of two variables divided by the product of their standard deviations (Rodgers and Nicewander 1988). The resulting matrix contains values ranging from zero (no correlation) to one (autocorrelation) which are represented by colours in the map. It is an immensely useful tool to examine the relations between two independent signals. Correlation coefficient values were also exported for further statistical analysis, using the xcorr function in Matlab.

Spectrograms

Short-time Fourier transforms (STFT) were calculated to obtain the instantaneous frequency components that constitute a signal in time (time-frequency map). This allows for observation of frequency changes in a specified time period of a single channel signal. For all -5:0:5 sec epoch a window size of 256 sample points was used, with an overlap of 250 sample points. The number of FFT points for the calculation was 2048 to ensure high resolution. Maps (the values of which were stored in matrix format) were scaled to show frequencies between 0 and 40 Hz.

FFT graphs

Fast Fourier Transforms were computed to transform the signals into frequency domain and to display them in a desired frequency range, revealing the proportionate strength of frequency components constituting the signal, using the one-sided implementation of Matlab's built in

periodogram function with input vector (continuous, sampled EEG data), and sampling frequency specified as parameters.

Filtering

All filterings were done using a zero phase shift FIR filter in Matlab (filtfilt command). This filter uses a special, two-way filtering method to avoid shifting in the signal. The filter characteristics were set for desired output signals. It then filtered the signal so that unwanted frequency components were suppressed with a specified attenuation. 4 Hz signal was obtained by a bandpass filter between 1-5 Hz, theta oscillation was obtained by a bandpass filter between 5-9 Hz.

Distribution analysis of 4Hz and theta peaks

Single trials were used for this analysis (not the averaged epochs) to increase detection reliability and achieve more detailed distribution analysis. Signal peaks were extracted from the epochs using bandpass filtering (within the corresponding frequency band), followed by root mean square transformation, threshold detection (mean + 2xSD), and peak detection. The peak detection algorithm did not register threshold crossing, but was looking for local maxima, to only pick signal peaks. Peak time codes were extracted in sample point values, then occurrence counts as well as inter-peak intervals were calculated.

Phase histograms

Hilbert transforms were calculated to get information on angular characteristics of a signal. Although Hilbert transform is a linear operator, it is still useful for the analysis of non-stationary signals by regarding frequency as a rate of change in phase, so that the frequency can change over time. Usually multiple time-varying frequencies coexist in raw signals, so in biological use it is advised to use a filter prior to transformation in order to remove irrelevant frequency bands. While Fast Fourier Transform (FFT) gives high frequency resolution, Hilbert transform provides better temporal resolution of fast changes in analytic state-variables of frequency, phase and amplitude, because the temporal resolution limited by the Nyquist criterion: digitization rate must be at least twice (and preferably more) the highest component frequency. Hilbert transforms were computed in Matlab using the combination of angle and hilbert functions (as the output of the hilbert command is a complex number that needs conversion to obtain the correct phase angles).

For phase histograms we need to filter the recorded signal in the desired frequency range. By doing so we get a sinusoid signal on which we can use the Hilbert transform, specifying the instantaneous phase of the oscillation. The outcome is a saw-tooth signal with small growths of phase lag. Peak values are then extracted from the signal using peak detection. Valid inter-peak intervals are regarded as one cycle of the oscillation and therefore divided into 360 degrees. A histogram is then computed using two time series containing peak information.
Weighted angular values are obtained by the cross product of valid bin indices and bin entries, divided by all counts.

Cross Power Spectral Density (CPSD) analysis

CPSD is an estimate of the cross power spectral density P_{xy} of discrete signals: *x,y*, using an averaged periodogram method for spectral estimation. The CPSD is the distribution of power per unit frequency.
It can be computed in Matlab using the cpsd command. It is a windowed function, therefore window length and overlap values, as well as number of FFT points must be specified. For the epochs 5% window length with 4% overlap was used. The number of FFT points was 256. Before multi-window comparison, data were normalized. The confidence interval was specified as 0.95.

Statistical analyses

All data are presented as means ± standard errors. Statistic tests were carried out using GraphPad Prism version 4.00 (GraphPad Software, Inc). Group differences were analysed using Student's t test or one-way ANOVA. Significance was tested by 95% confidence level. Permutation tests were used to identify differences in the powers of 4Hz activity and theta oscillation. Epoch power values were measured in pre-stimulus and peri-stimulus segments. Measurements were repeated *R* times in random order to obtain the statistic from the data by permutation of original samples.
Bartlett's test was run for equal variances, and Bonferroni's Multiple Comparison Test was computed following ANOVA to compare all sample pairs.
Cross-animal statistical analyses were carried out using two-level nested analysis of variance (nested ANOVA), testing groups (animals) and subgroups (sessions).

Results

Although altogether 15 animals were implanted with recording electrodes, due to a licence misinterpretation by the staff at [redacted], the food restriction process was suspended for 11 animals, rendering the experiments and experimental outcome useless. The staff argued that the licence covered visual stimuli only, while I was using auditory stimuli. 11 animals, that also had chronic microdrives implanted (see Appendices for details) did not respond anymore to the conditioning – extinction – reacquisition stages of the experiment, and therefore had to be [redacted]. One day after the food restriction was suspended, they included auditory stimulation in the licence, but it was too late by then for those 11 animals. This thesis and its findings are therefore based on four animals which had no microdrives, only fixed tetrodes implanted.

Still, a major result of my doctoral work is the successful development of a new, ultrasmall microdrive device, which is described in the Appendices of this thesis.

Histology

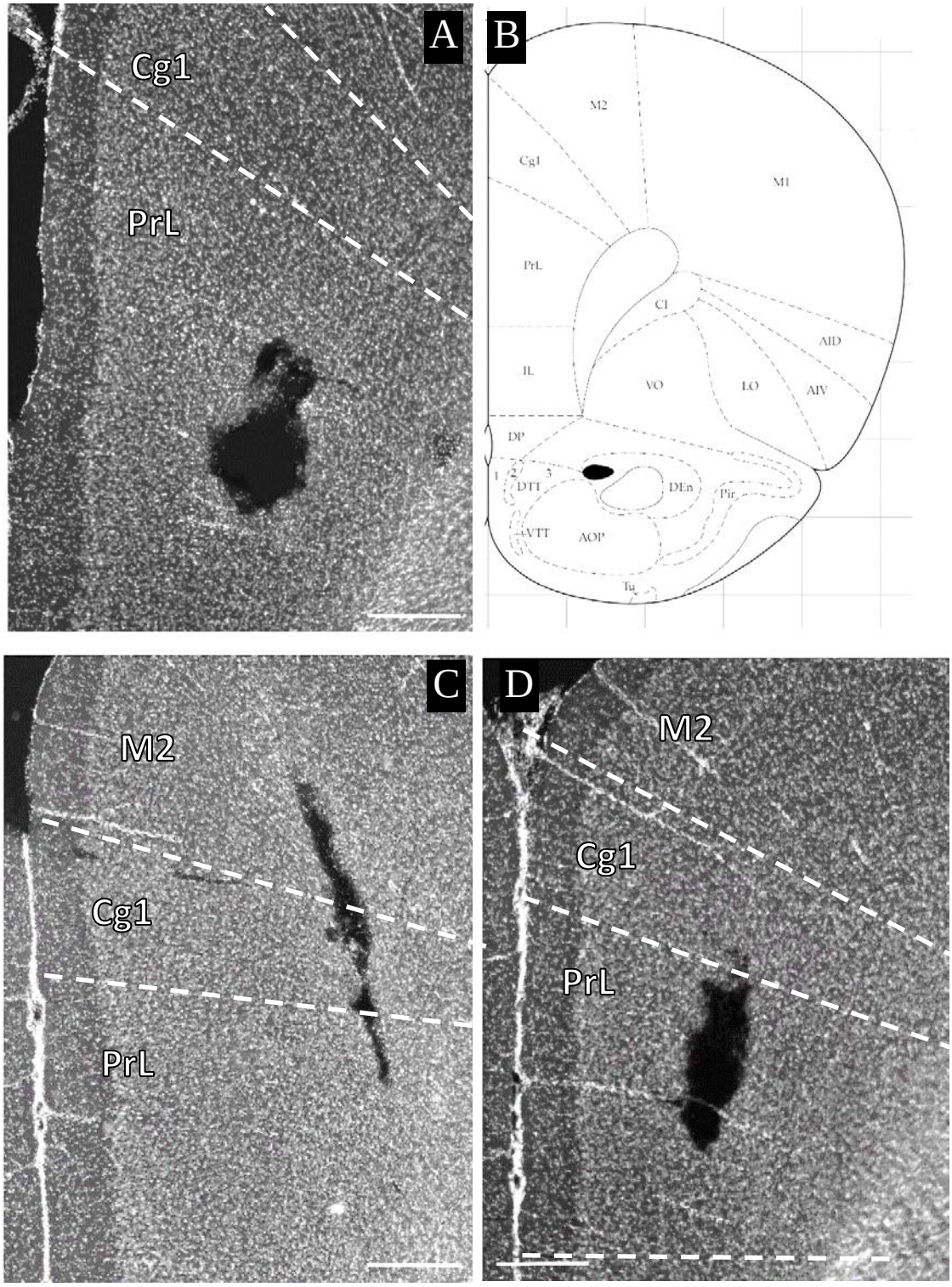

Figure 6: Examples of histological study with DAPI staining to show lesion sites (dark spots in the tissue) caused by the electrodes in the prefrontal cortex of animals (A-C-D).
B: Schematic map of targeted area. Cg1: cingulate cortex area 1, PrL: prelimbic cortex.
M2: secondary motor cortex. Scale bar: 300 μm.

LFP epochs

For visual examination and comparison, as a first approach, all channels were superimposed from all recording sites to display and compare waveforms and any peculiar deviations that can be seen by the naked eye and that can be assigned to any stimulus. Though the waveforms are devoid of any intrusive noise or artefacts, it is not easy to identify striking phenomena or consistent patterns (figure 7-9).

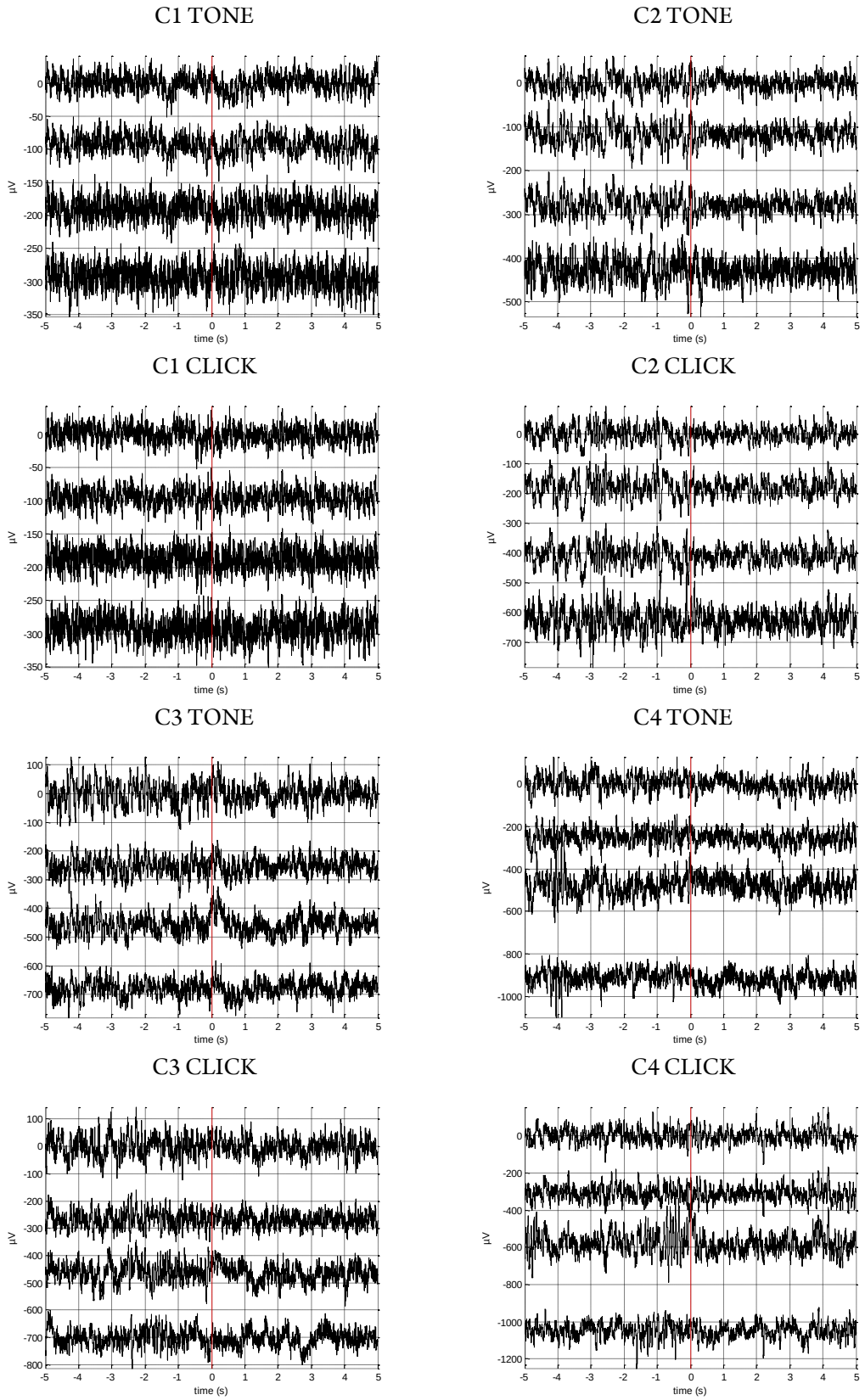

Figure 7: LFP epochs compared for TONE (CS) and CLICK (NS) stimuli from Rat1, conditioning day 1 through to day 4. Horizontal axis: time (s), vertical axis: amplitude (μV), displaying channels 1 (top) to 4 (bottom, 1:AMY-L, 2:AMY-R, 3:PFC-L, 4:PFC-R). Vertical red line indicates stimulus onset. Channels displaced vertically from zero.

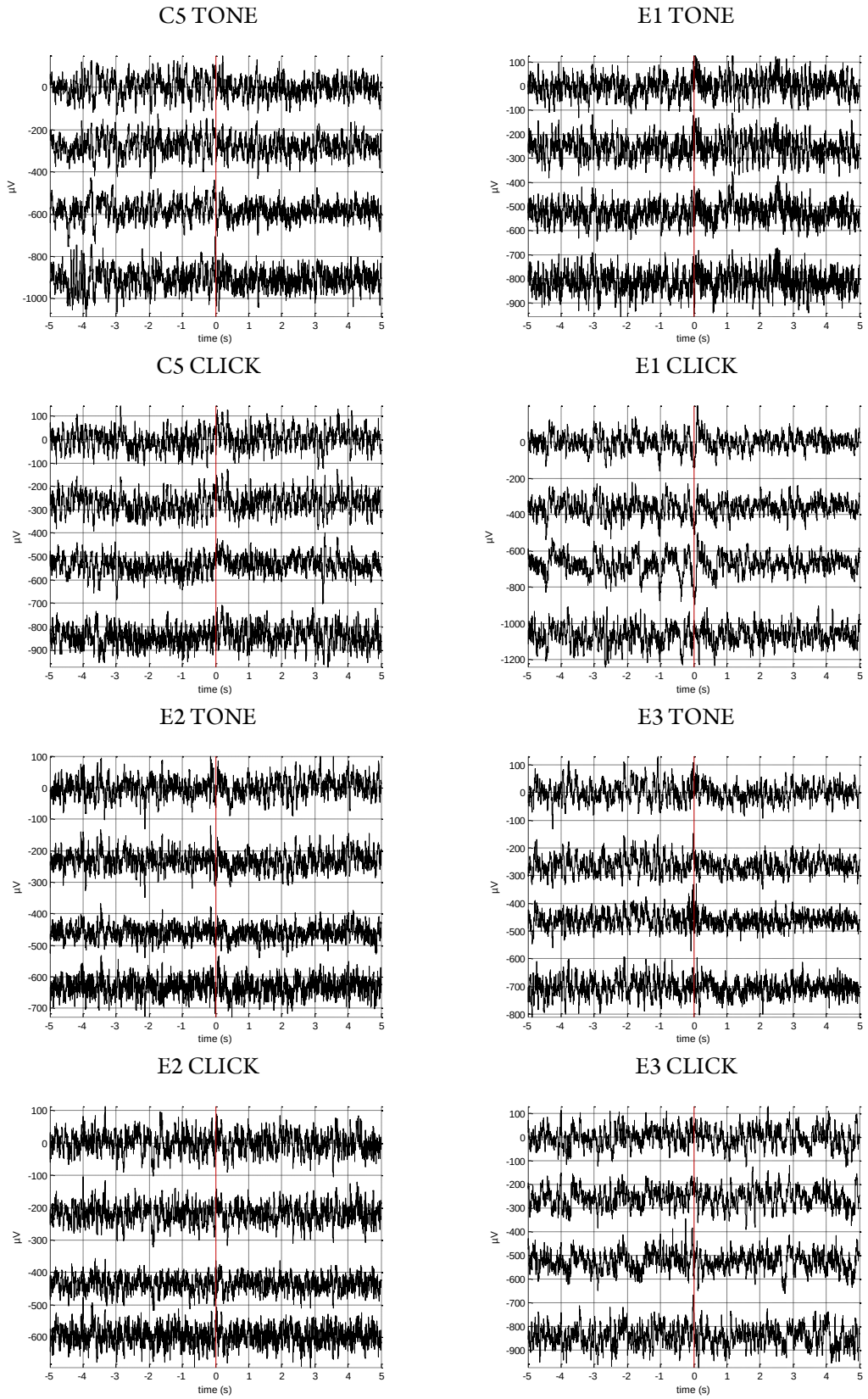

Figure 8: LFP epochs compared for TONE (CS) and CLICK (NS) stimuli from Rat1, conditioning day 5 through to extinction day 3. Horizontal axis: time (s), vertical axis: amplitude (μV), displaying channels 1 (top) to 4 (bottom, 1:AMY-L, 2:AMY-R, 3:PFC-L, 4:PFC-R). Vertical red line indicates stimulus onset. Channels displaced vertically from zero.

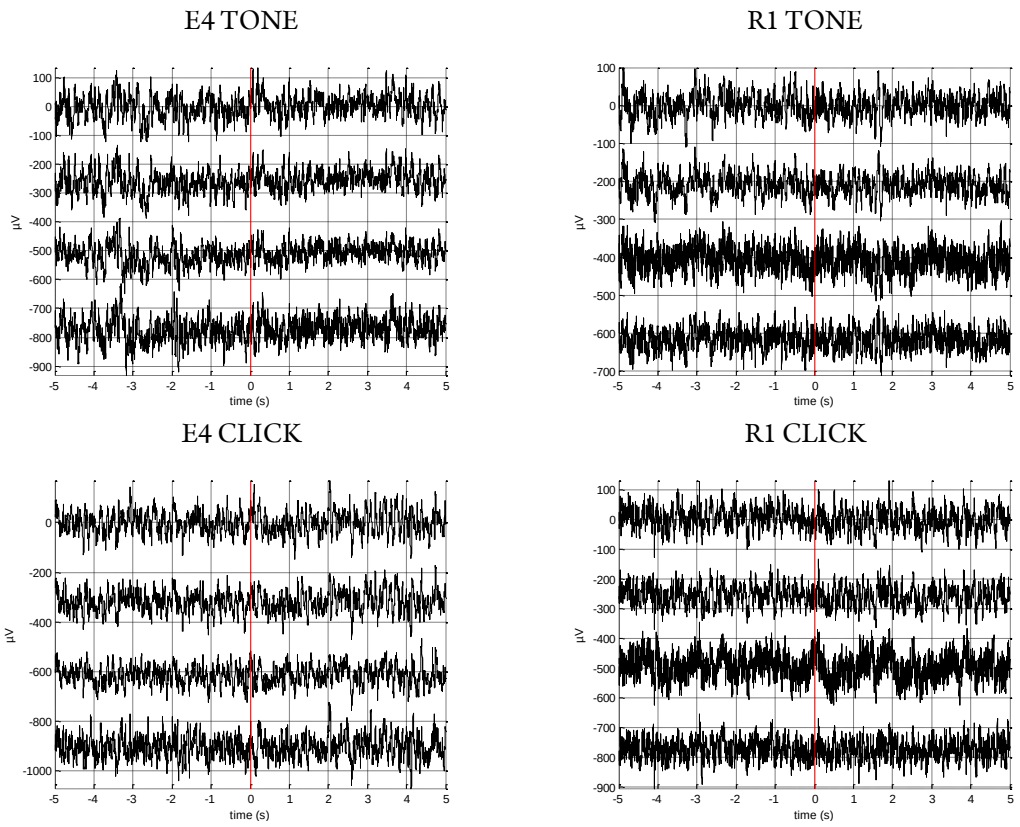

Figure 9: LFP epochs compared for TONE (CS) and CLICK (NS) stimuli from Rat1, extinction day 4 through to reacquisition day 1. Horizontal axis: time (s), vertical axis: amplitude (μV), displaying channels 1 (top) to 4 (bottom, 1:AMY-L, 2:AMY-R, 3:PFC-L, 4:PFC-R). Vertical red line indicates stimulus onset. Channels displaced vertically from zero.

Correlation analysis of LFP epochs

To assess the precise relation of signals from prefrontal and amygdala locations on both sides, it is crucial to quantify the correlation of the single waveforms. On the other hand, we need to take into consideration the time-variance and dependence of correlation function, because the signal is non-stationary. Therefore epochs were divided into pre-stimulus (-5000 ms to 0) and peri-stimulus (0 to +5000 ms) segments, in order to have a baseline, not affected by the stimulus (spontaneous segment), and a response period strongly linked to the stimulus. Thus, the separate examination of correlation on these segments is expected to be more beneficial for comparison. Figures (10-11) demonstrate the bi-segmental correlation of tone (CS) and click (NS) epochs for Rat1.

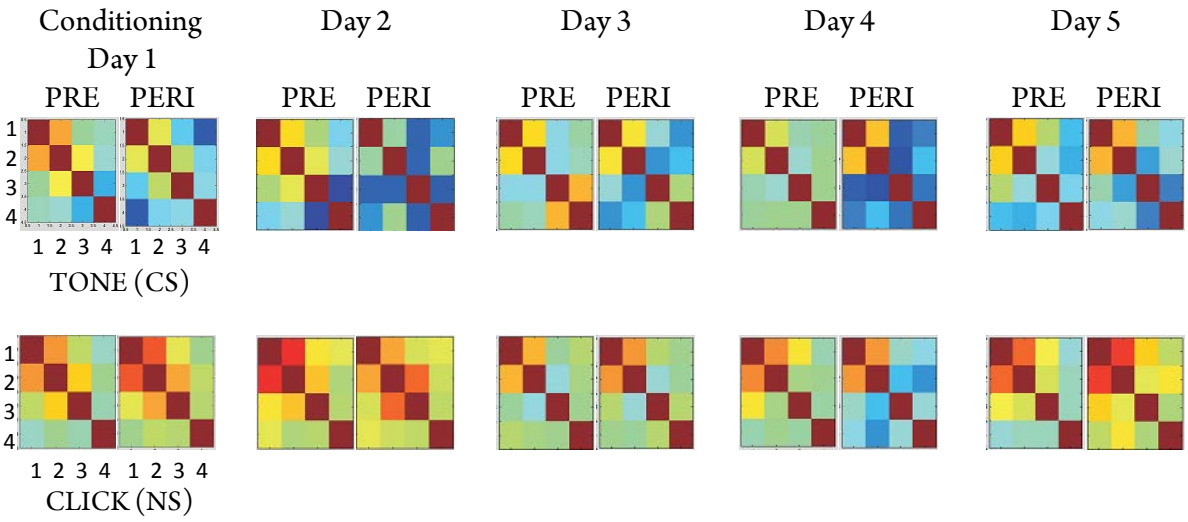

Figure 10: Comparison of correlations calculated for pre- (-5000 ms to 0, left) and peri-stimulus (0 to +5000 ms, right) segments of each epoch for the conditioning sessions from Rat1. Rows and columns: 1: AMY-L, 2: AMY-R, 3: PFC-L, 4: PFC-R. Colours indicate correlation values ranging from low (blue, 0) to high (red, 1) . Main diagonal: autocorrelation of corresponding channels. Maps below and above the main diagonal are symmetrical.

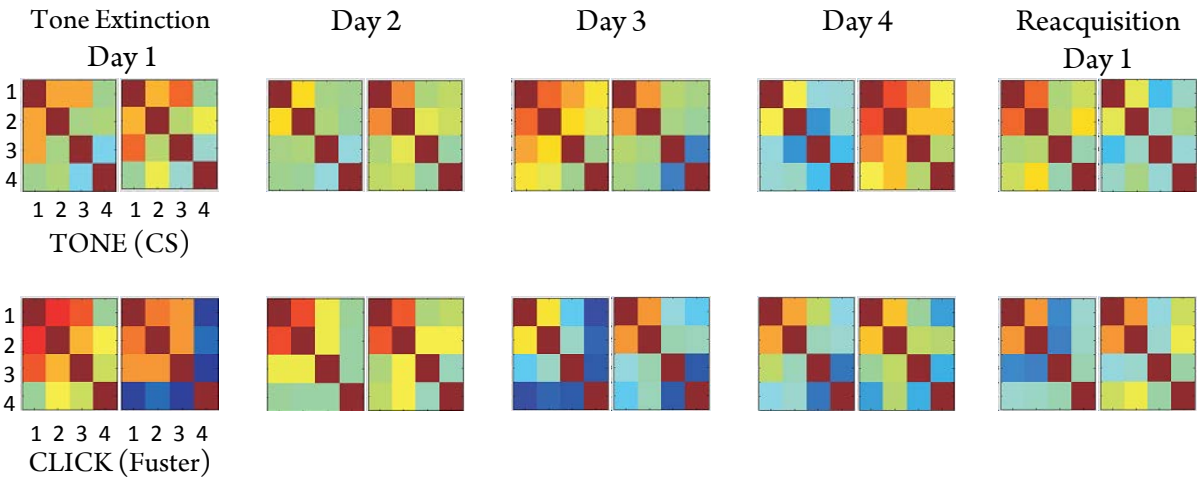

Figure 11: Comparison of correlations calculated for pre- (-5000 ms to 0, left) and peri-stimulus (0 to +5000 ms, right) segments of each epoch for the extinction and reaquisition sessions from Rat1. Rows and columns: 1: AMY-L, 2: AMY-R, 3: PFC-L, 4: PFC-R. Colours indicate correlation values ranging from low (blue, 0) to high (red, 1) . Main diagonal: autocorrelation of corresponding channels. Maps below and above the main diagonal are symmetrical.

Although the correlation maps show various colours in various patterns that seemingly have no systematic formations, but the correlation between the bilateral amygdalae is increased (> 0.6 by value) in every case, detailed statistics with the concrete values reveal additional information. The correlation between the two amygdalae is reassuringly consistent in all animals through all sessions in the conditioning phase (average ± standard error in pre-stimulus segment: 0.66 ± 0.03, peri-stimulus section: 0.594 ± 0.07, n=40).

The statistical analysis of the correlation of individual regions shows a general decrease of synchrony in the PERI segment of the epoch with TONE (CS) stimulus (figure 12-13).

Conditioning

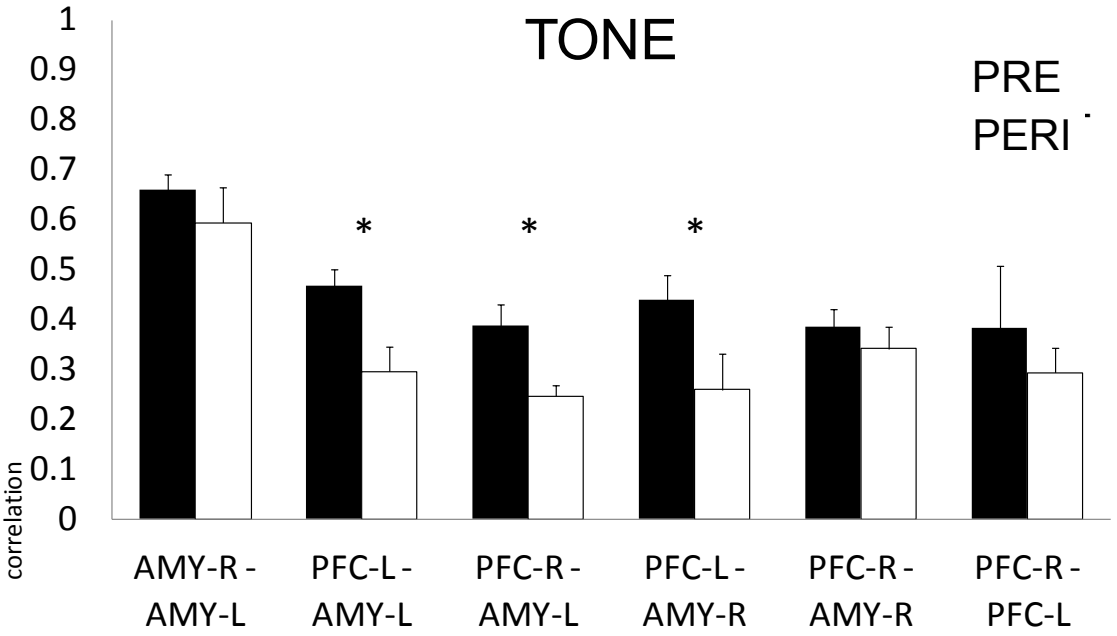

Figure 12: Cross-animal correlation averages in tone (CS) conditioning for pre-stimulus (dark) and peri-stimulus (light) segments with standard error. Significant differences are marked with * ($p<0.05$, n=200).

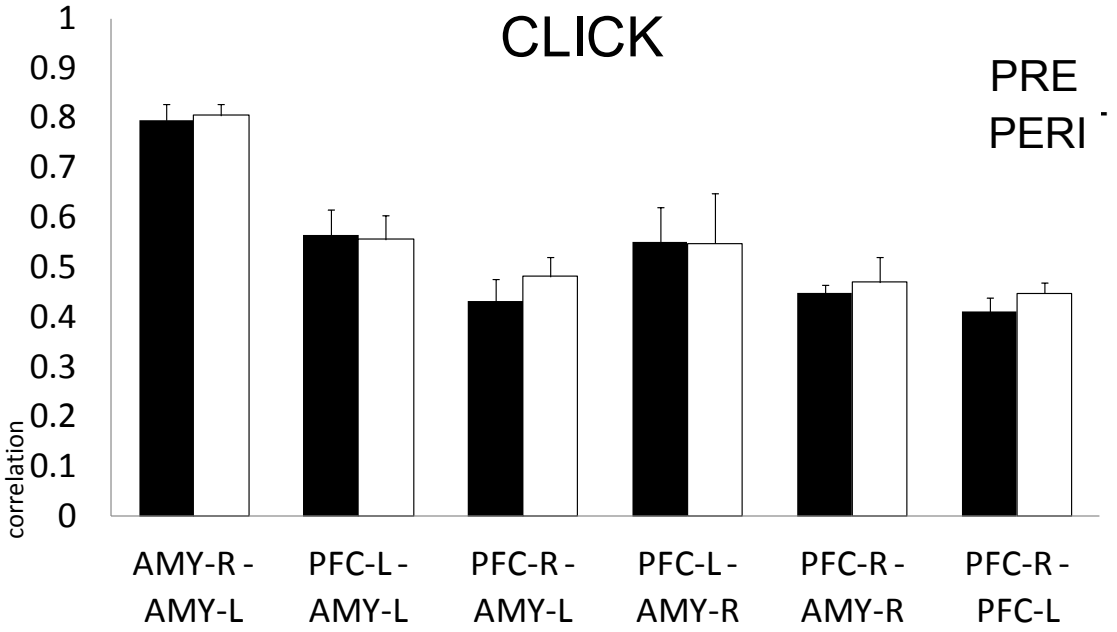

Figure 13: Cross-animal correlation averages in click (NS) conditioning for pre-stimulus (dark) and peri-stimulus (light) segments with standard error ($p<0.05$, n=200).

Correlation values during tone (CS) conditioning show decrease in all areas in the peri-stimulus phase, while there is no essential difference in synchrony during click (NS) stimulus phase. Furthermore, when we compare the pre- and peri-stimulus intervals of tone (CS) and click (NS) stimuli (that is pre-tone vs pre-click and peri-tone vs peri-click) in the conditioning sessions we find that there is a significant drop in the correlation of the peri-tone phase compared to the peri-click phase (while there is no significant difference in the pre-stages, figure 14).

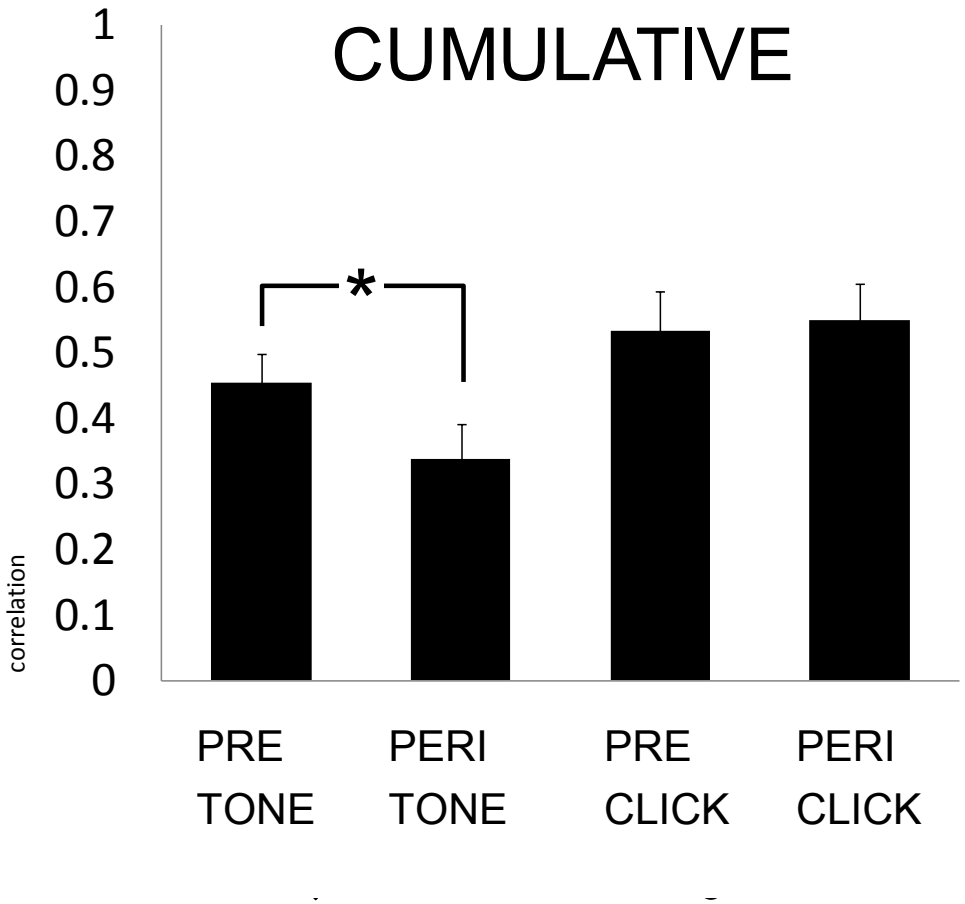

Figure 14: Cross-animal cumulated correlation averages and standard error values through the conditioning phase. Significant differences are marked with * ($p<0.05$, $n=200$).

Extinction

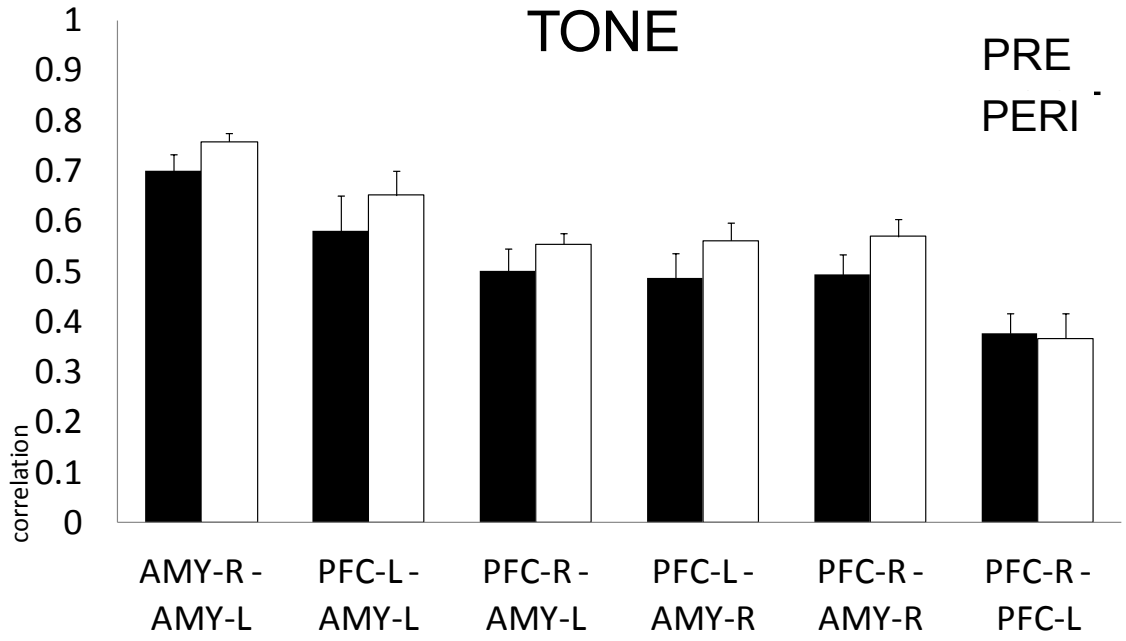

Figure 15: Cross-animal correlation averages in tone (CS) extinction for pre-stimulus (dark) and peri-stimulus (light) segments with standard error ($p<0.05$, n=200).

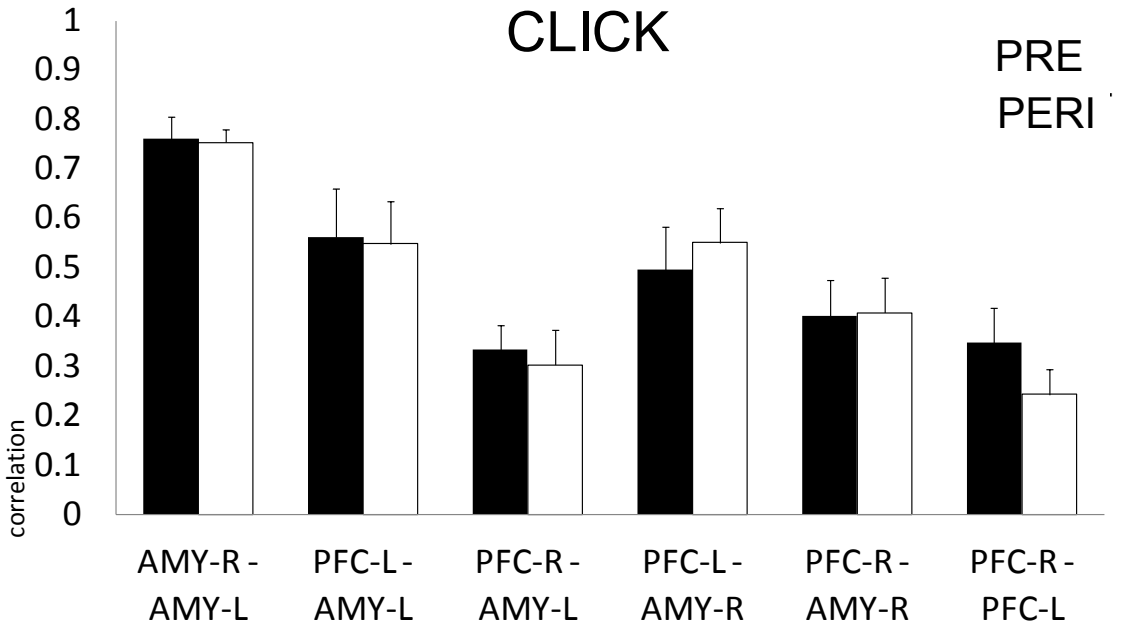

Figure 16: Cross-animal correlation averages in click (NS) extinction for pre-stimulus (dark) and peri-stimulus (light) segments with standard error ($p<0.05$, n=200).

During extinction, results show no statistically significant difference between peri-tone segments compared to pre-tone sections, and similarly, results in the cross-animal correlation averages show no significant differences between pre-click and peri-click segments in the extinction sessions, suggesting that a larger sample size would be necessary to test whether or not the changes are real.

When we compare the pre- and peri-stimulus intervals of tone (CS) and click (NS) stimuli (that is pre-tone vs pre-click and peri-tone vs peri-click) in the extinction phase we find quite the opposite of the conditioning phase as in this case there is no significant difference in the correlation average through peri-tone sections compared with pre-tone segments, and there is no observable change in the correlation averages between pre-click and peri-click segments (figures 15-17).

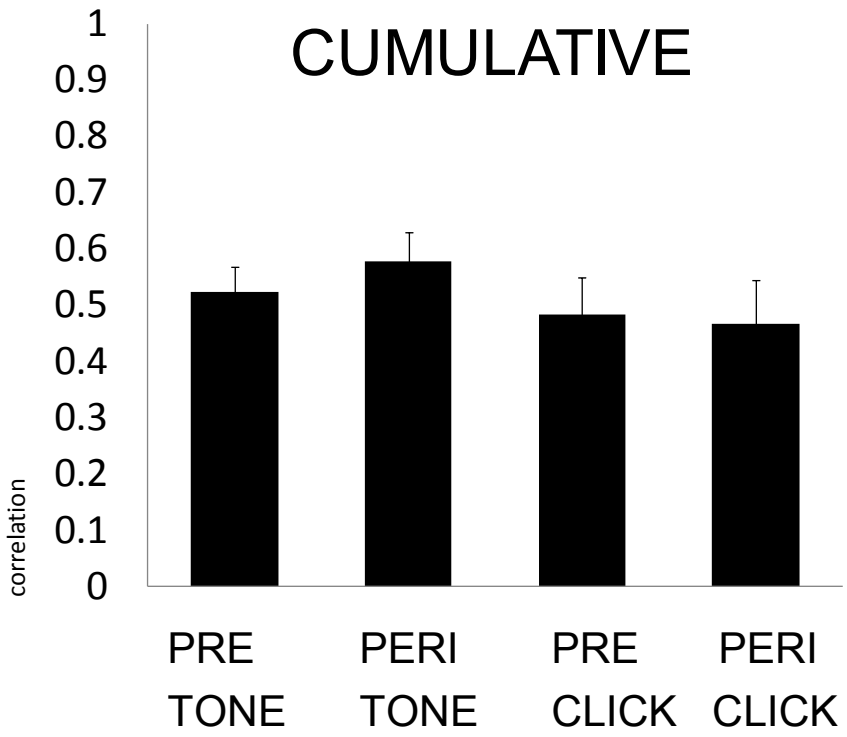

Figure 17: Cross-animal cumulated correlation averages and standard error values through the extinction phase ($p<0.05$, $n=200$).

The third stage of the experiments was the reacquisition phase where the animals were rewarded with food again. We performed the same series of analysis to get a detailed overview of the processes involved in reward conditioning. Results of the correlation calculations in the tone reacquisition phase show a remarkable phenomenon: a consistent and significant decrease in the correlation (increased desynchronization) in all areas during the peri-tone phase compared to the pre-tone segment. Correlation analysis shows no significant difference between correlation averages for the neutral click stimulus during reacquisition phase when pre-click and peri-click segments are compared (figure 18-20).

Reacquisition

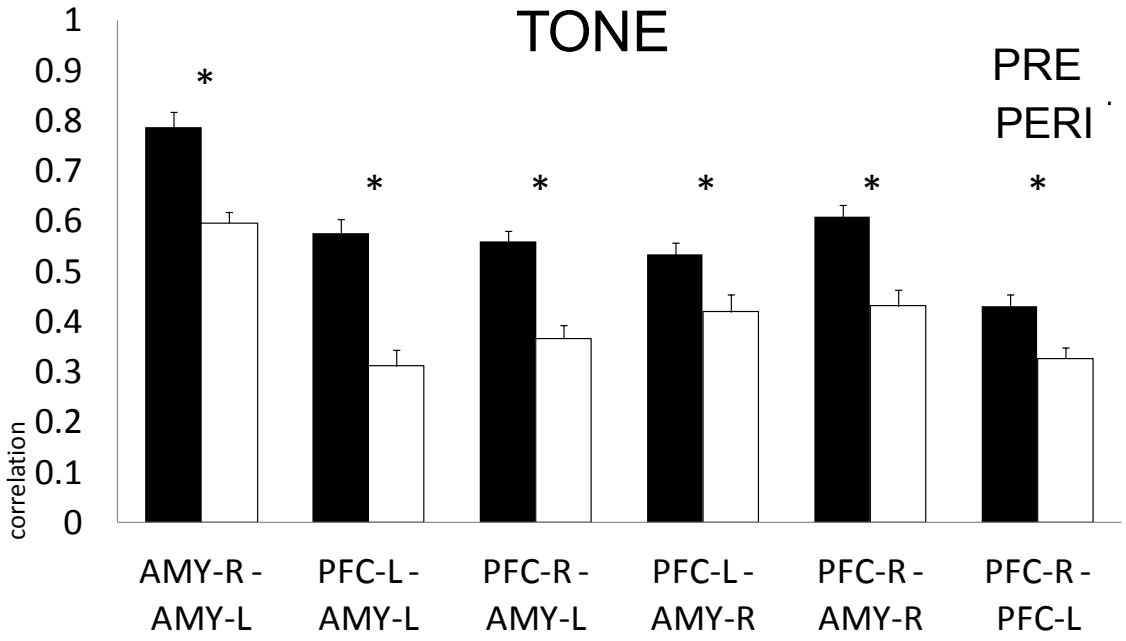

Figure 18: Cross-animal correlation averages in tone (PS) reacquisition for pre-stimulus (dark) and peri-stimulus (light) segments with standard error. Significant differences are marked with * ($p<0.05$, n=200).

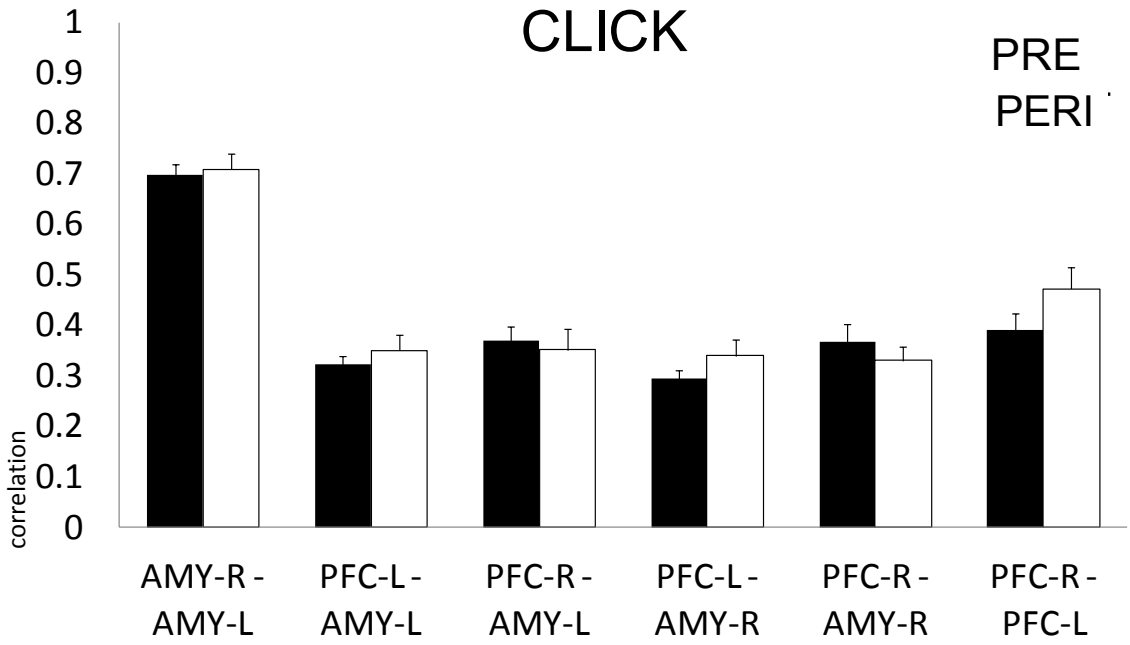

Figure 19: Cross-animal correlation averages in click (Fuster) reacquisition for pre-stimulus (dark) and peri-stimulus (light) segments with standard error ($p<0.05$, n=200).

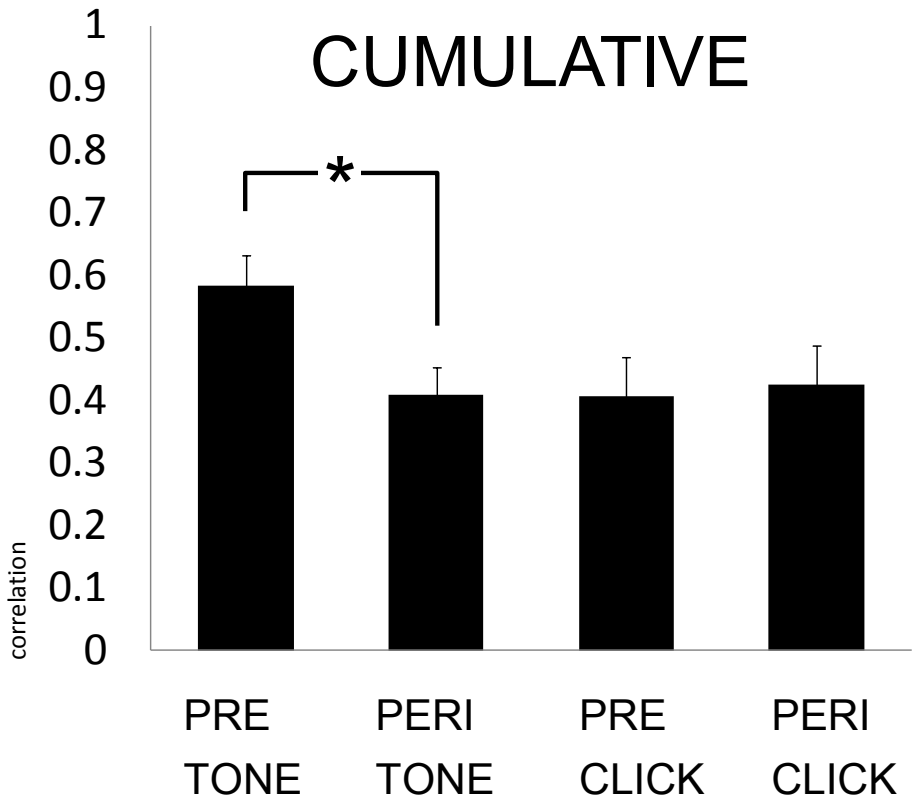

Figure 20: Cross-animal cumulated correlation averages and standard error values through the reacquisition phase. Significant differences are marked with * ($p<0.05$, $n=200$).

Spectral characteristics of LFP epochs

One essential and indispensable method of signal analysis is the examination of frequency components constituting the signal. Fourier analysis has been a powerful and popular tool for a long time, enabling us to extract spectral attributes of a signal and to produce a special, transformed view of the same signal (time domain -> frequency domain). Fourier transformation does not cause any loss of information, as it is fully reversible with the inverse Fourier transformation as long as phase part is used in addition to the power spectrum. Although the time variable is not present in the frequency domain, it is still possible to carry out time-frequency analyses in order to be able to relate frequency characteristics with time.

To inspect how frequencies perform during pre-stimulus and peri-stimulus phases it is advantageous to compute the Short Time Fourier Transform (STFT) of a signal that provides us with the time-frequency analysis of the recorded activity. The calculation is to be performed on the same epochs used in preceding analyses, thus we can also relate the outcome with previous results (figures 21-25).

Spectrograms:

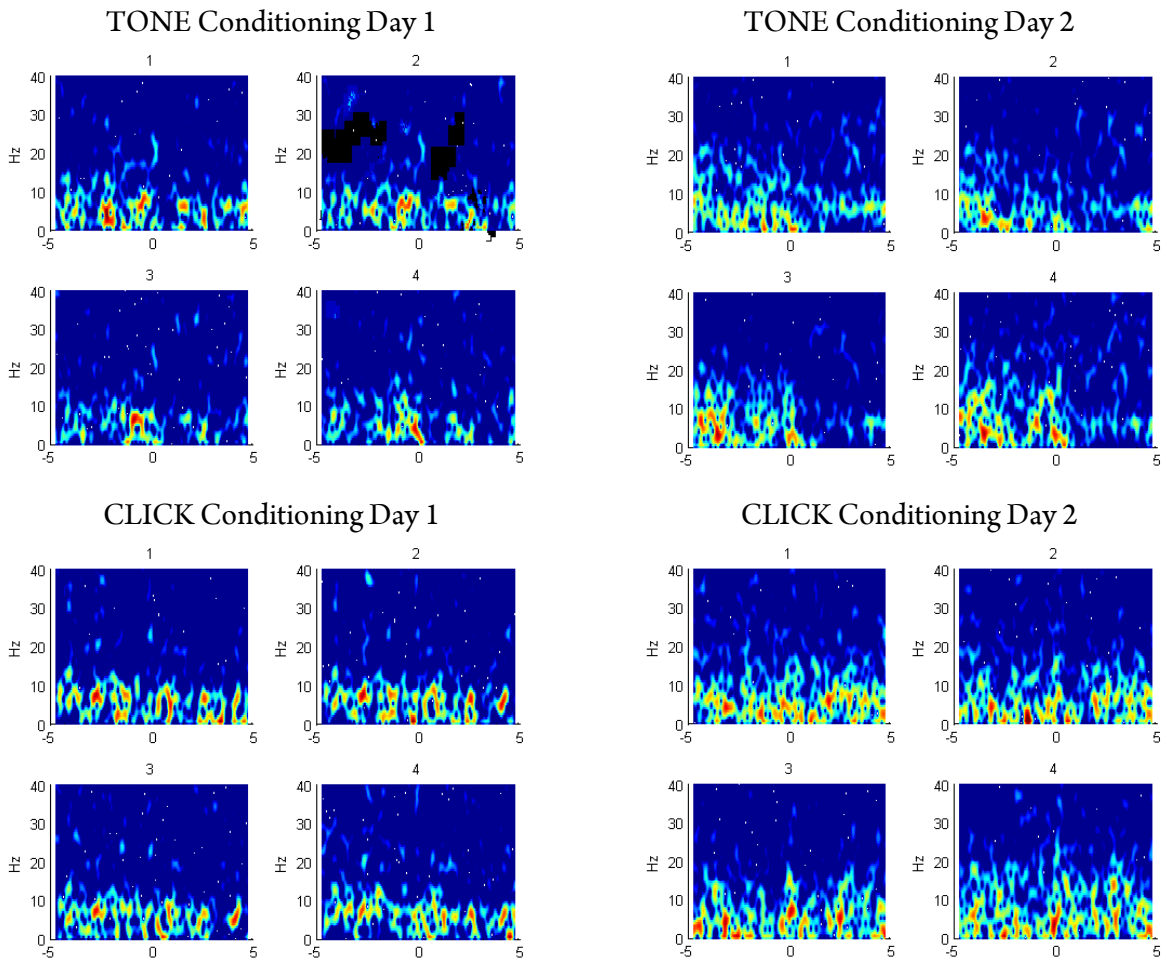

Figure 21: LFP epoch STFT-spectrograms compared for TONE (CS) and CLICK (NS) stimuli for Rat1, conditioning day 1 through to conditioning day 2. Horizontal axis: time (s), vertical axis: frequency (Hz), displaying channels 1 (top-left) to 4 (bottom-right, 1:AMY-L, 2:AMY-R, 3:PFC-L, 4:PFC-R). Zero time point on horizontal axis indicates stimulus onset. Colours indicate spectral power ranging from low (blue, 10 dB/Hz) to high (red, 25 dB/Hz)

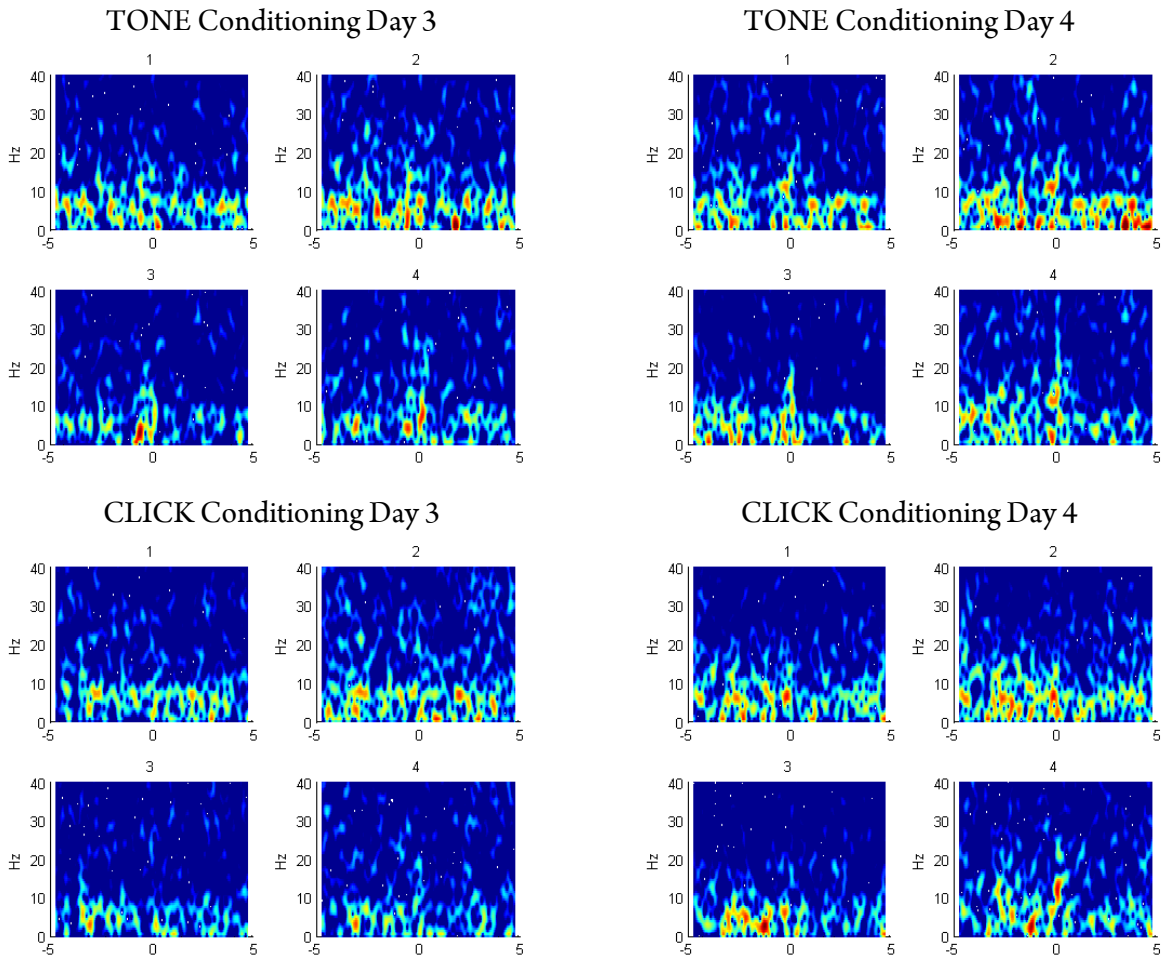

Figure 22: LFP epoch STFT-spectrograms compared for TONE (CS) and CLICK (NS) stimuli for Rat1, conditioning day 3 through to conditioning day 4. Horizontal axis: time (s), vertical axis: frequency (Hz), displaying channels 1 (top-left) to 4 (bottom-right, 1:AMY-L, 2:AMY-R, 3:PFC-L, 4:PFC-R). Zero time point on horizontal axis indicates stimulus onset. Colours indicate spectral power ranging from low (blue, 10 dB/Hz) to high (red, 25 dB/Hz) .

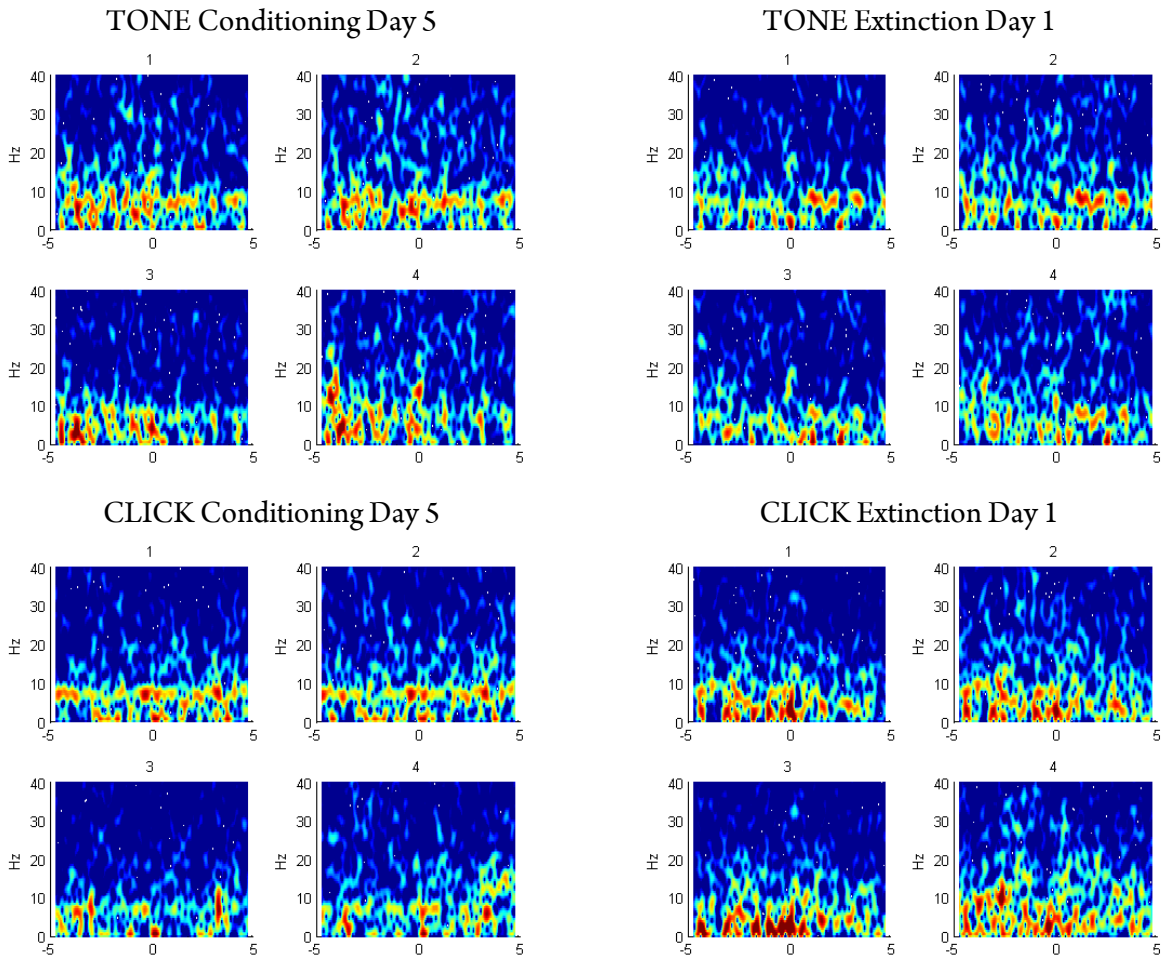

Figure 23: LFP epoch STFT-spectrograms compared for TONE (CS) and CLICK (NS) stimuli for Rat1, conditioning day 5 through to extinction day 1. Horizontal axis: time (s), vertical axis: frequency (Hz), displaying channels 1 (top-left) to 4 (bottom-right, 1:AMY-L, 2:AMY-R, 3:PFC-L, 4:PFC-R). Zero time point on horizontal axis indicates stimulus onset. Colours indicate spectral power ranging from low (blue, 10 dB/Hz) to high (red, 25 dB/Hz)

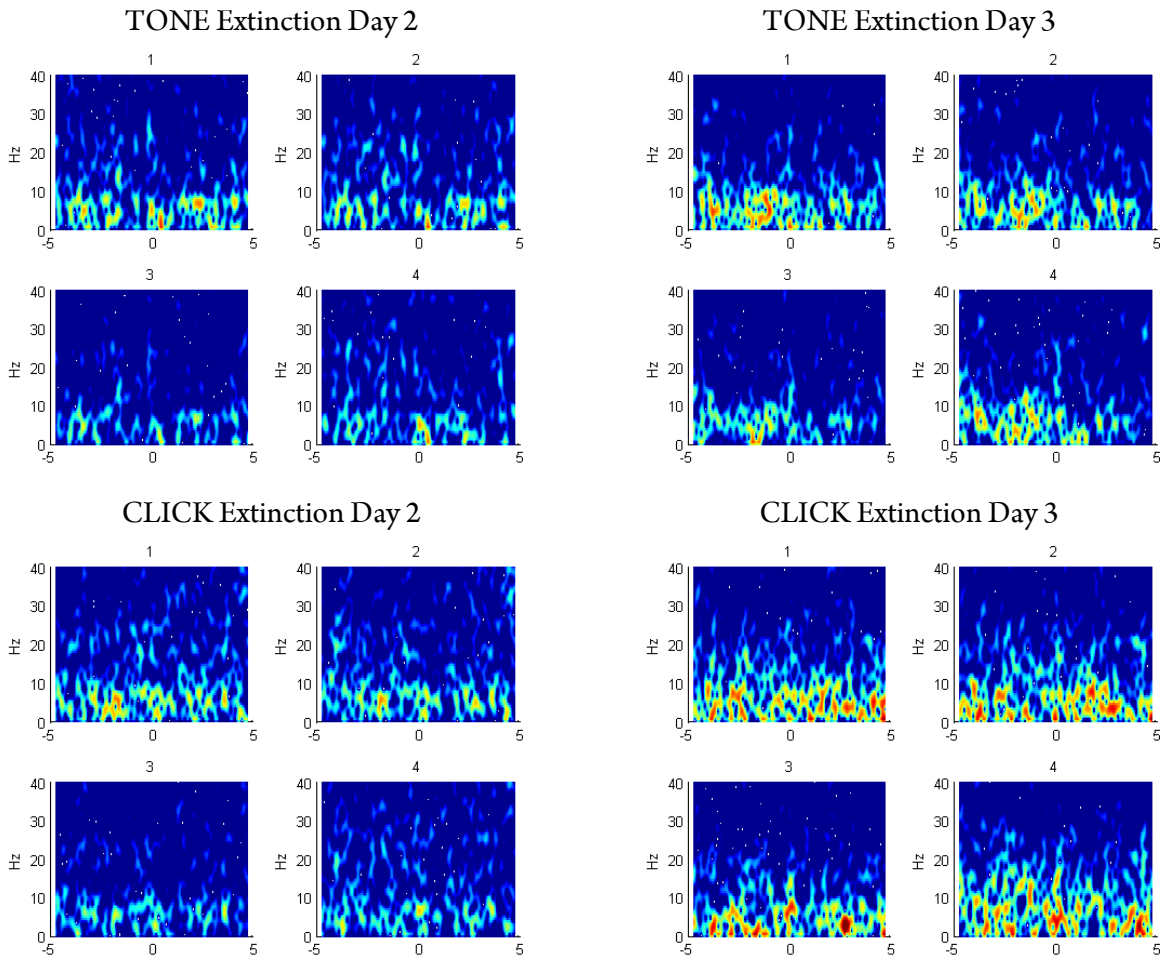

Figure 24: LFP epoch STFT-spectrograms compared for TONE (CS) and CLICK (NS) stimuli for Rat1, extinction day 2 through to extinction day 3. Horizontal axis: time (s), vertical axis: frequency (Hz), displaying channels 1 (top-left) to 4 (bottom-right, 1:AMY-L, 2:AMY-R, 3:PFC-L, 4:PFC-R). Zero time point on horizontal axis indicates stimulus onset. Colours indicate spectral power ranging from low (blue, 10 dB/Hz) to high (red, 25 dB/Hz) .

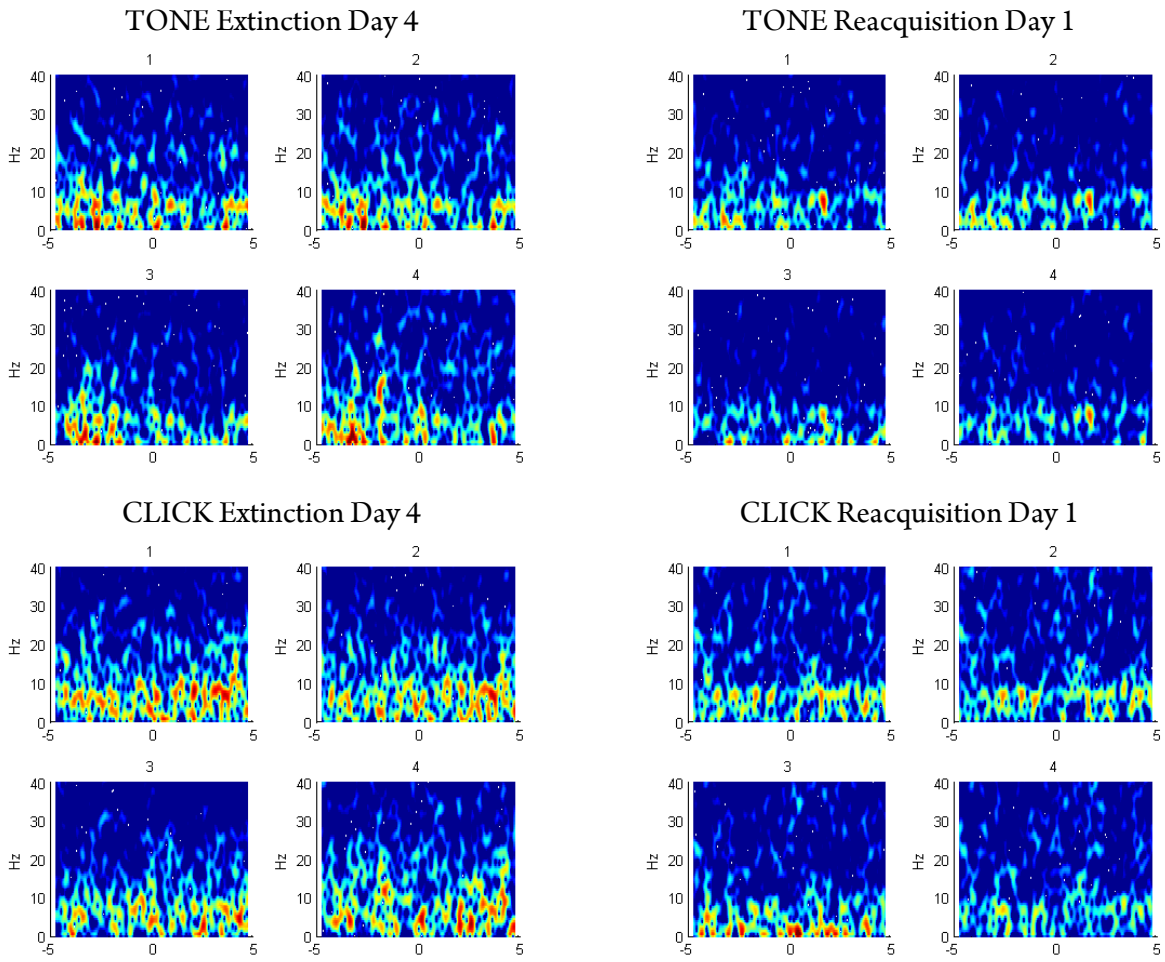

Figure 25: LFP epoch STFT-spectrograms compared for TONE (CS) and CLICK (NS) stimuli for Rat1, extinction day 4 through to reacquisition day 1. Horizontal axis: time (s), vertical axis: frequency (Hz), displaying channels 1 (top-left) to 4 (bottom-right, 1:AMY-L, 2:AMY-R, 3:PFC-L, 4:PFC-R). Zero time point on horizontal axis indicates stimulus onset. Colours indicate spectral power ranging from low (blue, 10 dB/Hz) to high (red, 25 dB/Hz)

The spectrograms show two solid and consistent frequency bands, one in the range of 1-5 Hz and a range of 5-9 Hz. Peak detection within these bands resulted in two distinct peaks, one at 3.78 ± 0.47 Hz, and another one at 8.24 ± 0.75 Hz. By mere visual inspection no recurring patterns are observable. It is also notable that the frequency bands above 15 Hz seem to lack power in the majority of cases, at least compared to the nominal power of the two aforementioned bands falling between 10-25 dB/Hz (figure 26).

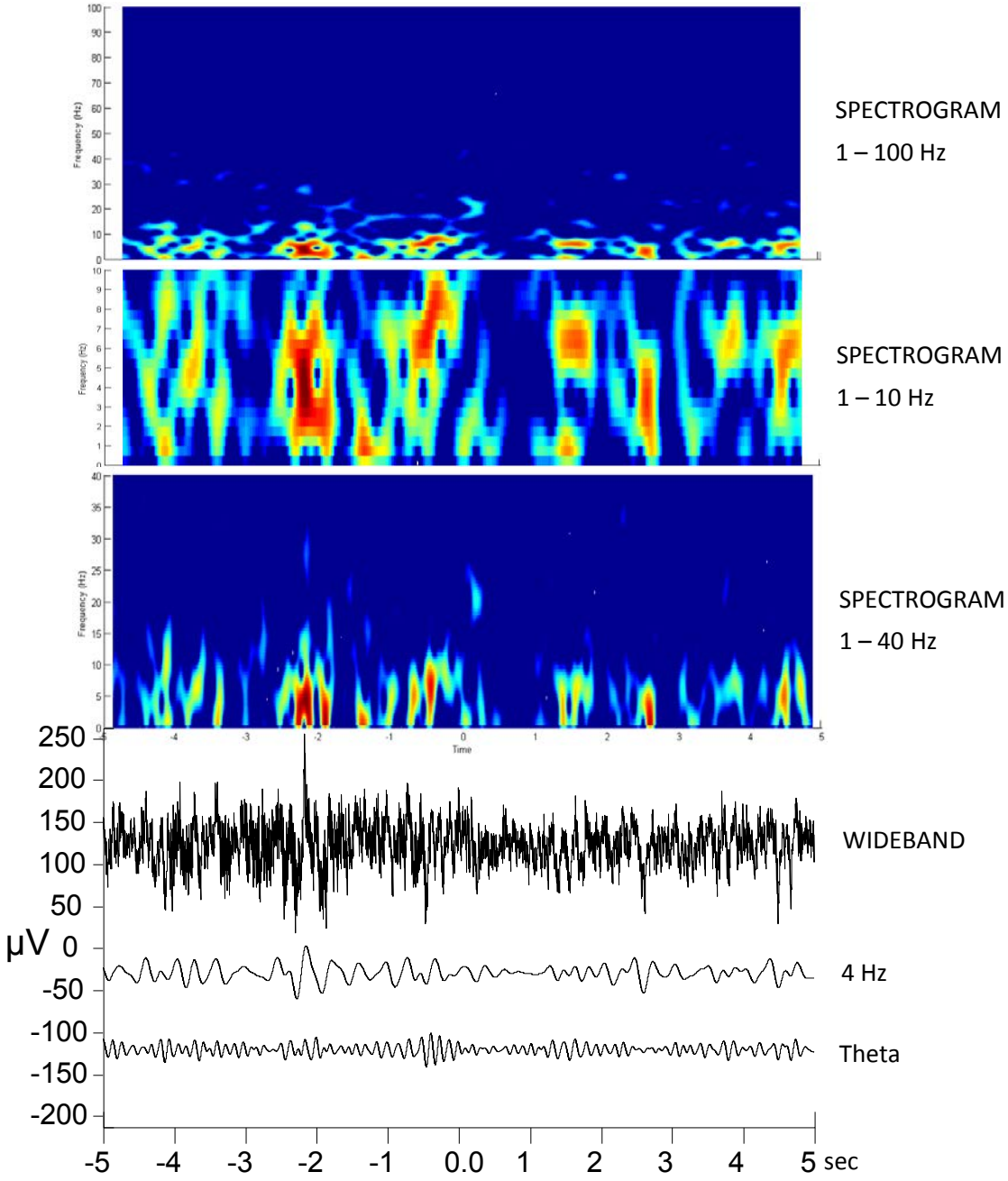

Figure 26: Rat2 example of LFP epoch spectral properties from Conditioning Day 1, recorded from AMY-L. From top to bottom: spectrogram of the wideband LFP epoch. Horizontal axis: time (s). Vertical axis: frequency (Hz). Colours indicate spectral power ranging from low (blue, 10 dB/Hz) to high (red, 25 dB/Hz) . Below: wideband and filtered signals (4 Hz: 2-5 Hz bandpass and Theta: 5-9 Hz bandpass).

Although the spectrogram maps have relatively good time resolution, it is hard to find a distinct activity that can be linked directly to the stimulus at the 0 time point. Any relation to the stimulus onset, and the distribution of the occurrence of the recurring activities will have to be examined using a detection algorithm to obtain the time codes within the epochs, and thorough statistical analysis to reveal systematic patterns, if there are any.

In order to assess the exact and accurate spectral characteristics, we need to run Fourier analysis on the bi-segmental epochs, which provides us with a quantifiable measure, through which the spectral performance of the PRE and PERI segments can be statistically compared. Since the correlation analysis showed no statistical differences between PRE-CLICK and PERI-CLICK segments, – compared to the differences between PRE-TONE and PERI-TONE segments – we now concentrate on the comparison of SPONTANEOUS (pre-tone) and EVOKED (peri-tone) segments, since should there be any detectable response evoked by the stimulus, it must appear as a difference between spontaneous and evoked stages (figure 27-31).

Frequency domain of the LFP epochs:

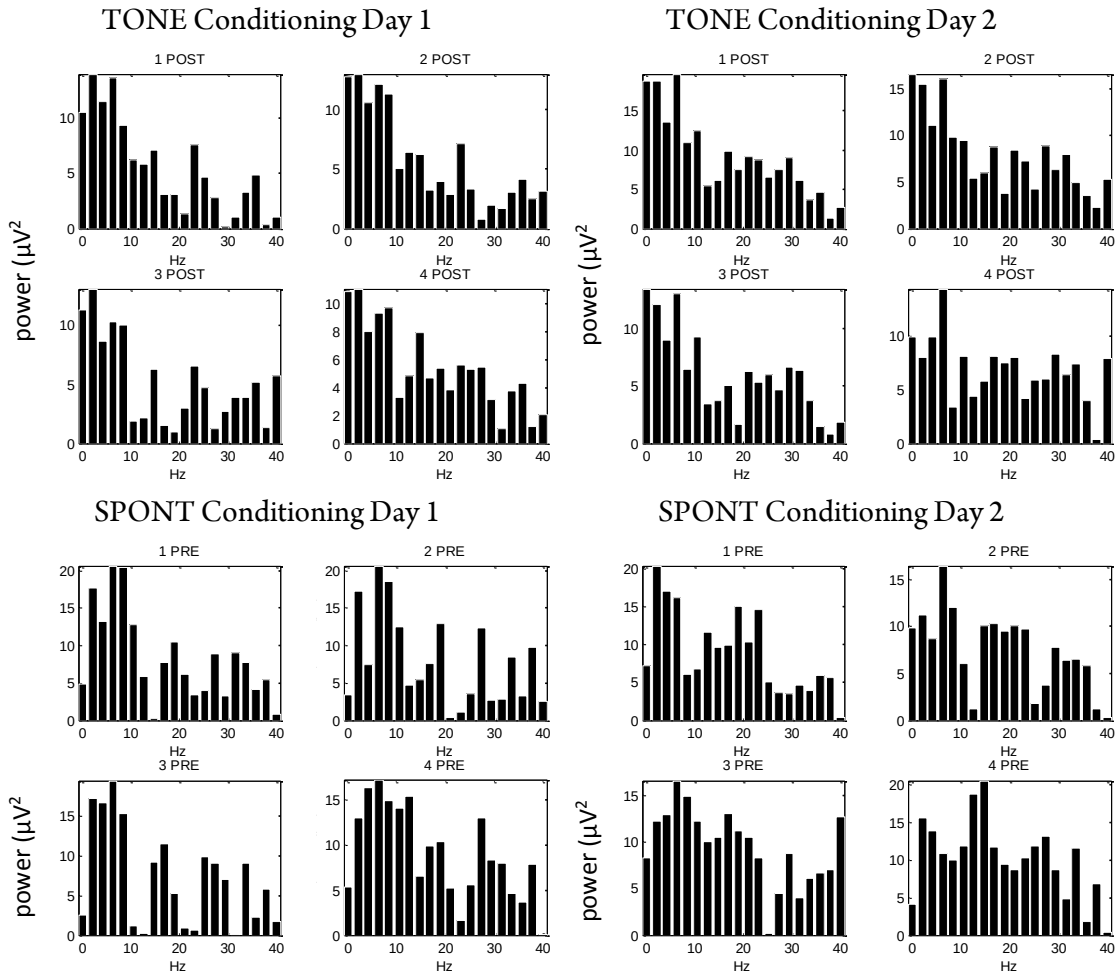

Figure 27: LFP epoch FFT graphs compared for TONE (CS) and SPONTANEOUS segments for Rat1, conditioning day 1 through to conditioning day 2. Horizontal axis: frequency (Hz), vertical axis: power (μV^2), displaying channels 1 (top-left) to 4 (bottom-right, 1:AMY-L, 2:AMY-R, 3:PFC-L, 4:PFC-R).

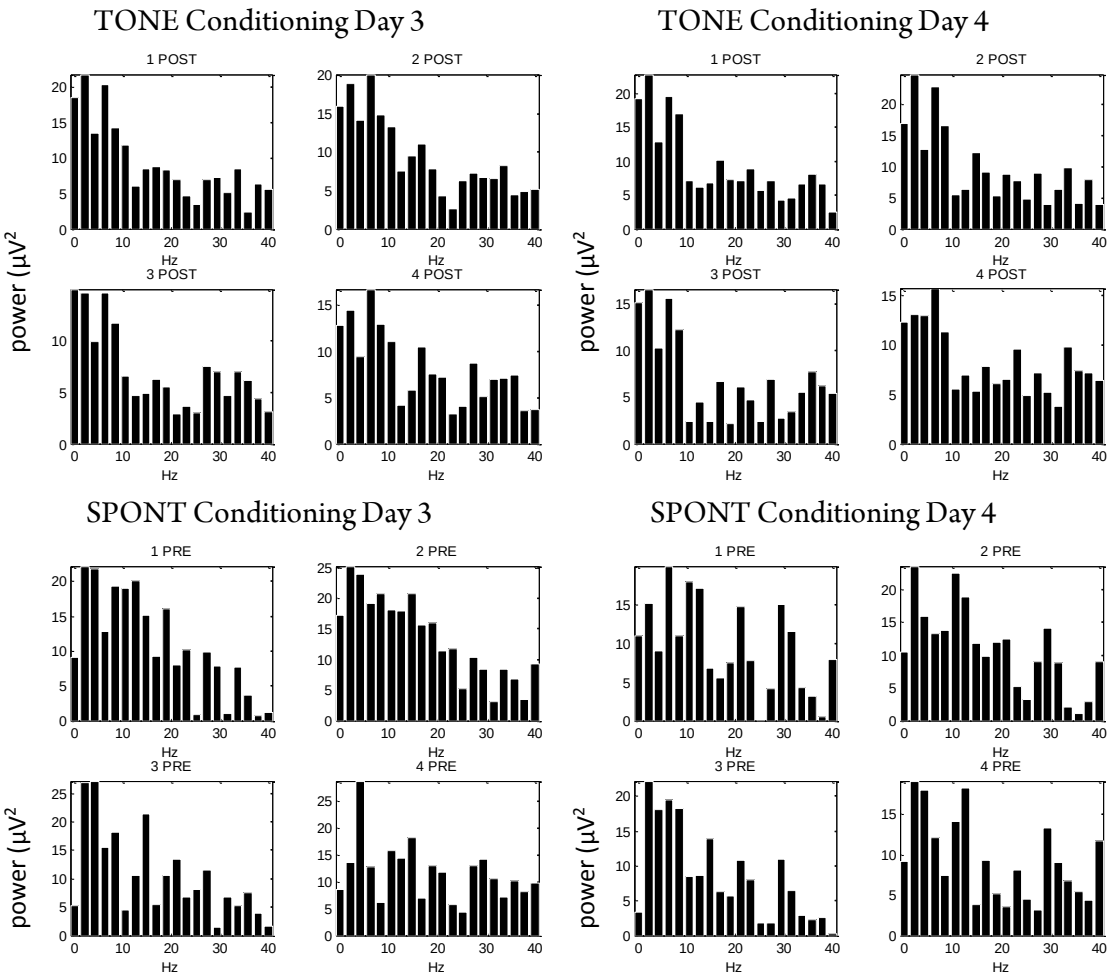

Figure 28: LFP epoch FFT graphs compared for TONE (CS) and SPONTANEOUS segments for Rat1, conditioning day 3 through to conditioning day 4. Horizontal axis: frequency (Hz), vertical axis: power (μV^2), displaying channels 1 (top-left) to 4 (bottom-right, 1:AMY-L, 2:AMY-R, 3:PFC-L, 4:PFC-R).

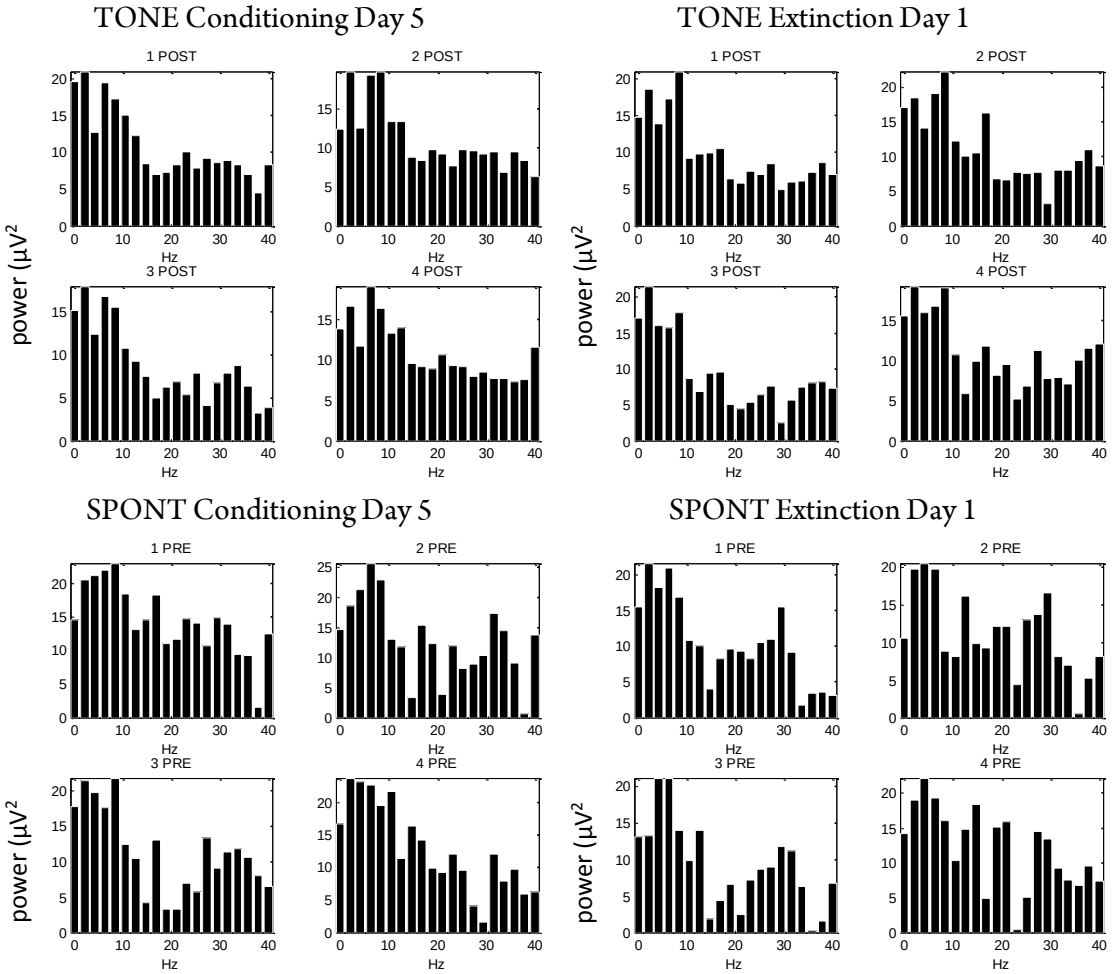

Figure 29: LFP epoch FFT graphs compared for TONE (CS) and SPONTANEOUS segments for Rat1, conditioning day 5 through to extinction day 1. Horizontal axis: frequency (Hz), vertical axis: power (μV^2), displaying channels 1 (top-left) to 4 (bottom-right, 1:AMY-L, 2:AMY-R, 3:PFC-L, 4:PFC-R).

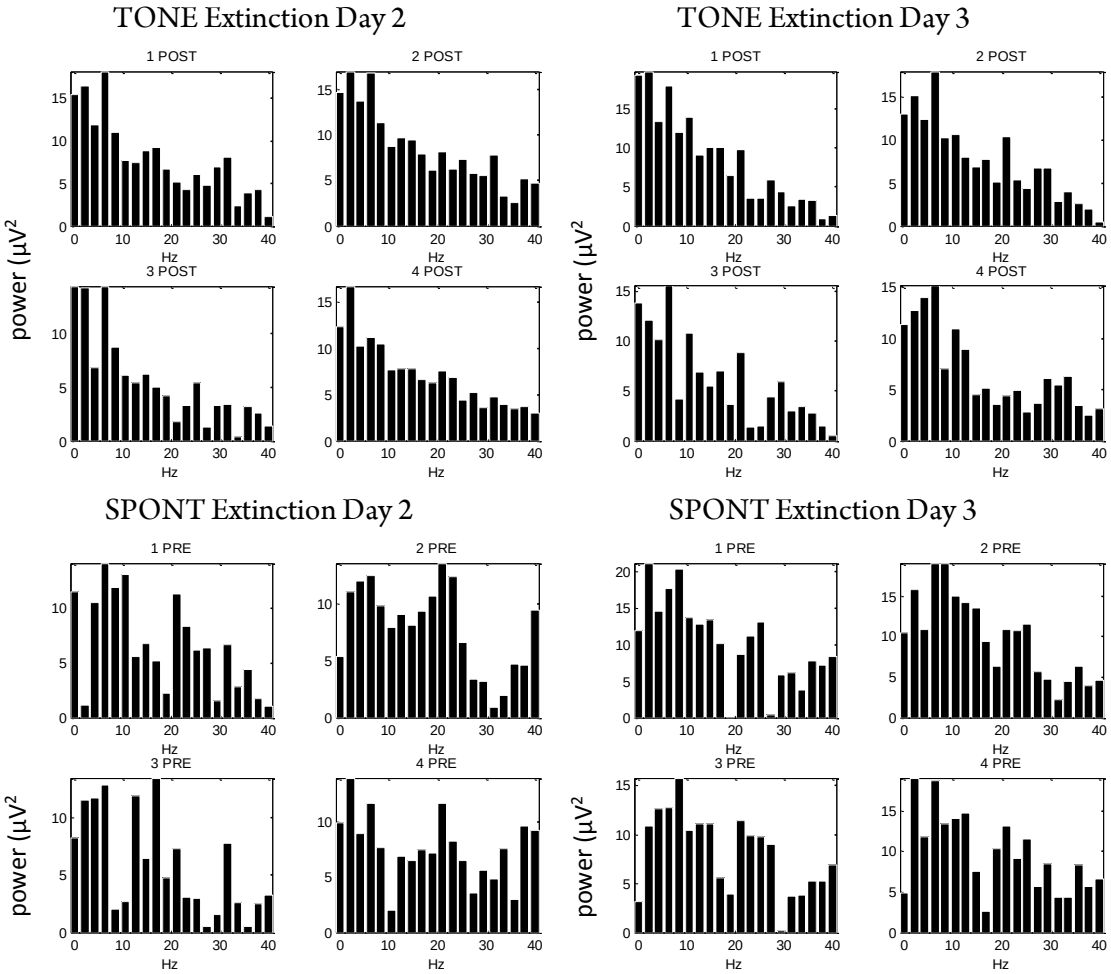

Figure 30: LFP epoch FFT graphs compared for TONE (CS) and SPONTANEOUS segments for Rat1, extinction day 2 through to extinction day 3. Horizontal axis: frequency (Hz), vertical axis: power (μV^2), displaying channels 1 (top-left) to 4 (bottom-right, 1:AMY-L, 2:AMY-R, 3:PFC-L, 4:PFC-R).

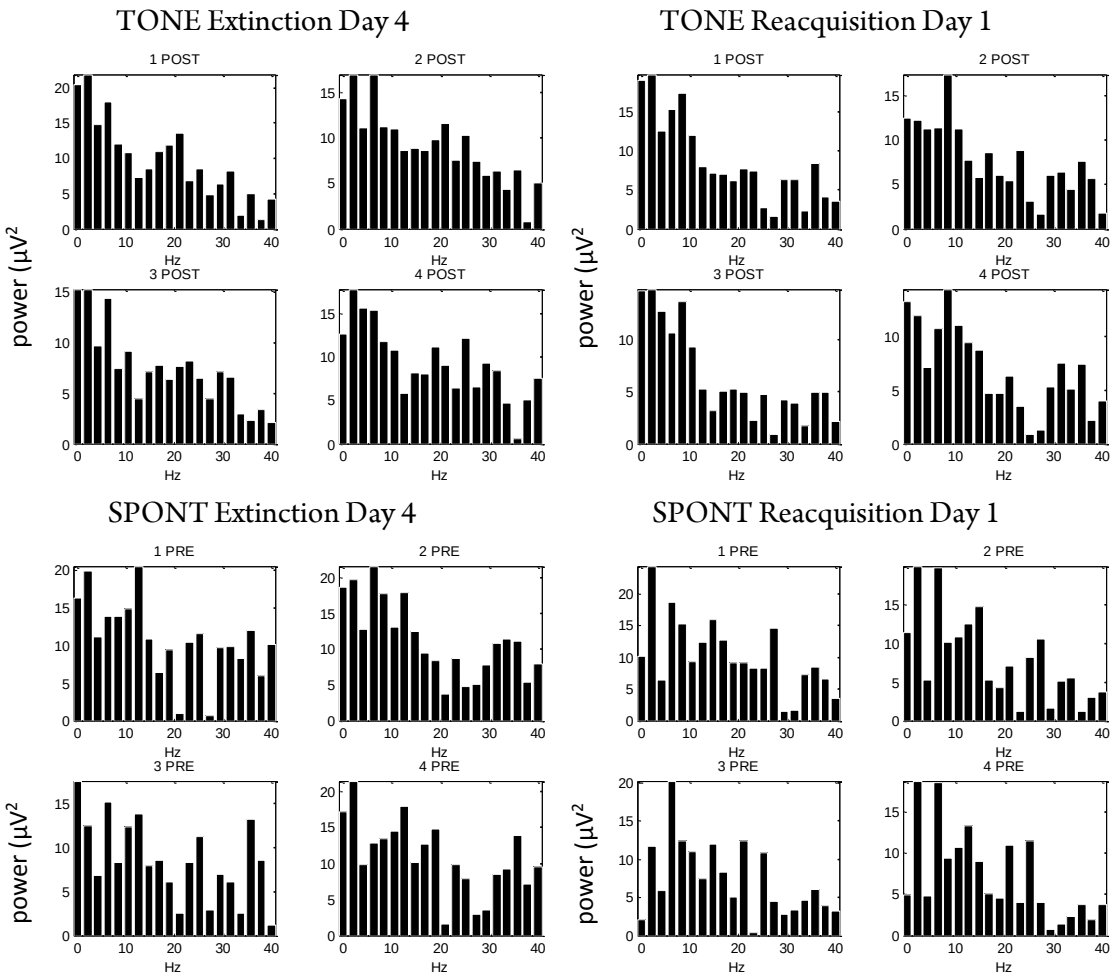

Figure 31: LFP epoch FFT graphs compared for TONE (CS) and SPONTANEOUS segments for Rat1, extinction day 2 through to extinction day 3. Horizontal axis: frequency (Hz), vertical axis: power (μV^2), displaying channels 1 (top-left) to 4 (bottom-right, 1:AMY-L, 2:AMY-R, 3:PFC-L, 4:PFC-R).

To make a quantitative comparison, spectral areas for both corresponding bands were calculated by integration. This resulted in a single value for each band in the spontaneous and in the peri-tone segment (figures 32-33).

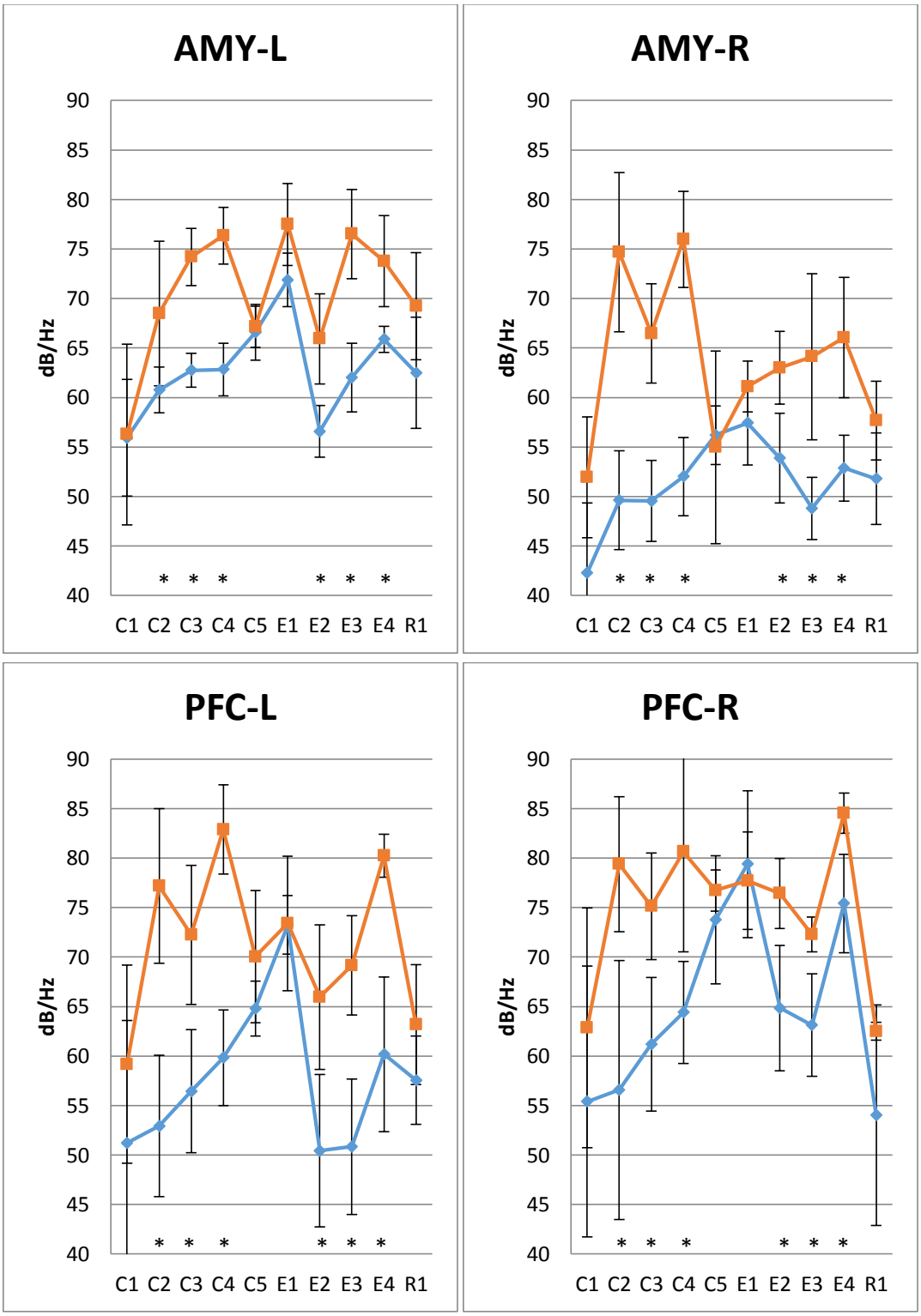

Figure 32: Cross-animal integrated power of 4Hz activity with standard error means (orange: spontaneous, blue = peri-tone). Horizontal axis: experiment sessions (conditioning: C1-C5, extinction: E1-E4, reacquisition: R1), vertical axis: integrated power (dB/Hz). Significant differences are marked with * ($p<0.05$, n=400 sessions).

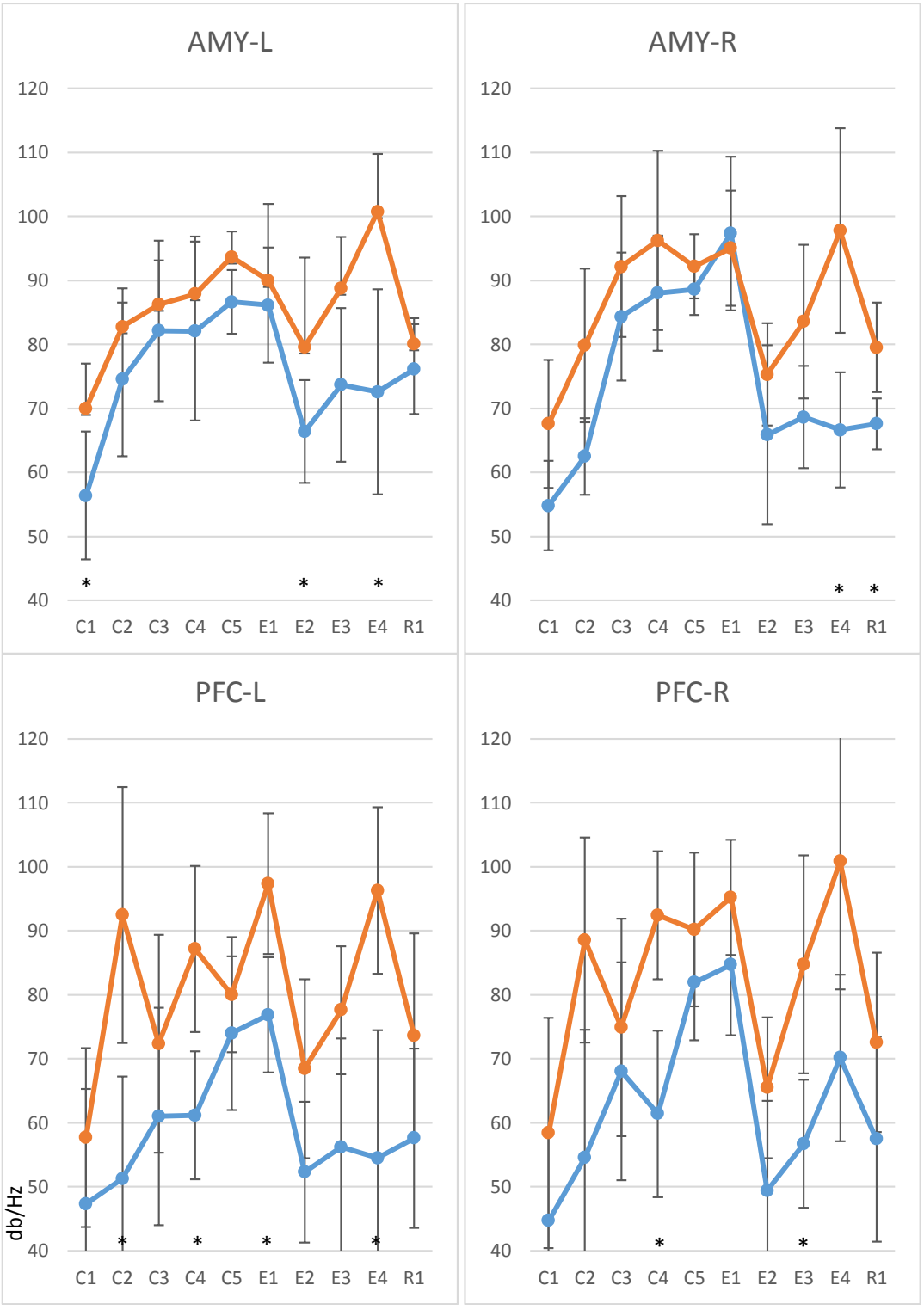

Figure 33: Cross-animal integrated power of Theta activity with standard error means (orange: spontaneous, blue = peri-tone). Horizontal axis: experiment sessions (conditioning: C1-C5, extinction: E1-E4, reacquisition: R1), vertical axis: power (dB/Hz). Significant differences are marked with * ($p<0.05$, n=400 sessions).

The comparison of integrated 4Hz and theta powers show remarkable differences. The 4Hz power analysis shows consistent significant differences on C2, C3, C4 and E2, E3, E4 days. These sessions are in the centre of experimental phases, meaning they contribute to, or are affected by learning / memory processes. Although theta power analysis also shows significant differences, these do not occur consistently.

Distribution of 4 Hz and theta peaks

To elucidate whether either the 4 Hz activity or the theta oscillation has any stimulus dependent features in terms of locking to the stimulus onset, it is important to examine how the occurrence of oscillation peaks distribute over the spontaneous and the stimulus related epoch segments (figure 34).

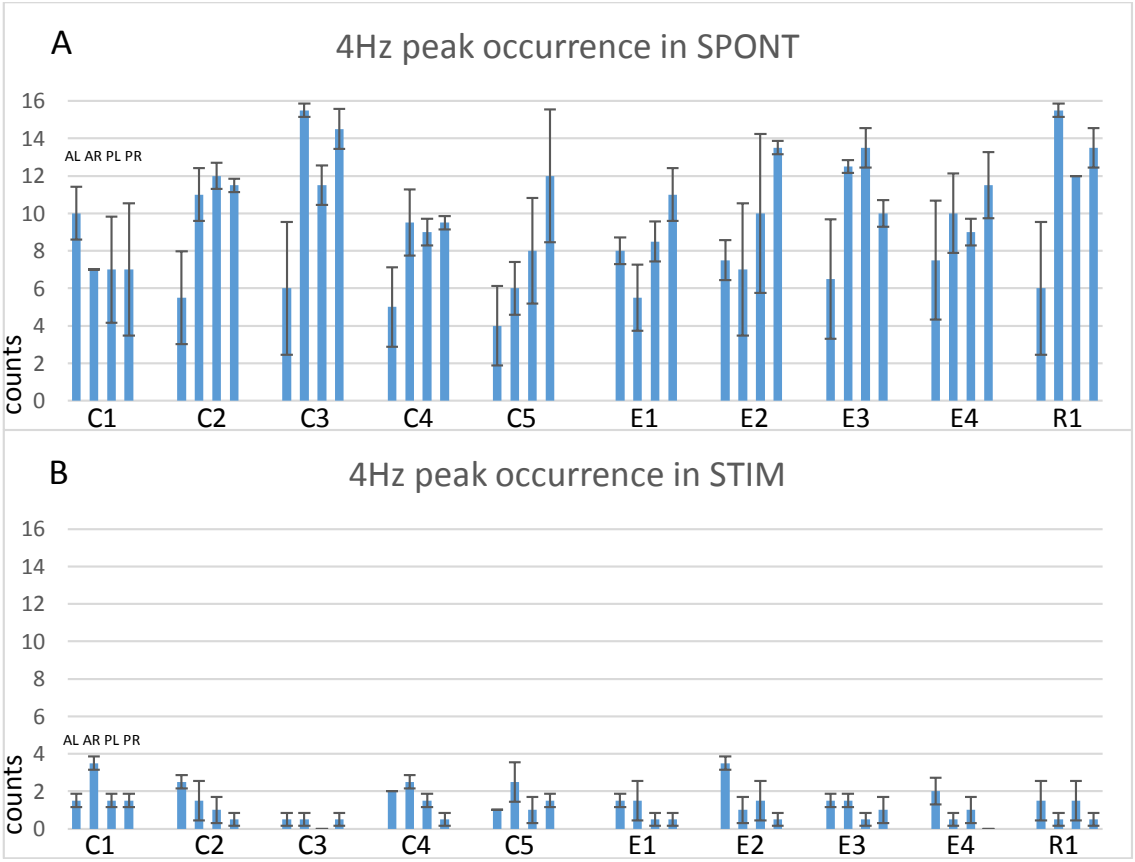

Figure 34: Cross-animal distribution of 4Hz peaks in spontaneous (A) and stimulus related (B) epoch segments in conditioning (C1-C5), extinction (E1-E4) and reacquisition (R1) sessions. Order in all groups: AMY-L (AL), AMY-R (AR), PFC-L (PL), PFC-R (PR).

Results show a remarkable difference in the occurrence rate of 4Hz oscillation peaks when spontaneous and stimulus related segments are compared. The occurrence rate drops significantly ($p<0.01$) after the tone (CS) stimulus is presented, making the 4Hz peaks quite sparse.

In order to see whether the occurrence is systematic and follows a pattern or it is more like a random process, we can compute the mean intervals between 4Hz peaks within each segment (figure 35).

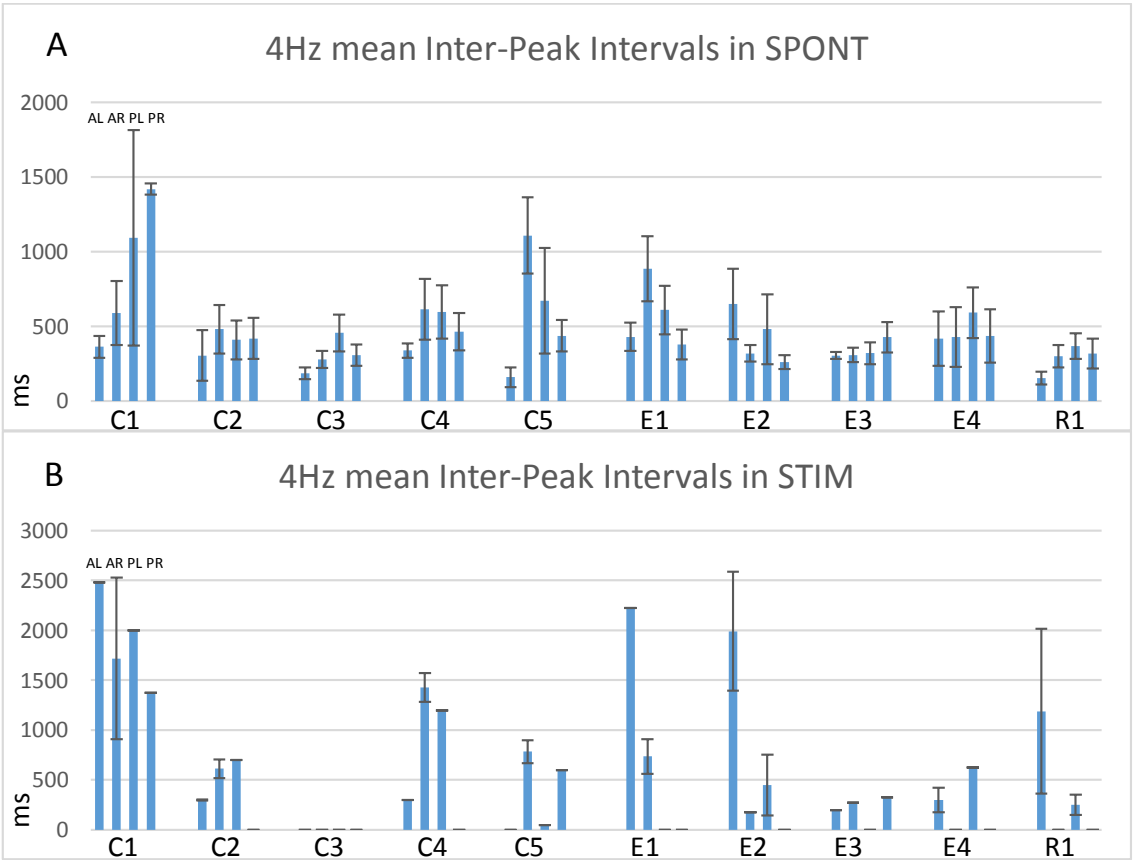

Figure 35: Cross-animal comparison of inter-peak intervals for the 4Hz activity in spontaneous (A) and stimulus related (B) epoch segments in conditioning (C1-C5), extinction (E1-E4) and reacquisition (R1) sessions. Order in all groups: AMY-L (AL), AMY-R (AR), PFC-L (PL), PFC-R (PR).

While there is little consistency in the interval length between peaks during spontaneous activity, there is even less systematic occurrence after the tone (CS) stimulus, meaning there is no consistent pattern formed, more likely it reduces consistency even further. To see if there is any direct relation between the stimulus onset and the 4Hz peaks (whether it is an evoked response or not), we need to examine the interval distribution of the first peak occurrences after the tone (CS) stimulus (figure 36).

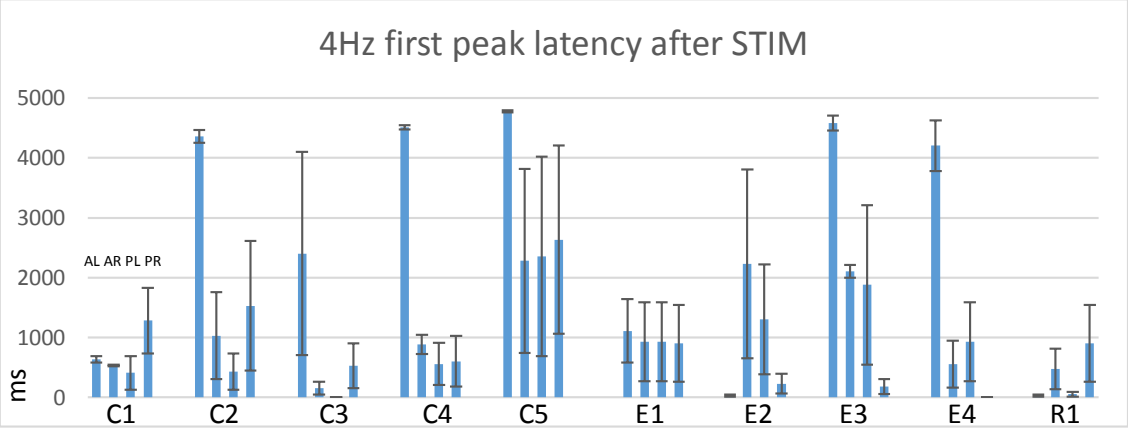

Figure 36: Cross-animal distribution of 4Hz first peak occurrence latencies after the tone (CS) stimulus in conditioning (C1-C5), extinction (E1-E4) and reacquisition (R1) sessions. Order in all groups: AMY-L (AL), AMY-R (AR), PFC-L (PL), PFC-R (PR).

By the mere variability of latency values it would be difficult to find direct relationship between the stimulus onset and the appearance of the first 4Hz peak, but when we also consider the low occurrence rates within the stimulus related epoch segment, it can be stated that there is no direct connection.

In contrast, occurrence rates must be calculated for the theta rhythm as well for comparison with the 4Hz activity (figure 37).

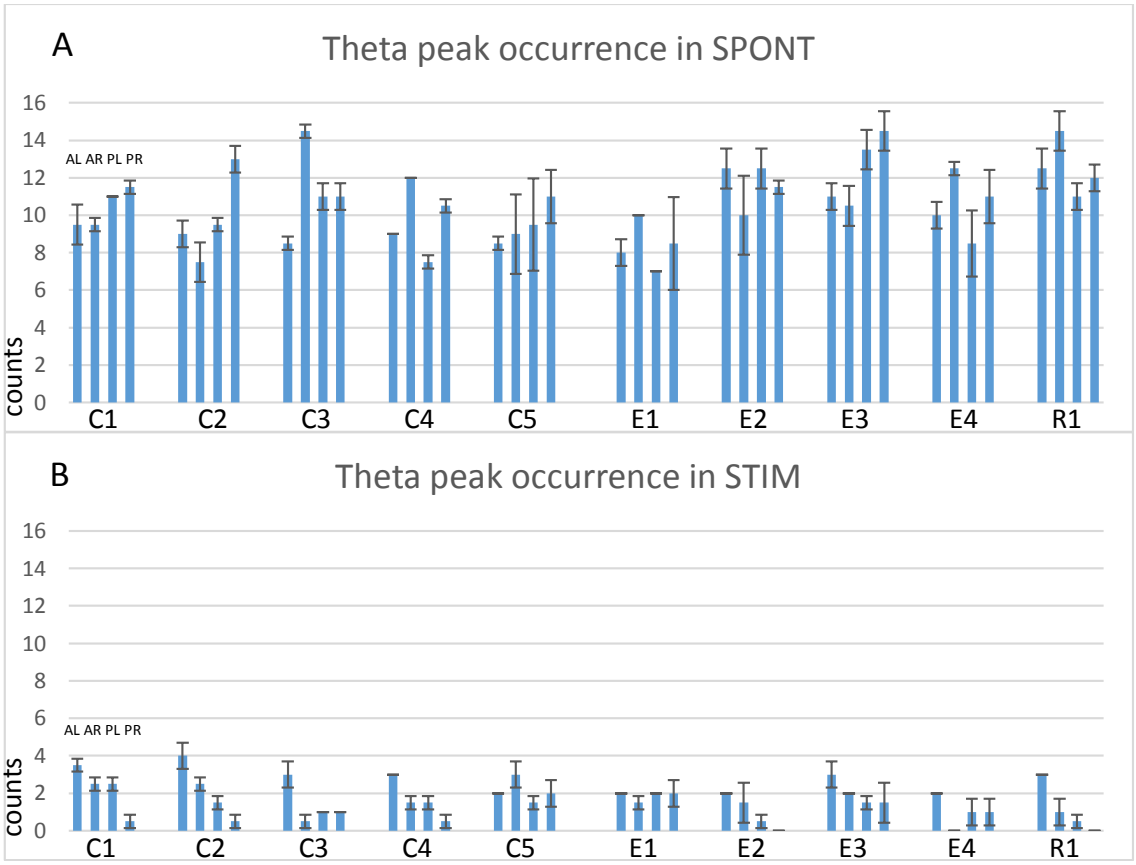

Figure 37: Cross-animal distribution of 4Hz peaks in spontaneous (A) and stimulus related (B) epoch segments in conditioning (C1-C5), extinction (E1-E4) and reacquisition (R1) sessions. Order in all groups: AMY-L (AL), AMY-R (AR), PFC-L (PL), PFC-R (PR).

Again, the results reveal a significant difference in the occurrence rate of theta oscillation peaks when spontaneous and stimulus related segments are compared. There is a significant ($p<0.01$) overall drop in the occurrence rate after the tone (CS) stimulus is presented, leading to quite sparse theta activity.

To see how systematic the occurrence is, we need a measure for the mean intervals between theta peaks within each segment (figure 38).

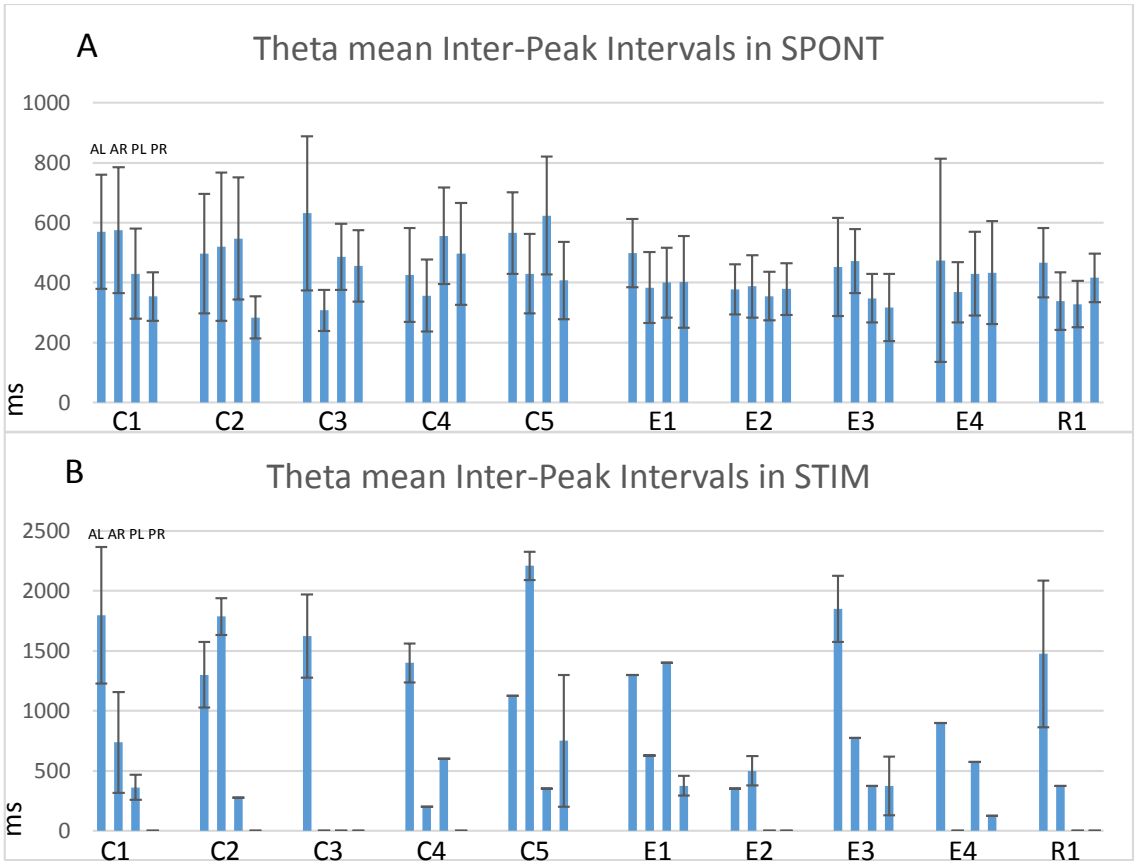

Figure 38: Cross-animal comparison of inter-peak intervals for the theta activity in spontaneous (A) and stimulus related (B) epoch segments in conditioning (C1-C5), extinction (E1-E4) and reacquisition (R1) sessions. Order in all groups: AMY-L (AL), AMY-R (AR), PFC-L (PL), PFC-R (PR).

It is reassuring, that during spontaneous activity there is consistency in the inter-peak intervals as there is no significant difference either between experimental sessions (C1-C5-E1-E4-R1), or between AMY-PFC area pairs. However, when compared to the stimulus related segments, we can see a huge variance in the cross-animal inter-peak interval means, again, meaning that there is no direct systematic effect triggered by the tone (CS) stimulus.

Once again, it needs to be examined whether there is an evoked response in the theta range following the stimulus onset, by computing the interval distribution of the first peak occurrences after the tone (CS) stimulus (figure 39).

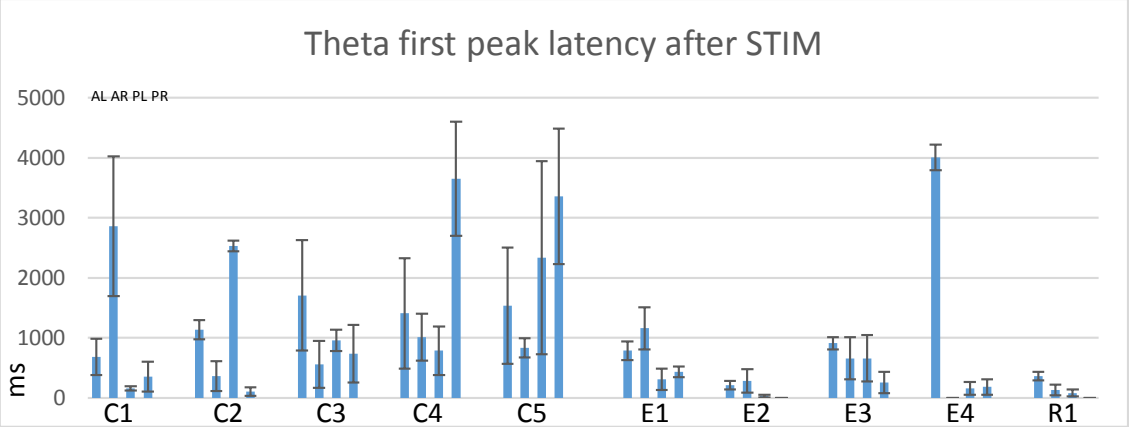

Figure 39: Cross-animal distribution of theta first peak occurrence latencies after the tone (CS) stimulus in conditioning (C1-C5), extinction (E1-E4) and reacquisition (R1) sessions. Order in all groups: AMY-L (AL), AMY-R (AR), PFC-L (PL), PFC-R (PR).

By the evaluation of variability of latency values and by the consideration of how low occurrence rates within the stimulus related epoch segment are, it can be stated that there is no direct connection.

Phase relationship between 4Hz activity and theta oscillation

Oscillations usually have no static spectral characteristics as both internal and external effects can modulate their frequency attributes as well as amplitude physiognomies. Distinct neuronal oscillations often affect each other and it is a frequently observable means of transient communication across spatially separated brain regions. These oscillations show phasic characteristics, and their joint oscillatory attributes can be analysed by the examination of phase relationship between the two rhythmic activities.

Having seen how the 4Hz activity and the theta oscillation dominate the spectral domain in this particular experimental setting, it is vital to obtain precise information on how they 1) synchronise or desynchronise within their frequency band and across the two bands, and 2) how they synchronise or desynchronise across the prefrontal cortex and the amygdala.

To obtain the phase relationship of these rhythmic activities, phase histograms can be calculated showing the precise level of phasic cooperation by a 360-degree resolution of the oscillation cycles. Phase histograms can reveal phase-lock properties as well as phase latency or precedency. Firstly we compared the 4Hz activity between the left amygdala and the left prefrontal cortex (figure 40).

C1 SPONT

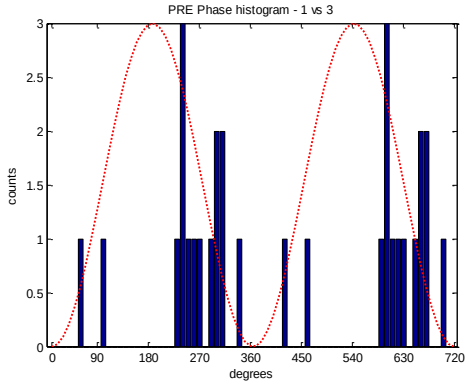

C2 SPONT

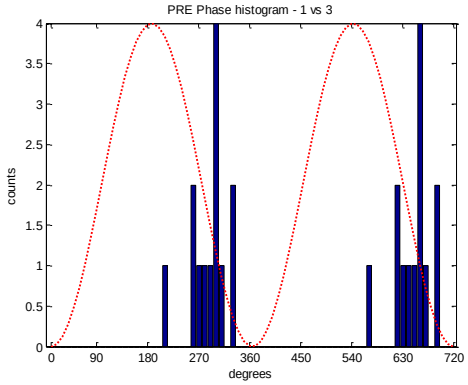

C1 STIM

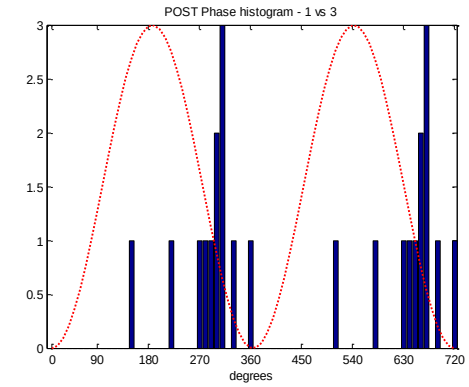

C2 STIM

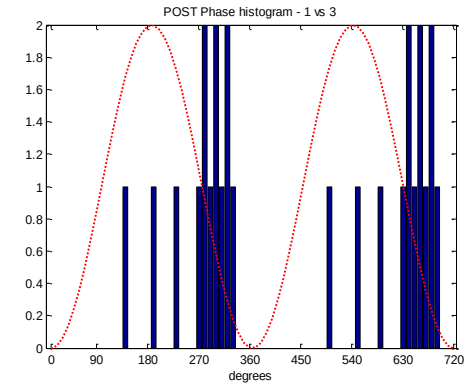

figure continued on next page

C3 SPONT

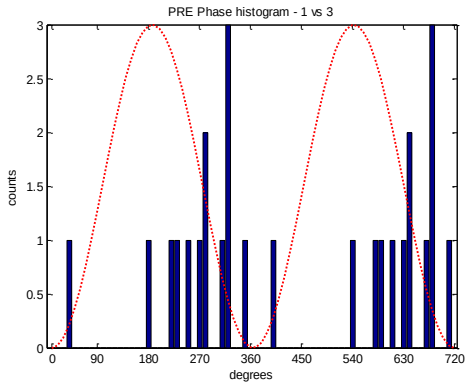

C4 SPONT

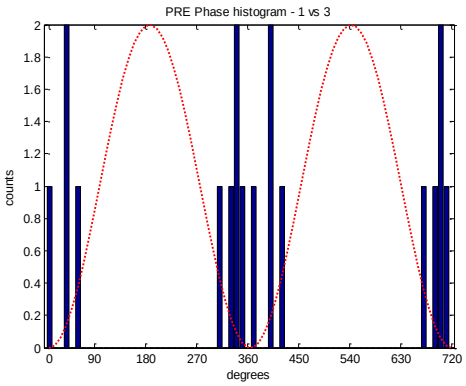

C3 STIM

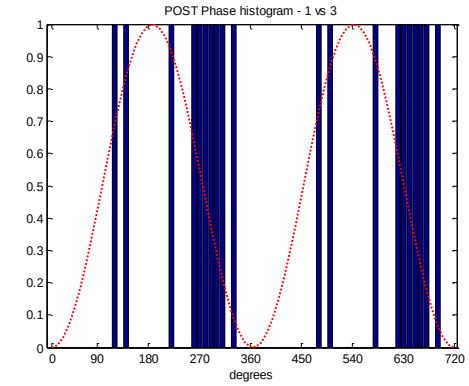

C4 STIM

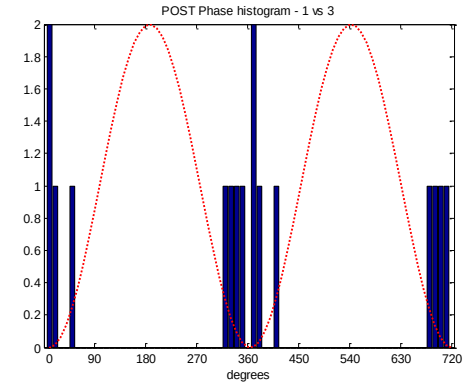

C5 SPONT

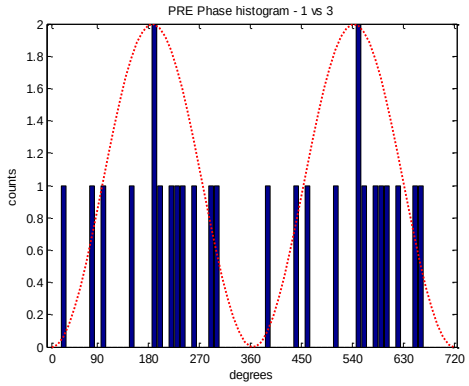

E1 SPONT

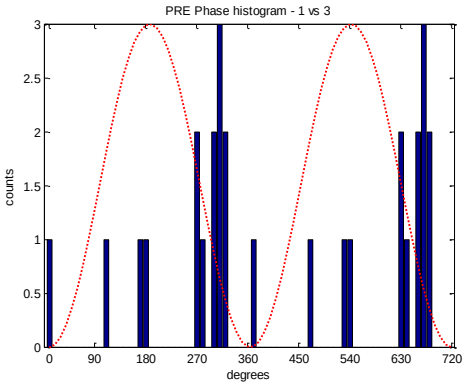

C5 STIM

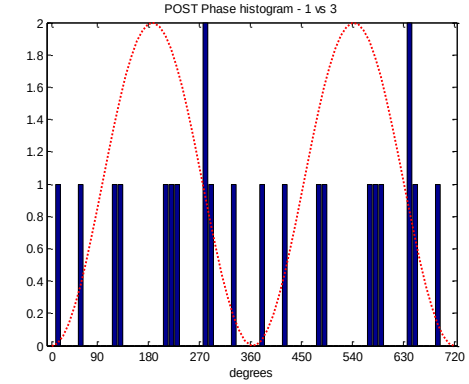

E1 STIM

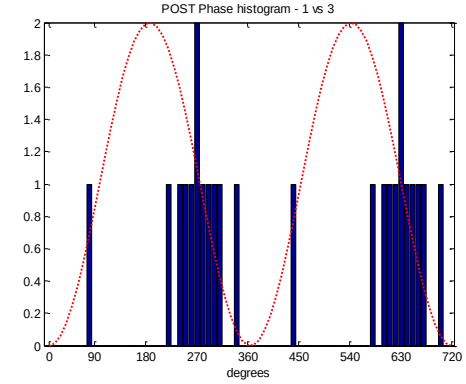

figure continued on next page

E2 SPONT

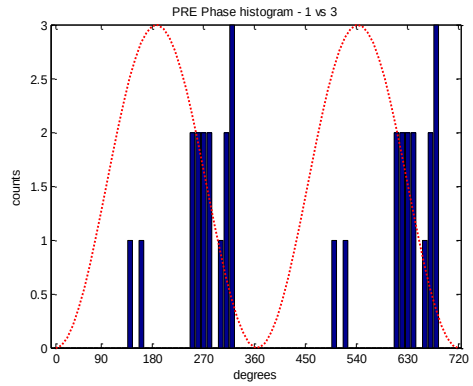

E3 SPONT

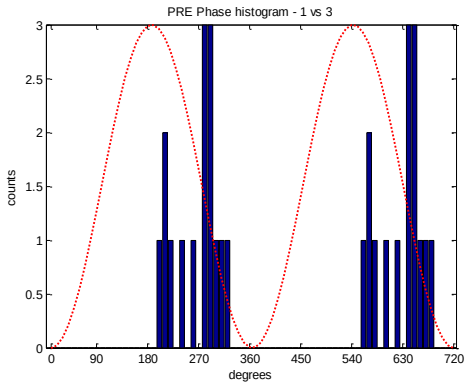

E2 STIM

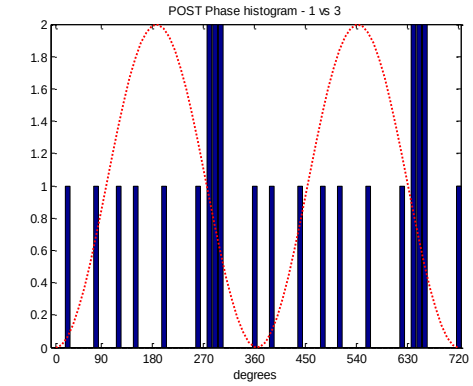

E3 STIM

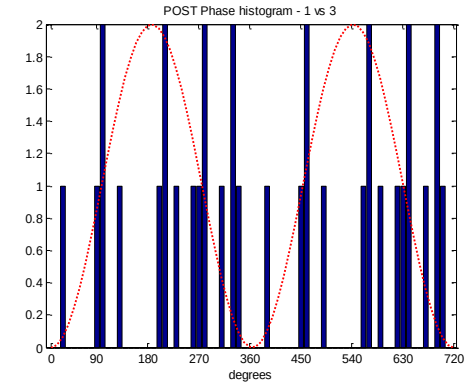

E4 SPONT

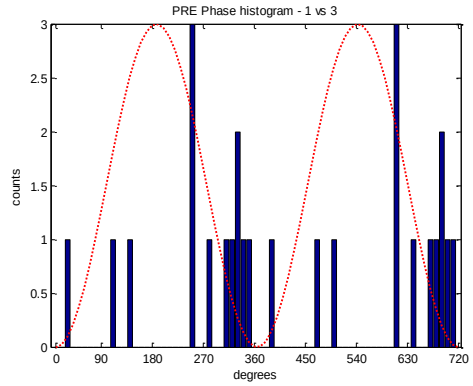

R1 SPONT

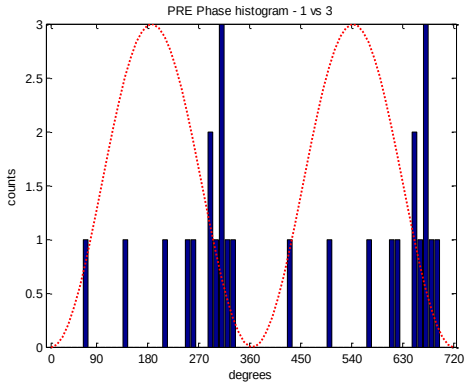

E4 STIM

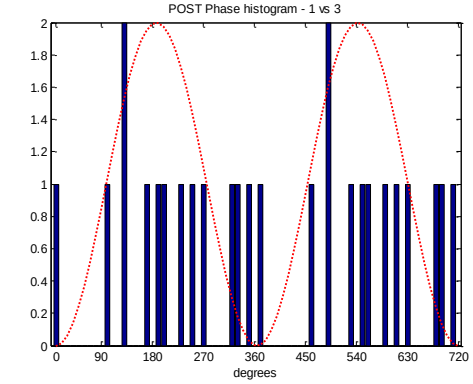

R1 STIM

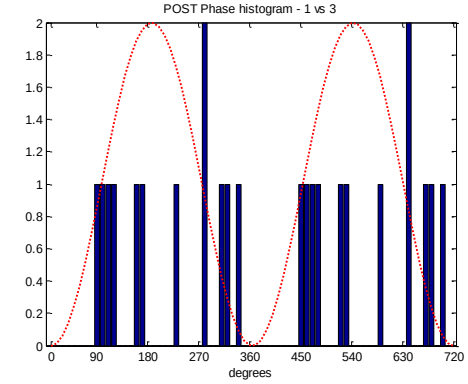

Figure 40: Phase histograms of 4Hz activity between left amygdala and left prefrontal cortex in all sessions (C1-C5-E1-E4-R1) for spontaneous and stimulus related epoch segments in Rat1. One full cycle shown twice (0-720 degrees).

Peaks in the phase histograms for the 4Hz activity between the left amygdala and the left prefrontal cortex show a negative shift from the cycle onset, suggesting that there is a certain level of phase relationship between the two areas in the domain of the 4Hz activity. To get a detailed insight, weighted average shift values were computed and compared in figure 41.

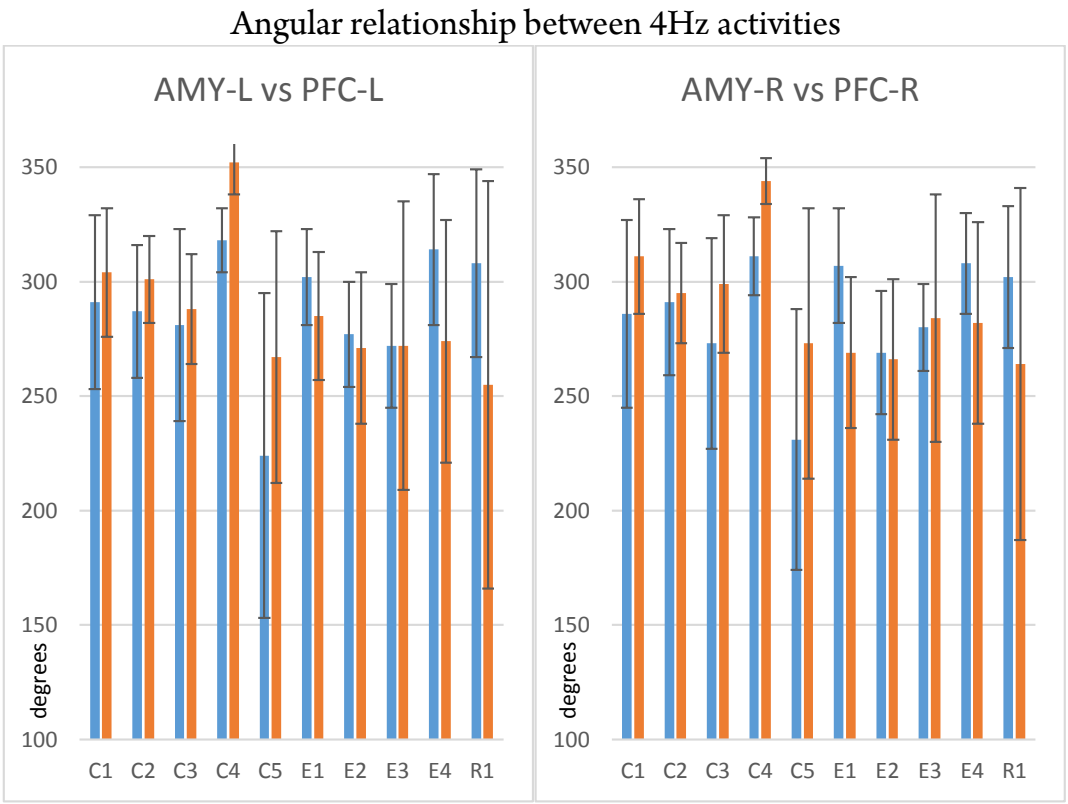

Figure 41: Cross-animal angular relationship between the 4Hz activities in ipsilateral amygdala and prefrontal cortex areas. Blue: spontaneous, orange: stimulus related segment. Bars indicate degrees ± standard error, n=400.

Results show a negative angular shift in the 4Hz activity synchronisation between both ipsilateral amydalar and prefronto- cortical regions. There is no significant difference in the shift between the two sides (AMY-L vs PFC-L spontaneous angle: 287.4±33.9, stimulus related angle: 286.9±40.6, while AMY-R vs PFC-R spontaneous angle: 285.8±31.7, stimulus related angle: 288.7±38.9).

Next we proceeded with the comparison of the theta oscillation between the amygdala and the prefrontal cortex (figure 42).

C1 SPONT

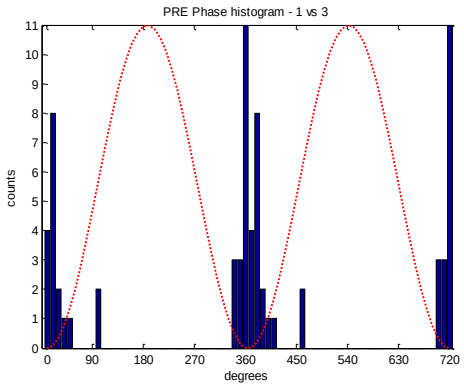

C2 SPONT

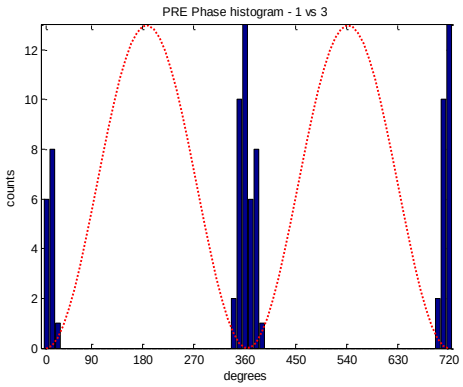

C1 STIM

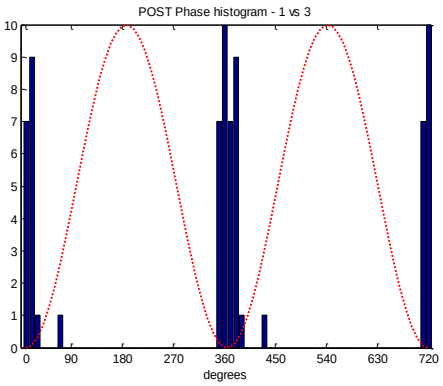

C2 STIM

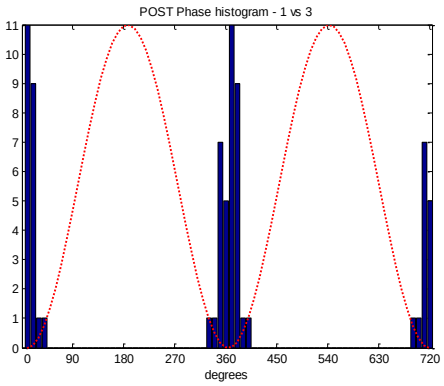

figure continued on next page

C3 SPONT

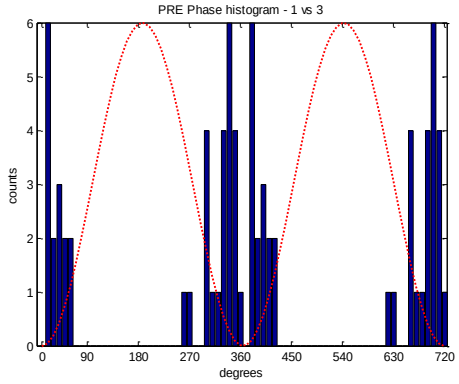

C4 SPONT

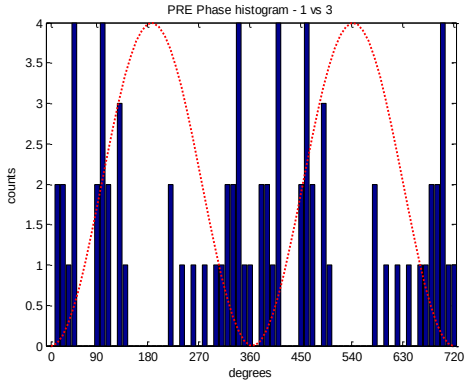

C3 STIM

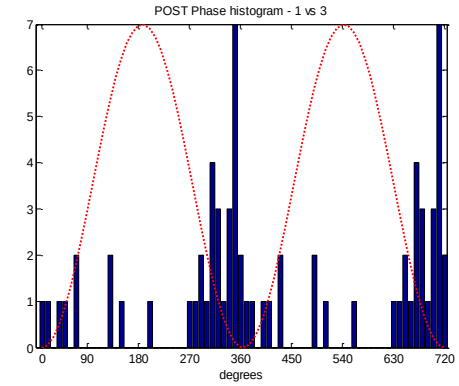

C4 STIM

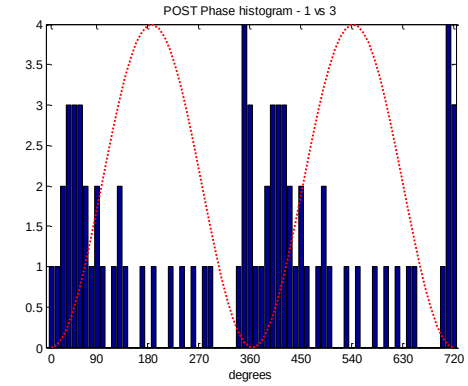

C5 SPONT

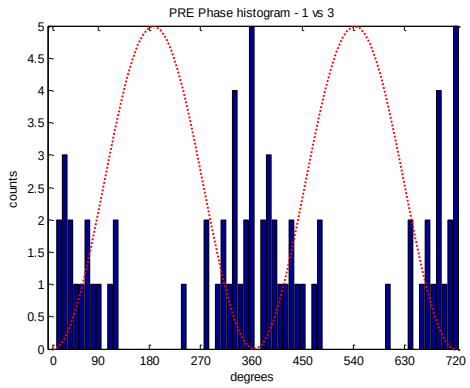

E1 SPONT

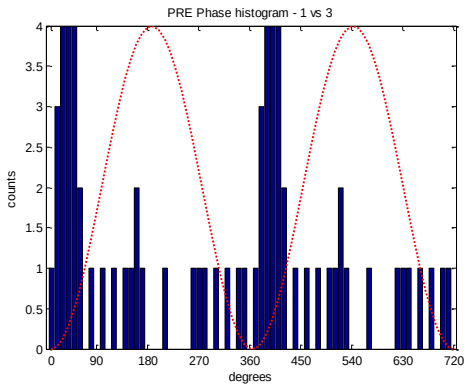

C5 STIM

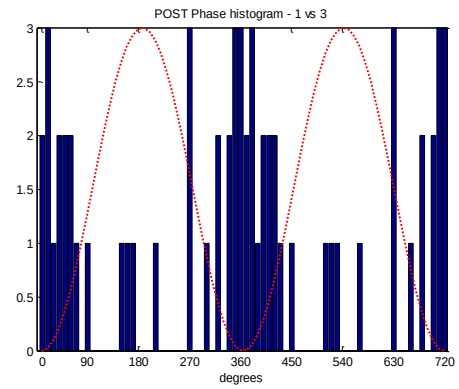

E1 STIM

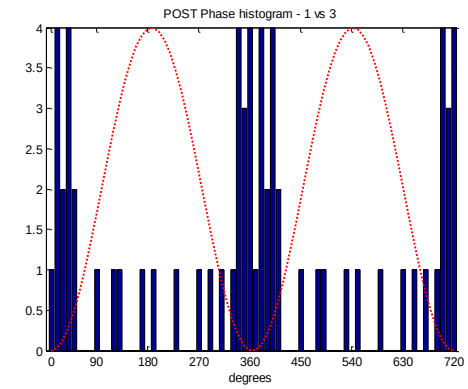

figure continued on next page

E2 SPONT

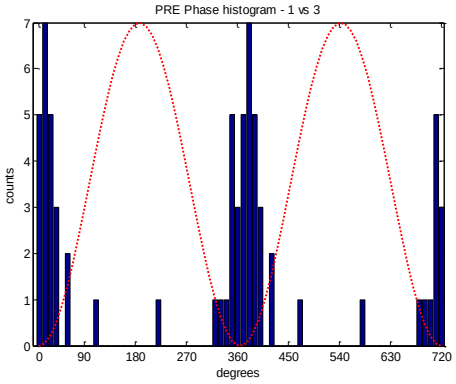

E3 SPONT

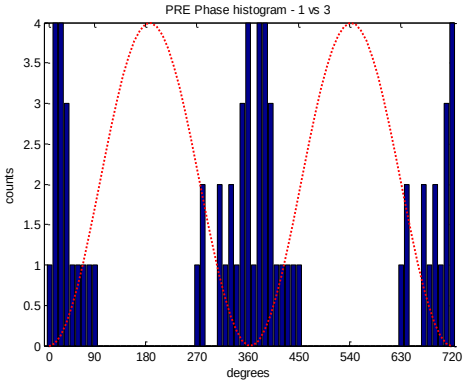

E2 STIM

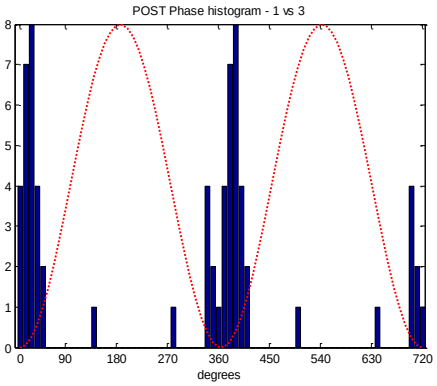

E3 STIM

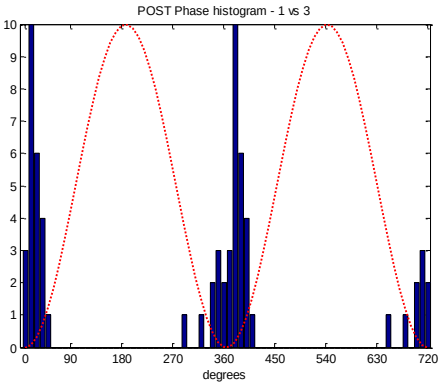

E4 SPONT

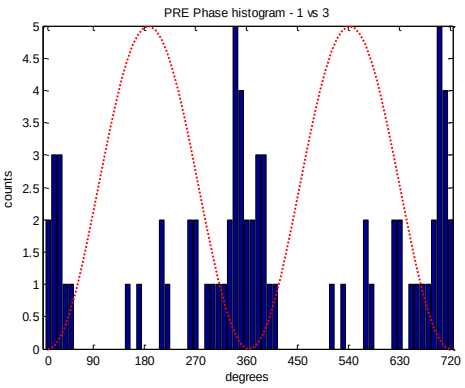

R1 SPONT

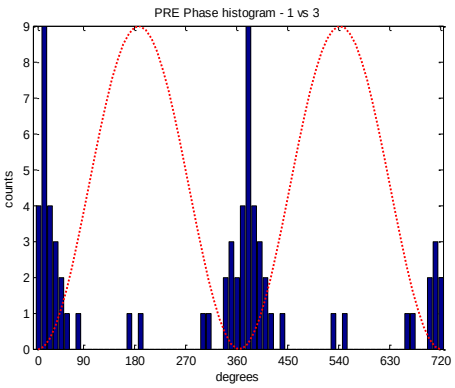

E4 STIM

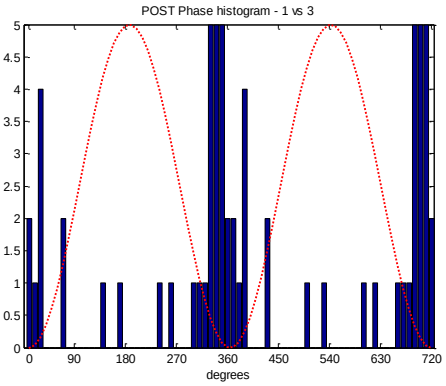

R1 STIM

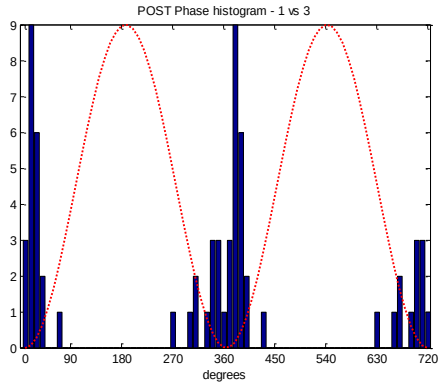

Figure 42: Phase histograms of theta activity between left amygdala and left prefrontal cortex in all sessions (C1-C5-E1-E4-R1) for spontaneous and stimulus related epoch segments in Rat1. One full cycle shown twice (0-720 degrees).

Peaks in the phase histograms for the theta activity between the left amygdala and the left prefrontal cortex are clearly linked to the cycle onset at 360 degrees, suggesting that there is an increased level of phase relationship between the two areas in the theta activity domain. Again, for a detailed insight, weighted average shift values were computed and compared in figure 43.

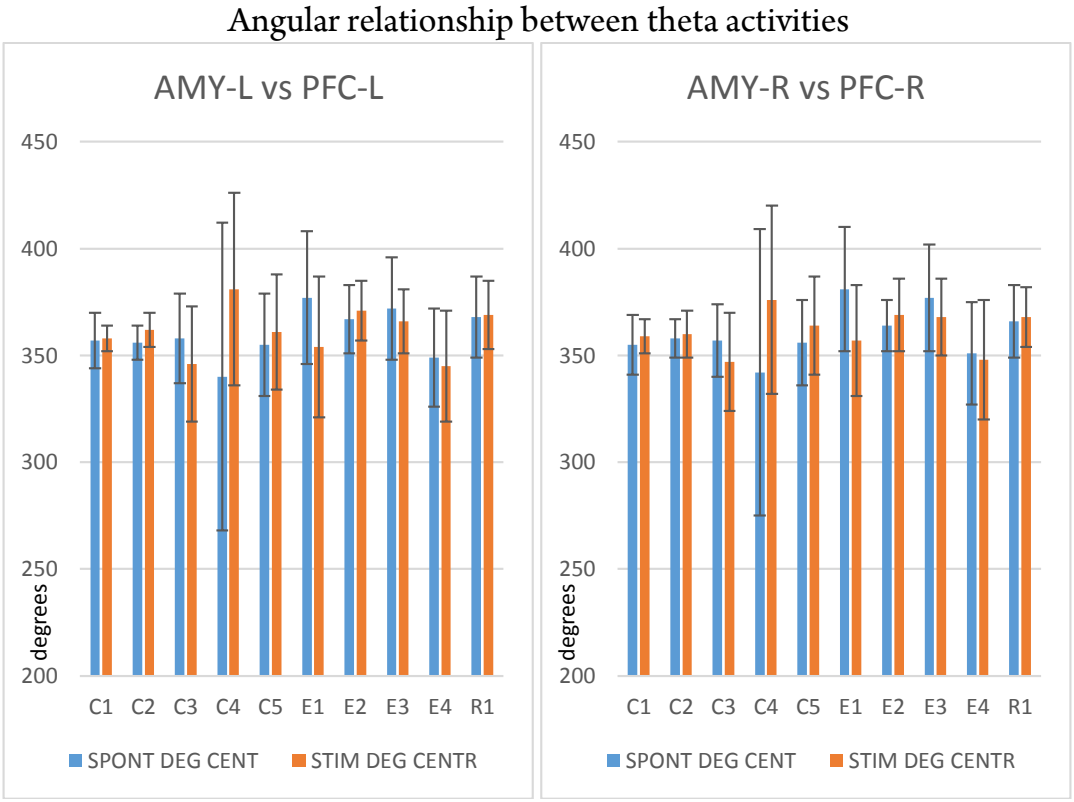

Figure 43: Cross-animal angular relationship between the theta activities in ipsilateral amygdala and prefrontal cortex areas. Blue: spontaneous, orange: stimulus related segment. Bars indicate degrees ± standard error, n=400.

Results show a clear angular preference in the theta activity synchronisation between both ipsilateral amydalar and prefronto- cortical regions around 360 degrees. There is no significant difference in the shift between the two sides (AMY-L vs PFC-L spontaneous angle: 359.9±25.1, stimulus related angle: 361.3±21.7, while AMY-R vs PFC-R spontaneous angle: 360.7±23.4, stimulus related angle: 361.6±21.2).

These data suggest that the theta oscillation is clearly phase locked to the cycle onset in both the prefrontal cortex and the amygdala, while there is a negative shift of around 74 degrees in the 4Hz activity synchronisation. There is a statistically significant difference between the two groups' angular shift in the phase-lock ($p<0.05$, $n=400$ sessions).

Last but not least, we need to examine whether there is phase relationship across the two frequency bands, the 4Hz activity and the theta oscillation (figure 44).

C1 4Hz vs theta within AMY-L, SPONT

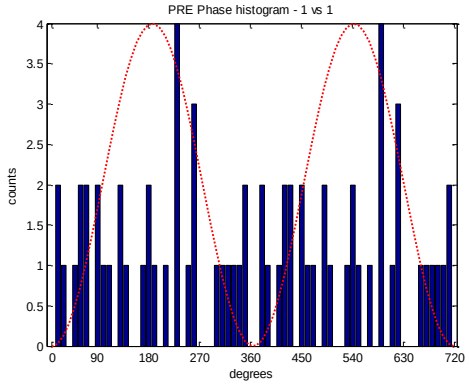

C1 4Hz vs theta within AMY-L, STIM

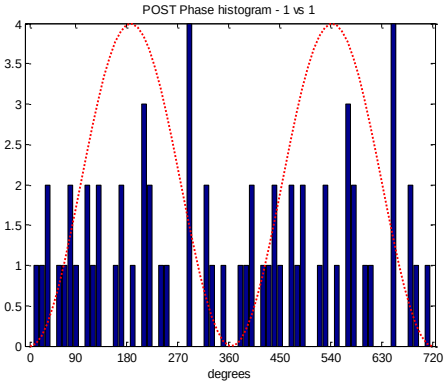

C5 4Hz vs theta within AMY-L, SPONT

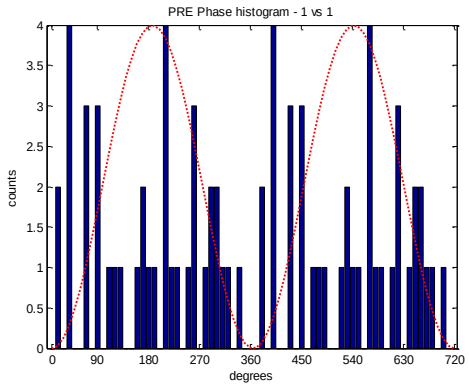

C5 4Hz vs theta within AMY-L, STIM

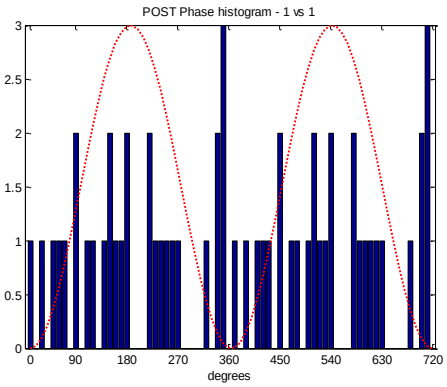

E1 4Hz vs theta within AMY-L, SPONT

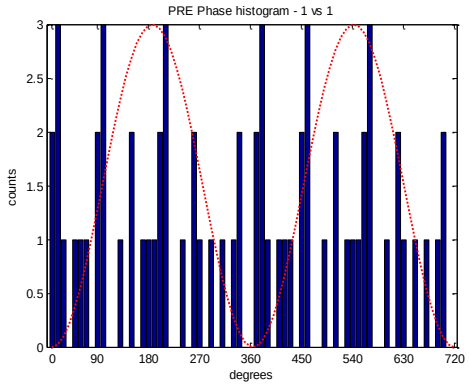

E1 4Hz vs theta within AMY-L, STIM

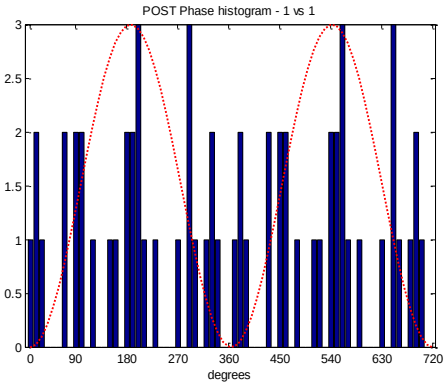

figure continued on next page

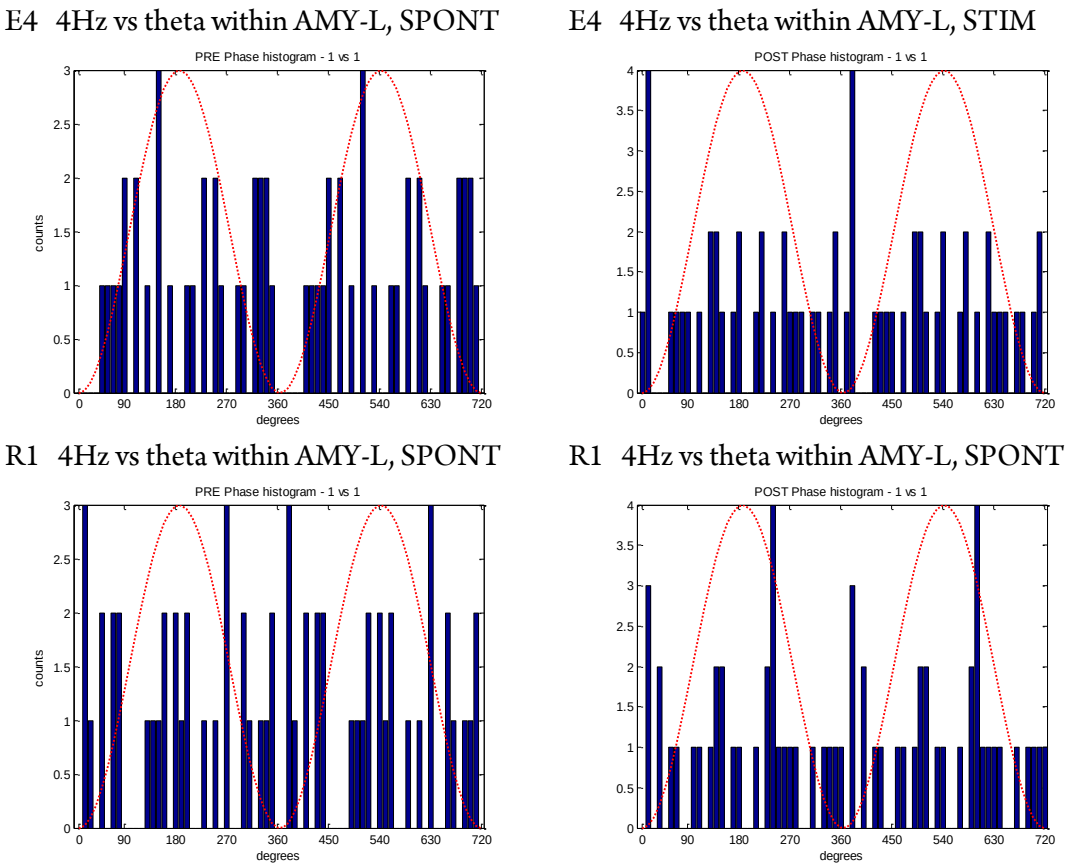

Figure 44: Phase histograms of 4Hz vs theta activity within the left amygdala in selected sessions (C1,C5,E1,E4,R1) for spontaneous and stimulus related epoch segments in Rat1. One full cycle shown twice (0-720 degrees).

These results show no phase relationship between the 4Hz activity and the theta oscillation when computed within the left amygdala, and the same analysis shows the same results for the right amygdala as well.

In the next step we take the same actions for the prefrontal cortex (figure 45).

C1 4Hz vs theta within PFC-L, SPONT

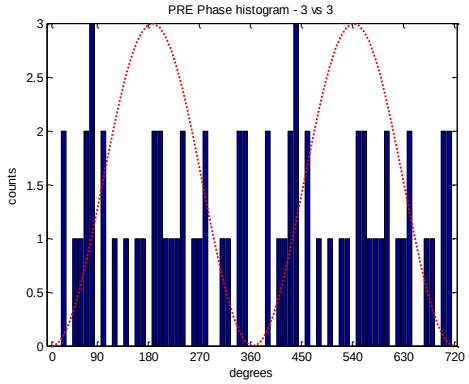

C1 4Hz vs theta within PFC-L, STIM

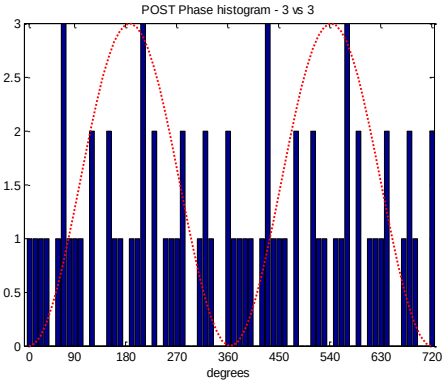

C5 4Hz vs theta within PFC-L, SPONT

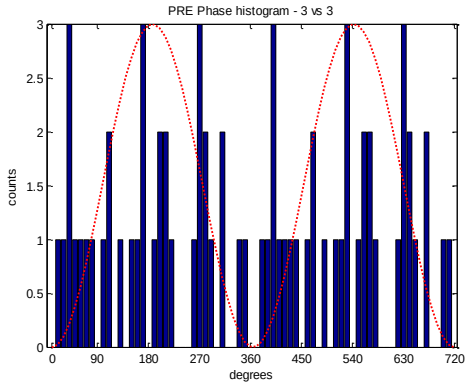

C5 4Hz vs theta within PFC-L, STIM

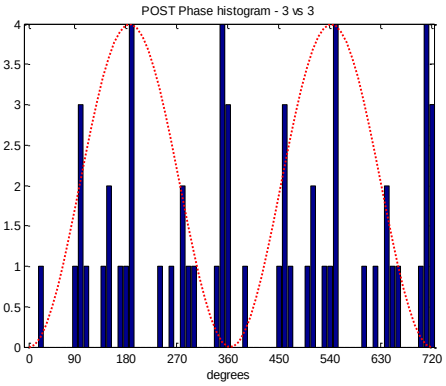

E1 4Hz vs theta within PFC-L, SPONT

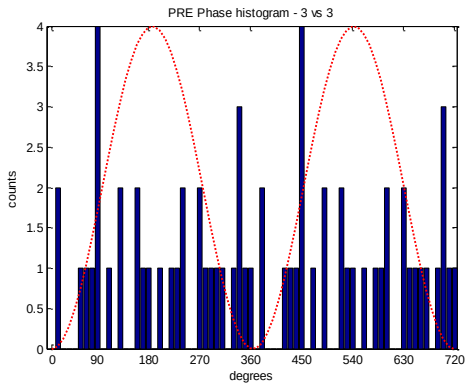

E1 4Hz vs theta within PFC-L, STIM

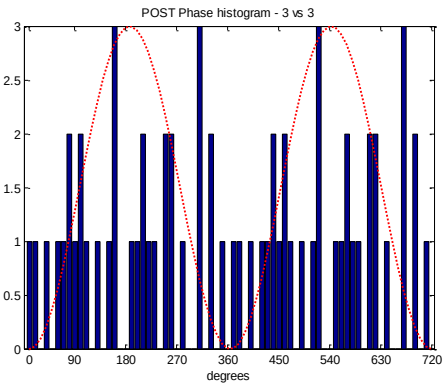

E4 4Hz vs theta within PFC-L, SPONT

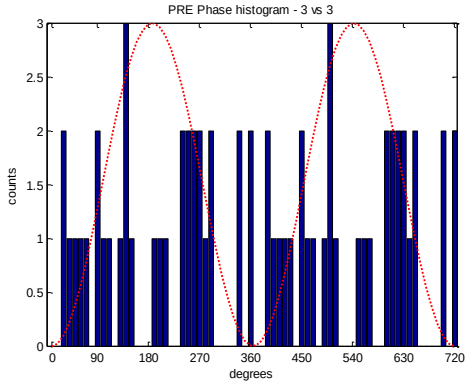

E4 4Hz vs theta within PFC-L, STIM

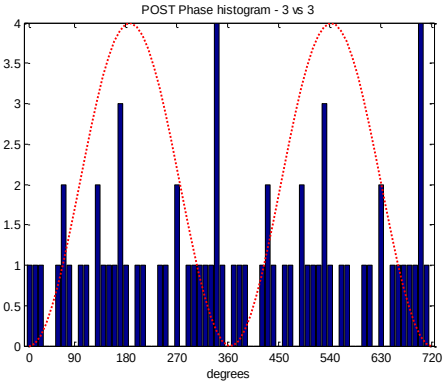

figure continued on next page

R1 4Hz vs theta within PFC-L, SPONT

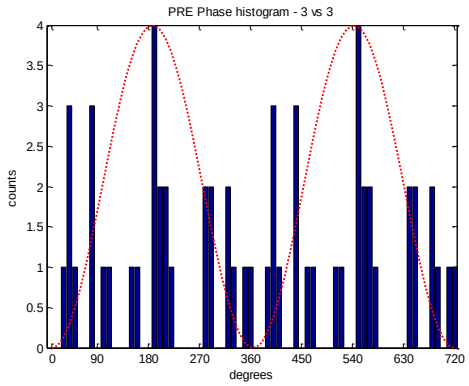

R1 4Hz vs theta within PFC-L, STIM

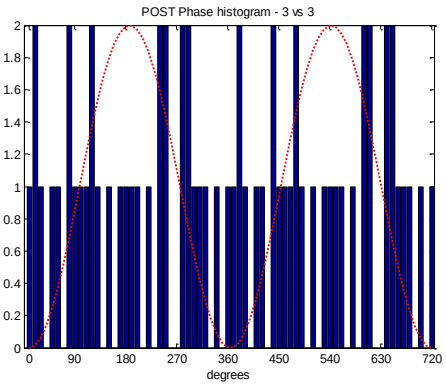

Figure 45: Phase histograms of 4Hz vs theta activity within the left prefrontal cortex in selected sessions (C1,C5,E1,E4,R1) for spontaneous and stimulus related epoch segments in Rat1. One full cycle shown twice (0-720 degrees).

Again, the results show no phase relationship between the 4Hz activity and the theta oscillation within the left prefrontal cortex either, and when calculated for the right prefrontal cortex, we get the same conclusion.

Finally, we need to assess the phase relationship between the two oscillations across the targeted brain regions, by performing the analysis looking for phase synchrony between the amygdala 4Hz activity and the prefrontal theta oscillation (figure 46).

C1 4Hz vs theta, AMY-L vs PFC-L, SPONT

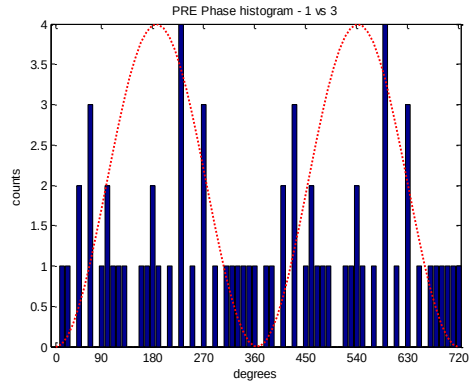

C1 4Hz vs theta, AMY-L vs PFC-L, STIM

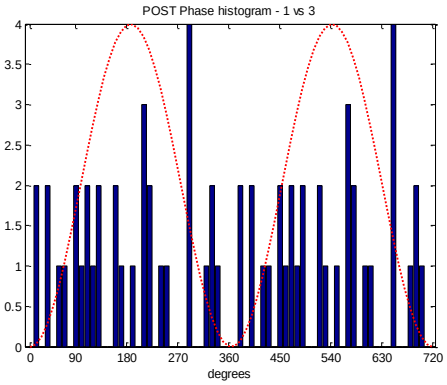

C5 4Hz vs theta, AMY-L vs PFC-L, SPONT

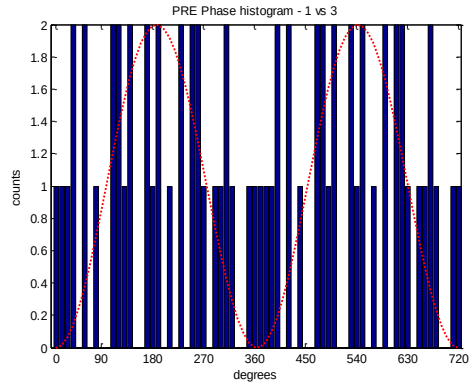

C5 4Hz vs theta, AMY-L vs PFC-L, STIM

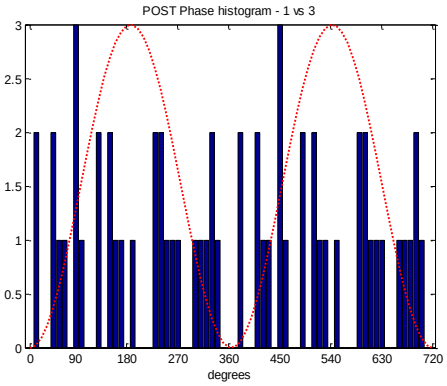

E1 4Hz vs theta, AMY-L vs PFC-L, SPONT

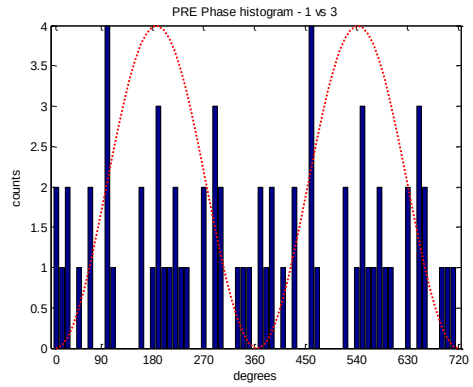

E1 4Hz vs theta, AMY-L vs PFC-L, STIM

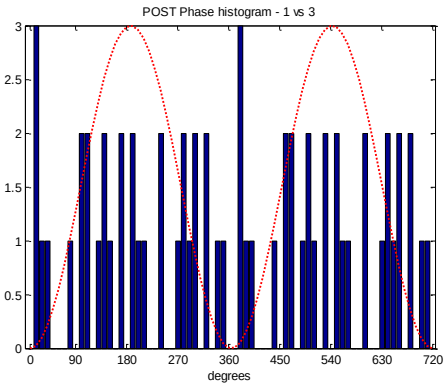

E4 4Hz vs theta, AMY-L vs PFC-L, SPONT

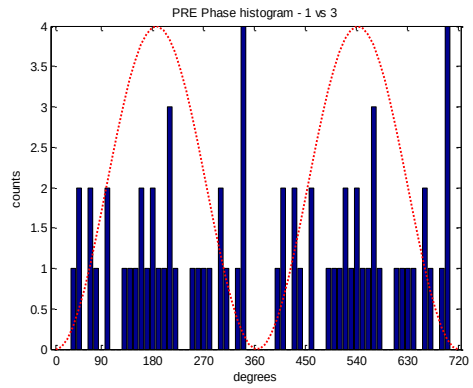

E4 4Hz vs theta, AMY-L vs PFC-L, STIM

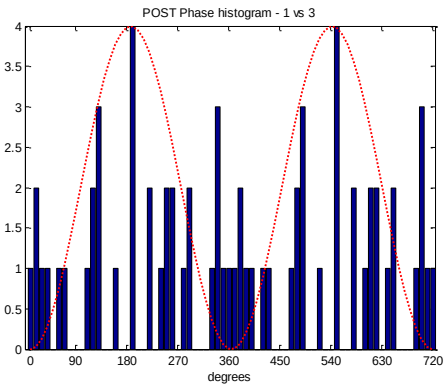

figure continued on next page

R1 4Hz vs theta, AMY-L vs PFC-L, SPONT

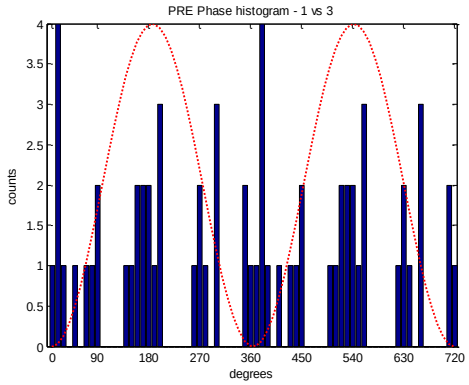

R1 4Hz vs theta, AMY-L vs PFC-L, STIM

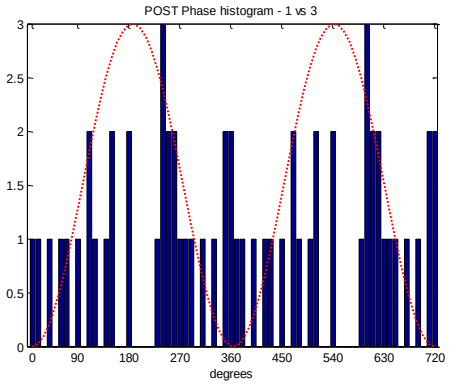

Figure 46: Phase histograms of 4Hz vs theta activity comparing left amygdala and left prefrontal cortex in selected sessions (C1,C5,E1,E4,R1) for spontaneous and stimulus related epoch segments in Rat1. One full cycle shown twice (0-720 degrees).

These results suggest that there is no phase relationship between the 4Hz activity and the theta oscillation when the left amygdala and the left prefrontal cortex are compared, and this result holds for the contralateral side as well.

Cross power spectral density analysis

Phase histograms revealed the phase relationship within the distinct frequency regions in the domain of the 4Hz and theta activity. What the histograms fail to reveal though, is the power or magnitude of relationship between the oscillations. This is important, because phase relationship analysis does not reflect power, and although it exposes the angular characteristics within the cycles of the oscillation, we are still unaware of 1) how this is reflected in the epochs instantaneously, and 2) what the magnitude is as far as cross frequency performance is concerned.

CPSD, or cross power spectral density analysis was designed to provide these crucial pieces of information by revealing coherent energy transfer between frequencies, while also delivering high temporal resolution and statistically significant results at a given confidence level. Thus, CPSD maps were computed for all epochs and animals to elucidate spectral transfer functions in our experimental settings (figures 47-51).

Conditioning Day 1

Conditioning Day 2

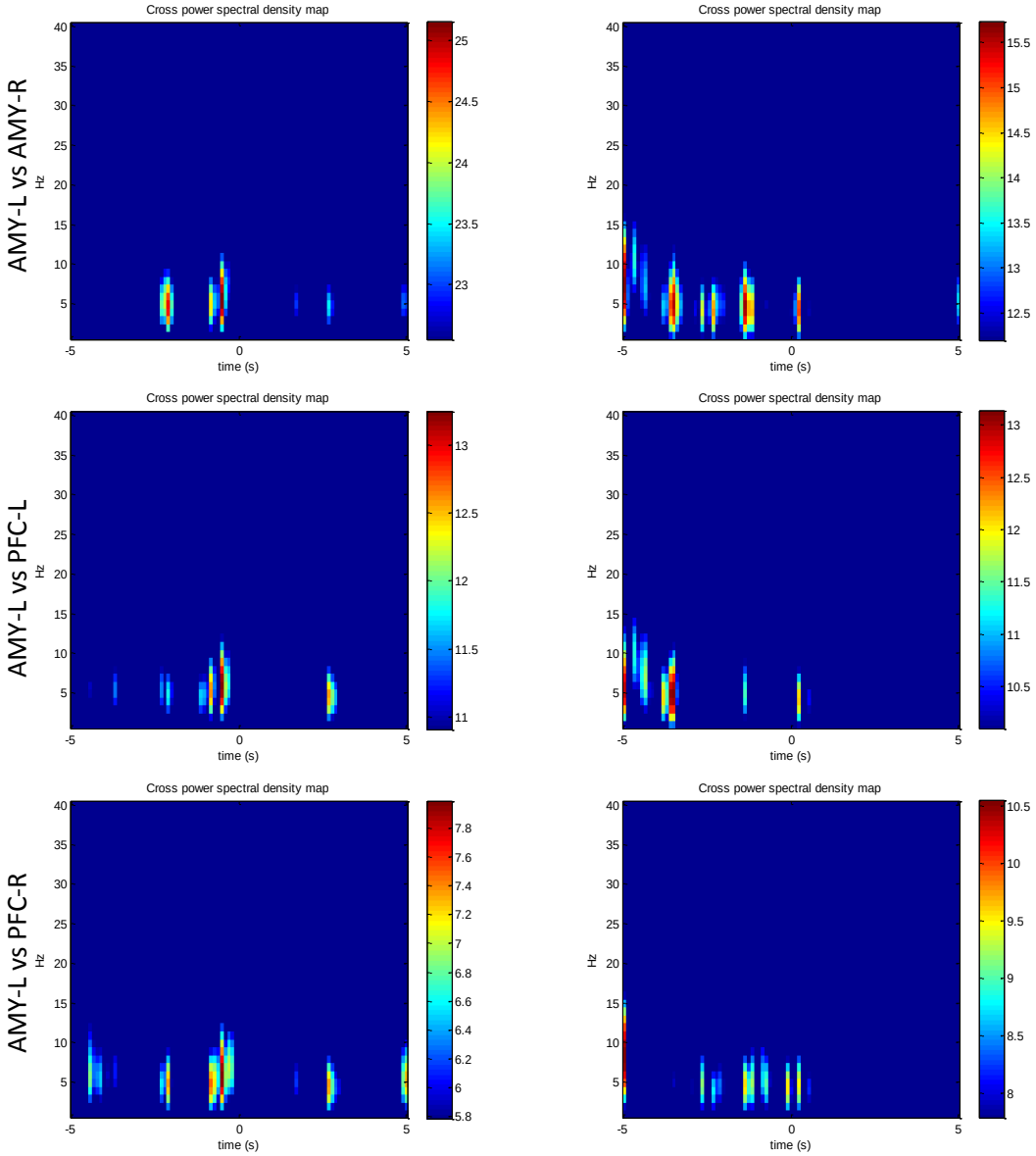

figure continued on next page

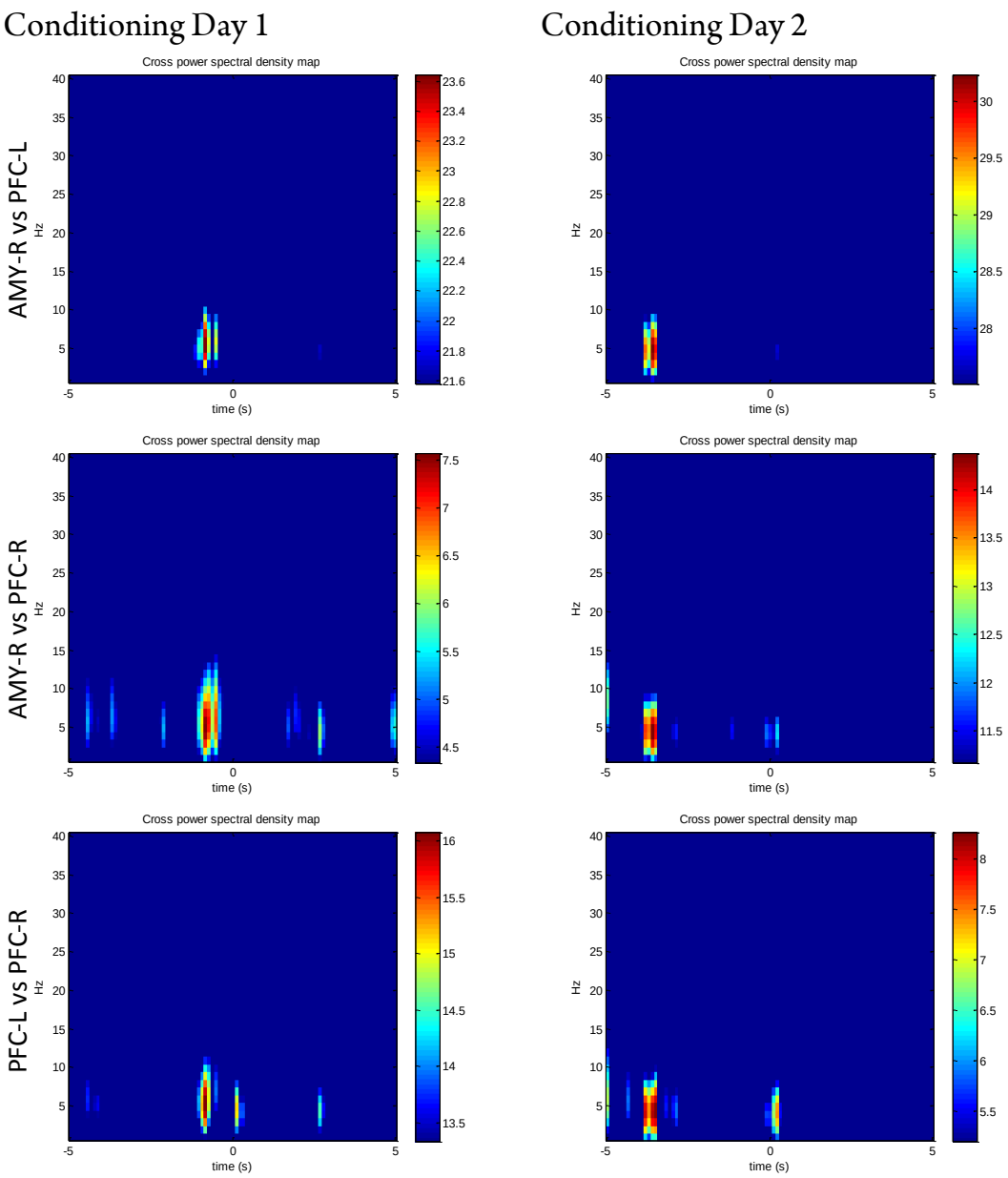

Figure 47: Cross power spectral density maps comparing all area-pairs. Horizontal axis: time (s). Vertical axis: frequency (Hz). Colours ranging from blue (low) to red (high) represent power density (dB/Hz). Zero time point indicates tone stimulus onset.

Conditioning Day 3

Conditioning Day 4

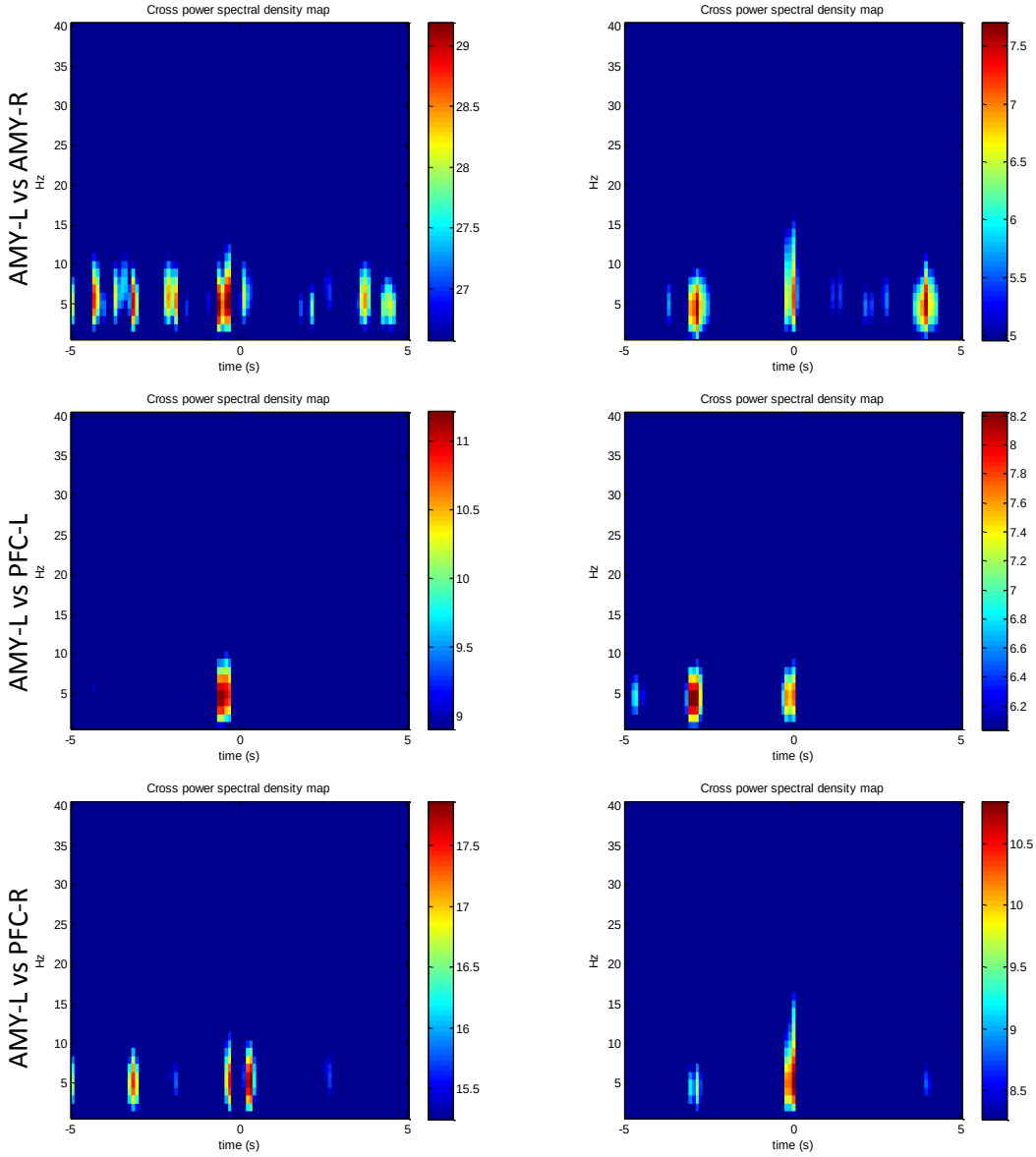

figure continued on next page

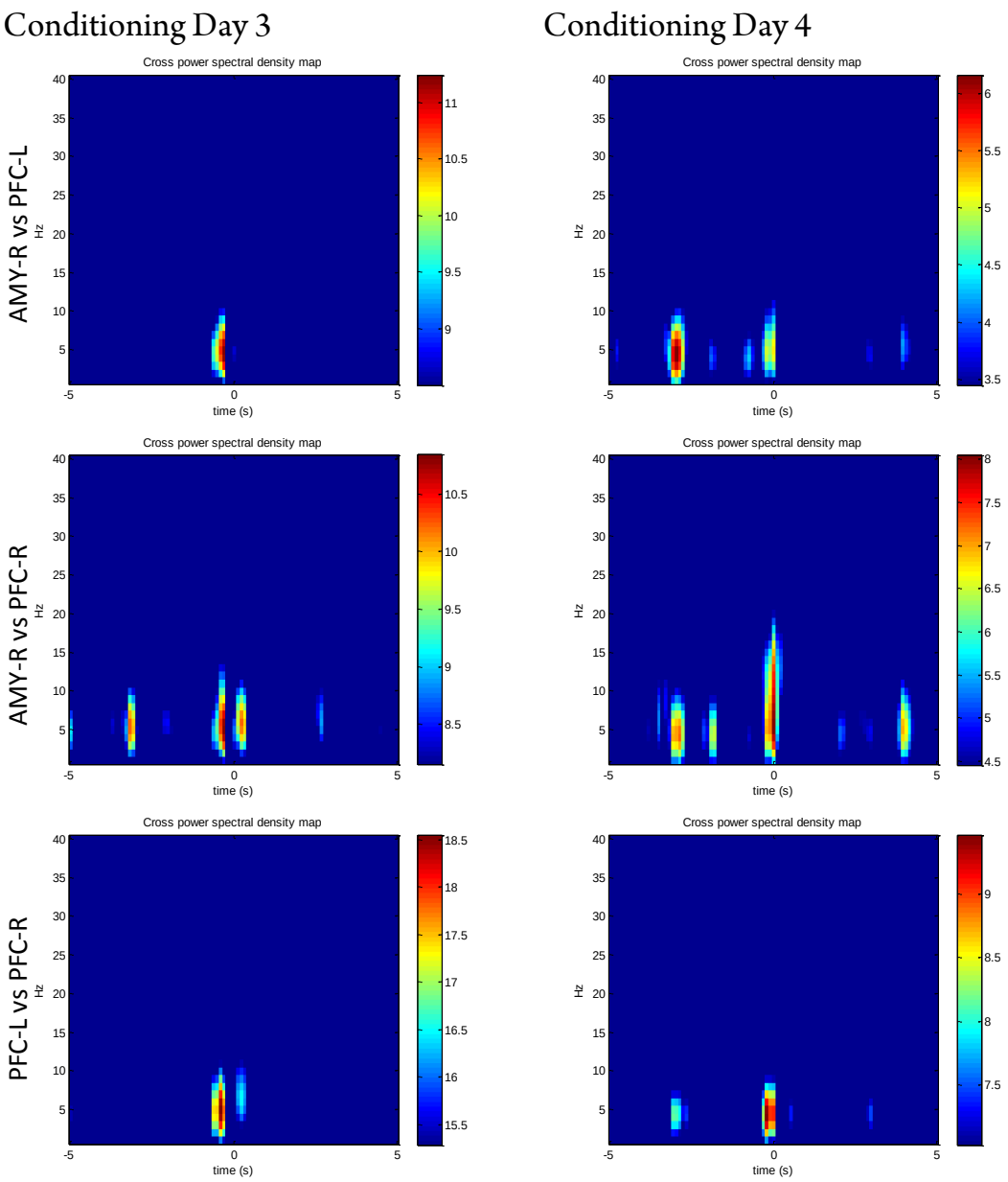

Figure 48: Cross power spectral density maps comparing all area-pairs. Horizontal axis: time (s). Vertical axis: frequency (Hz). Colours ranging from blue (low) to red (high) represent power density (dB/Hz). Zero time point indicates tone stimulus onset.

Conditioning Day 5

Extinction Day 1

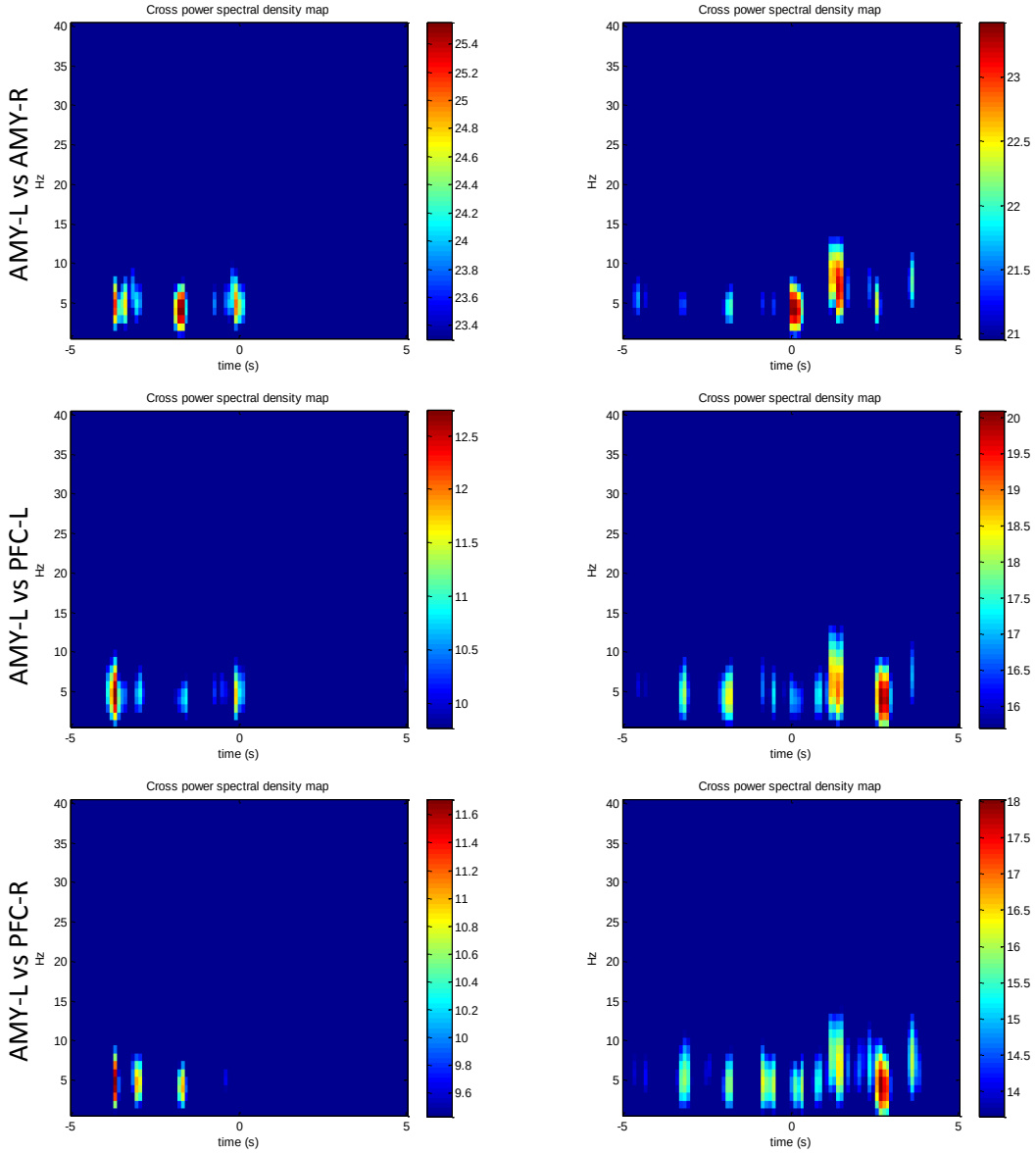

figure continued on next page

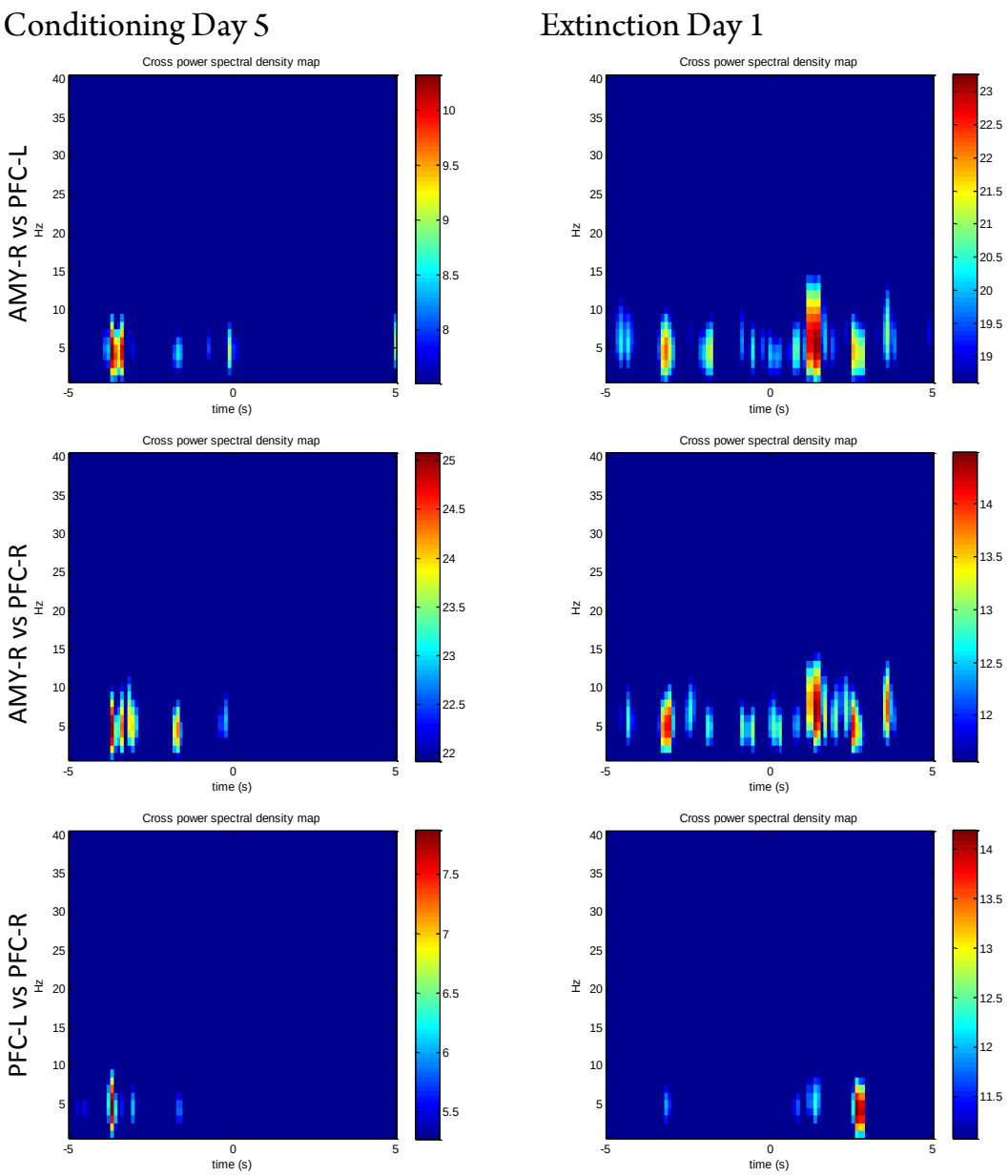

Figure 49: Cross power spectral density maps comparing all area-pairs. Horizontal axis: time (s). Vertical axis: frequency (Hz). Colours ranging from blue (low) to red (high) represent power density (dB/Hz). Zero time point indicates tone stimulus onset.

Extinction Day 2

Extinction Day 3

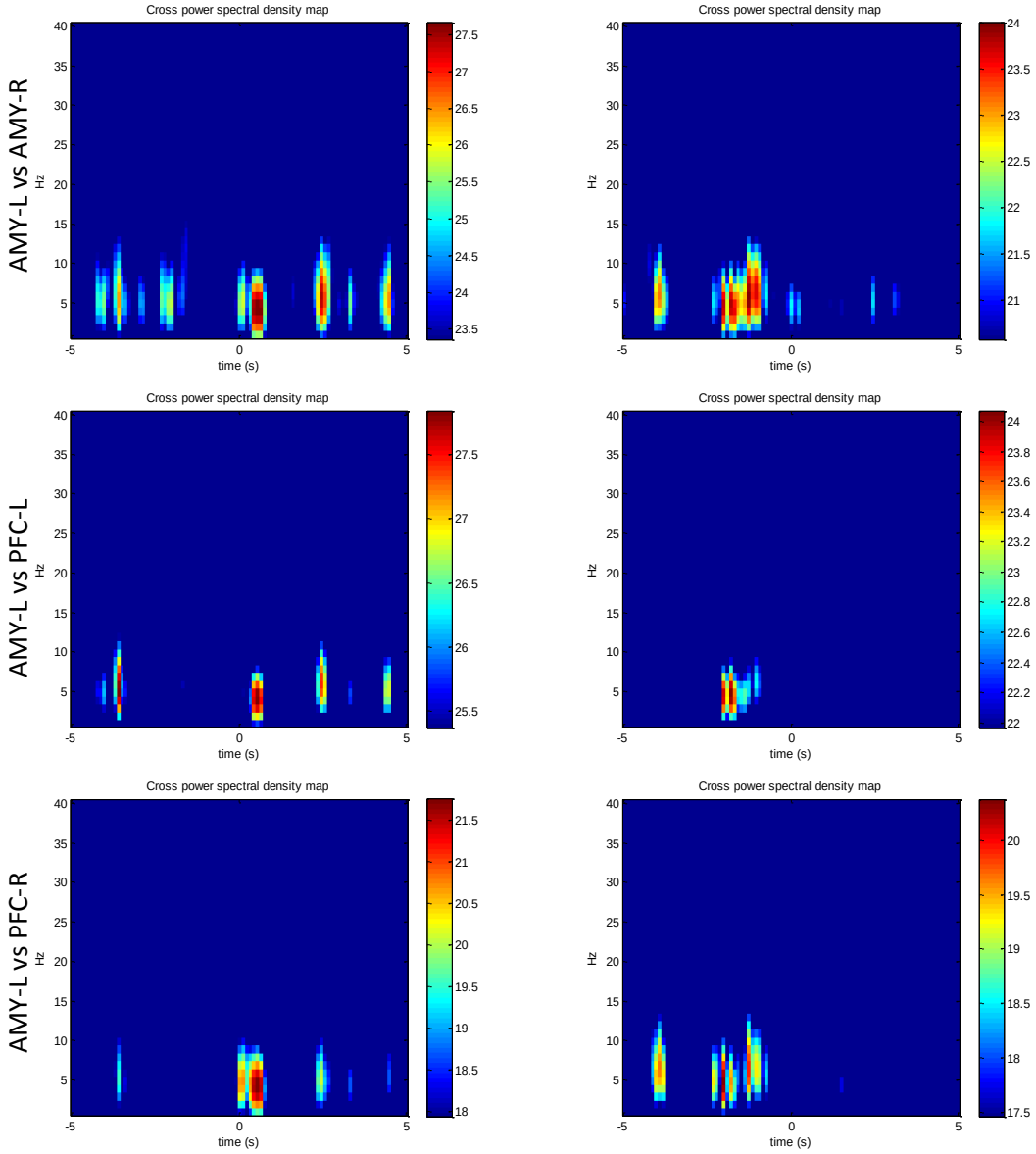

figure continued on next page

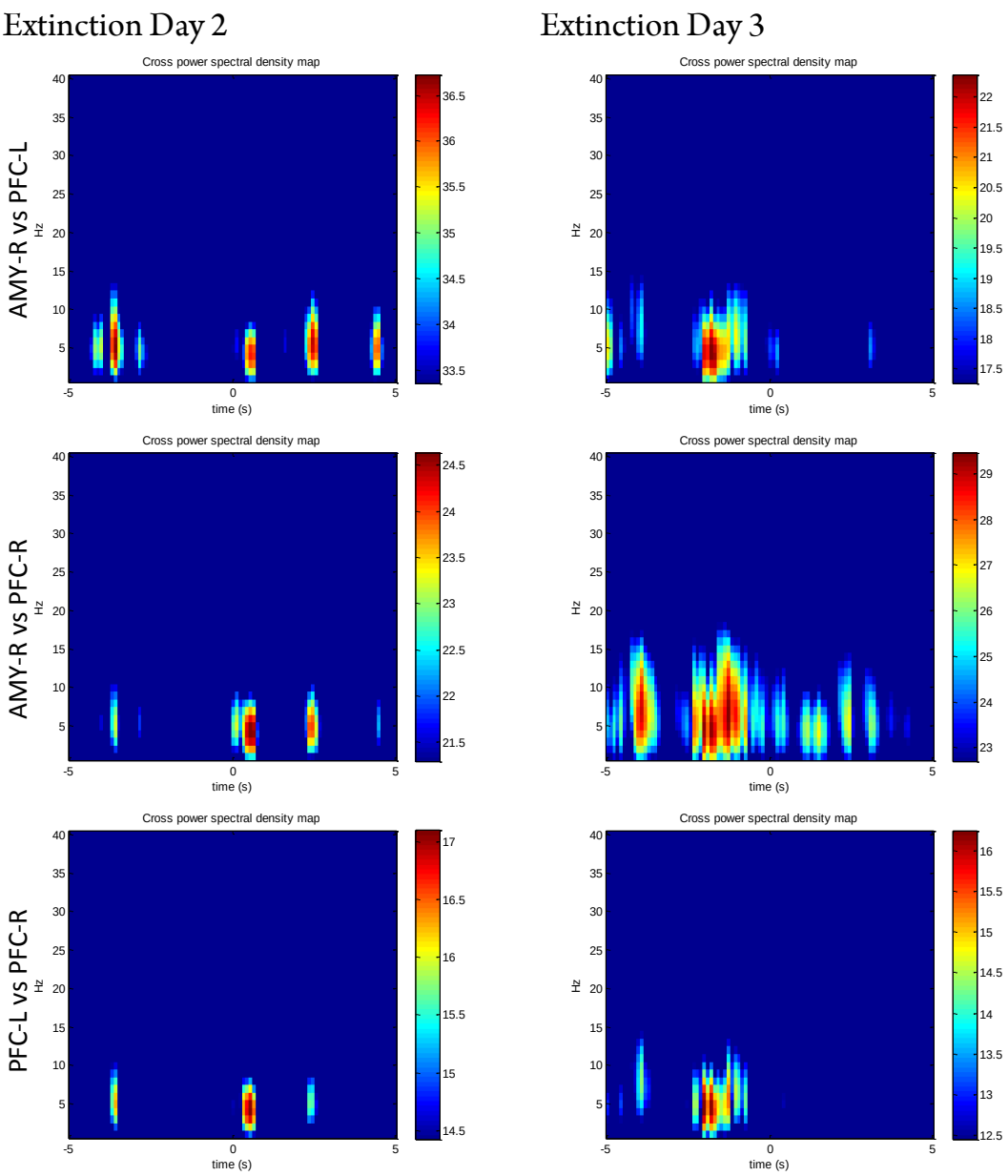

Figure 50: Cross power spectral density maps comparing all area-pairs. Horizontal axis: time (s). Vertical axis: frequency (Hz). Colours ranging from blue (low) to red (high) represent power density (dB/Hz). Zero time point indicates tone stimulus onset.

Extinction Day 4

Reacquisition Day 1

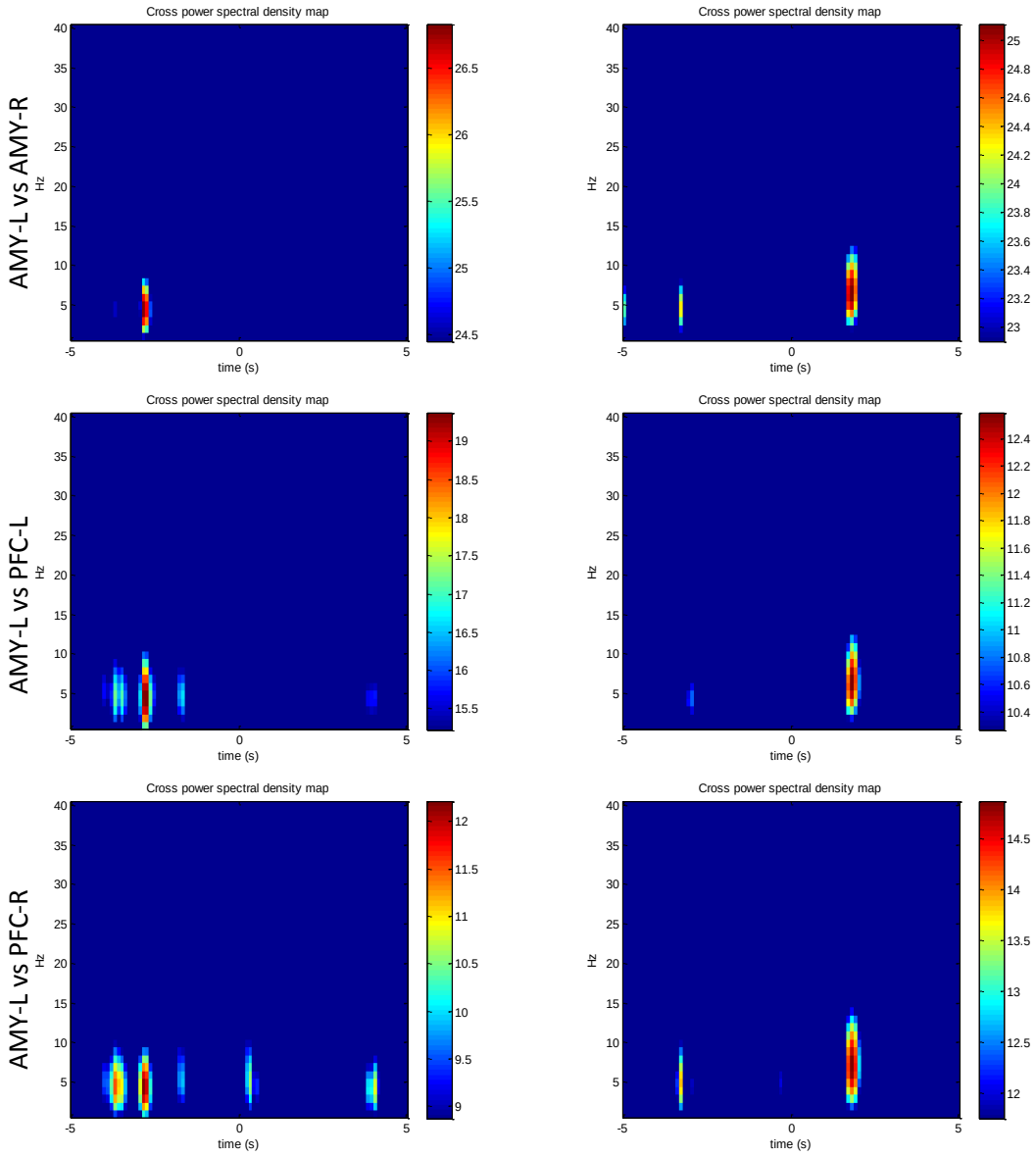

figure continued on next page

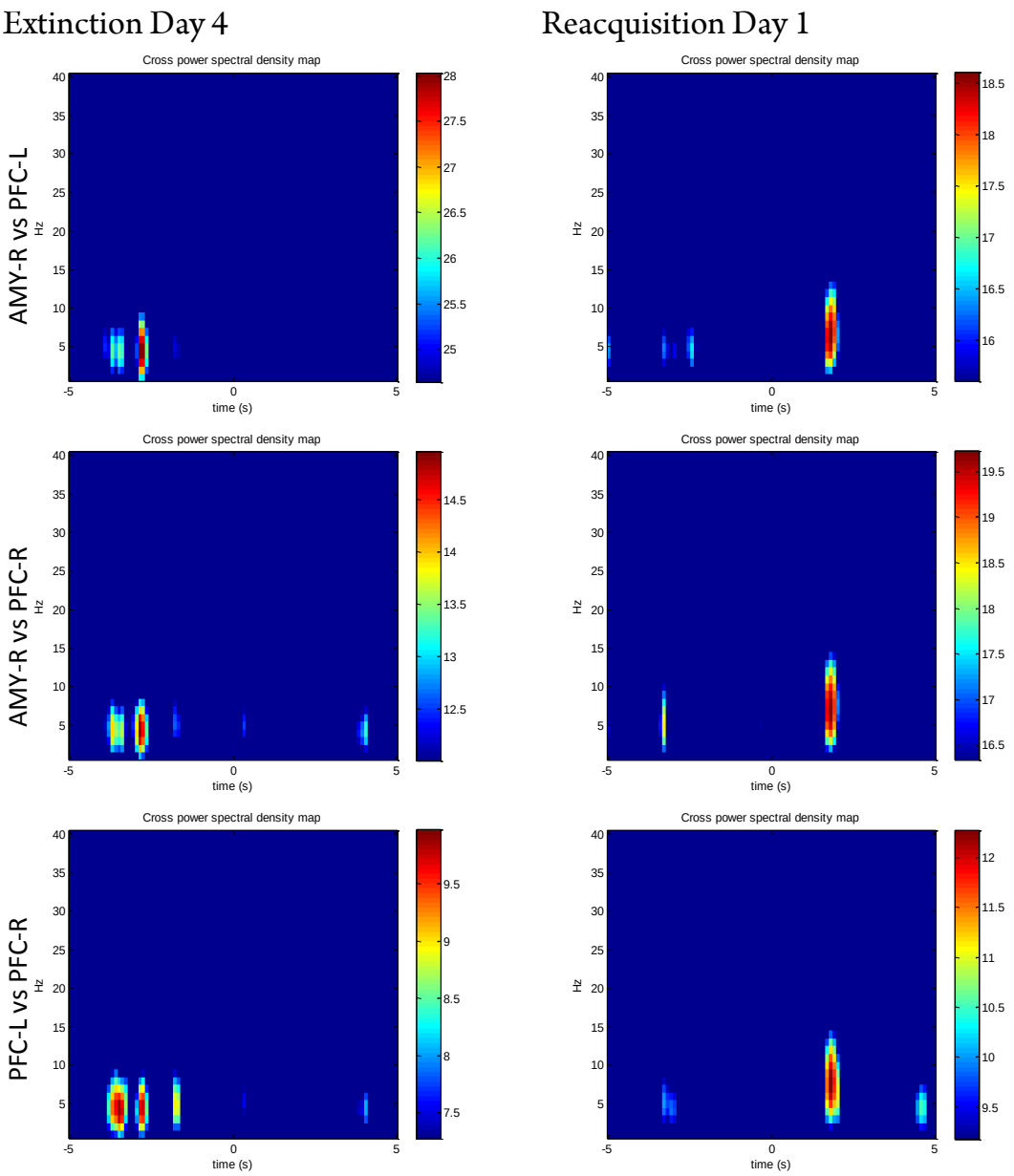

Figure 51: Cross power spectral density maps comparing all area-pairs. Horizontal axis: time (s). Vertical axis: frequency (Hz). Colours ranging from blue (low) to red (high) represent power density (dB/Hz). Zero time point indicates tone stimulus onset.

Cross power spectral density results reveal only one statistically significant frequency ($f=4.17\pm0.27$, $p<0.05$, $n=400$ sessions). This 4Hz activity is present consistently in all CPSD maps. These results suggest that there is a coherent, instantaneous cross spectral energy transition among amygdala and prefrontal cortical regions at this 4Hz frequency. It is also revealed, that in the majority of cases the cross spectral power of other frequencies (including theta) is not significant.

To directly compare the CPSD performance of spontaneous and stimulus related epoch segments, the integrated power of the 4Hz activity has also been calculated (figure 52).

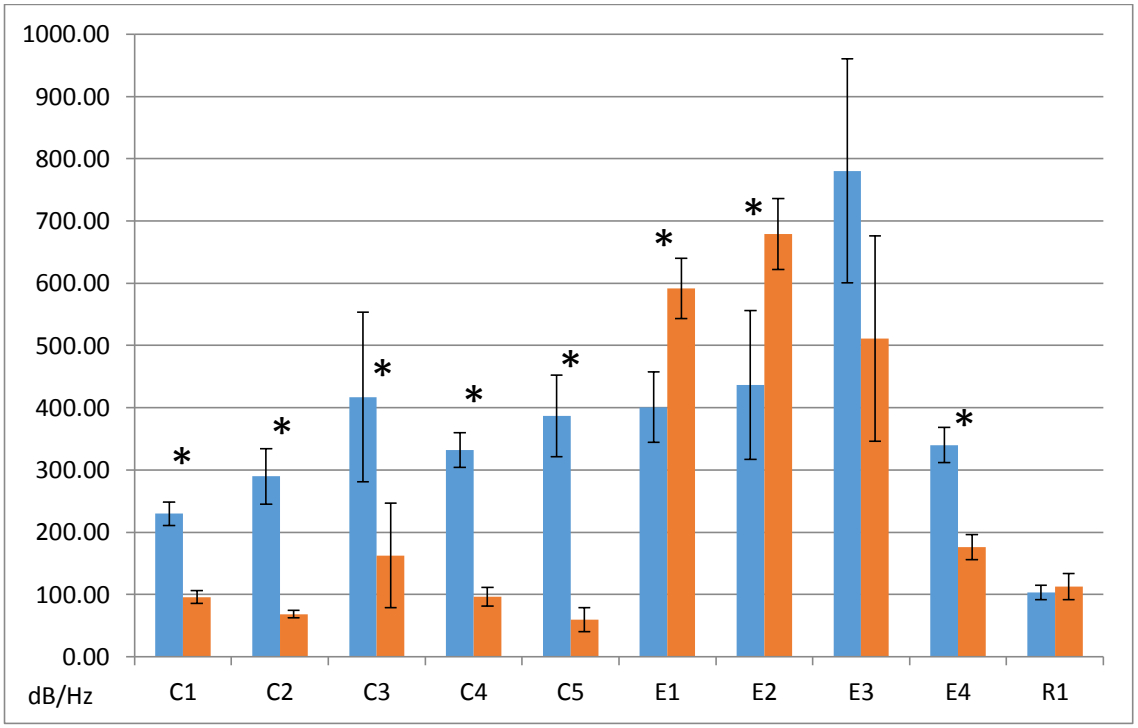

Figure 52: Cross-animal integrated power of 4Hz cross power spectral density. Horizontal axis: experimental sessions (conditioning, extinction, reacquisition). Vertical axis: integrated power (dB/Hz). Blue: spontaneous, red: stimulus related epoch segment. * indicates significant difference ($p<0.05$, $n=400$).

Integrated CPSD values across all animals and experimental sessions show a consistent and significant drop in the cross spectral power within the 4Hz activity domain throughout the conditioning phase (C1-C5) when the spontaneous and stimulus related epoch segments are compared. It then turns around and on the first two days of the extinction phase there is a significant increase in the cross-4Hz power following the tone (CS) stimulus. This increase, again, has a turning point and becomes a significant decrease by the fourth day. In the reacquisition session the power levels remain equally low, and there is no significant difference between the pre- and peri-stimulus segments. These results suggest a direct connection between the stages of the experiment (conditioning, extinction, and reacquisition) and the power of the 4Hz activity across both amygdala and prefrontal regions.

Discussion

We have successfully designed, fabricated and tested a novel miniature microdrive, to be able to increase the number of implantable recording devices. We designed and conducted the classical Pavlovian reward conditioning experiments successfully and managed to measure distinctive differences in correlation values and spectral properties, which revealed two distinct activities, one around 4Hz and another in the theta range of 5-9 Hz. The distribution of oscillation peaks revealed significant drop in the stimulus-related epoch segments, which supported the primary correlation results. Phase histograms demonstrated a significant difference in the phase-locking mechanism – while the 4Hz activity showed negative angular shift of about 74 degrees, the theta was mostly locked to the cycle onset. Cross power spectral density analysis revealed consistent presence in the 4Hz domain only.

Correlation of wideband pre- and peri-stimulus epochs

Judging by the experimental procedures, simplification and insistence on controlled parameters turned out to be more than beneficial as they managed to keep variables and uncontainable degrees of freedom at a minimum level. No matter how informative some analytical methods are, the examination of the electrophysiological correlates in a behaving animal can be quite challenging. All throughout the series of correlation maps it is remarkable that the correlation between contralateral central amygdaloid nuclei is consistently elevated. This consistency can be seen through the conditioning phase, the extinction phase, and in the reacquisition phase as well. Comparing the values of correlation through the conditioning phase between pre-tone and peri-tone segments, we get a decreased synchrony in the peri-tone segment. The difference might be small, but it should be taken into account, that the animal is awake, its sensory systems are all engaged. Still, an increased sample size could possibly further increase the differences. When the same values are computed for all possible site-pairs within the rectangle of both central amygdalae and both medial prefrontal cortical regions the results are even more appealing. The comparison of correlation values demonstrates a decrease in the synchrony between all pairs in the peri-tone segment versus the pre-tone segment, meaning that the tone stimulus induces desynchronization on all channel-pairs. To elucidate whether this phenomenon can be attributed to the conditioned tone stimulus we need to examine the

processes during the presentation of the neutral click stimulus. It is discernible that no similar changes can be identified, correlation values in the pre-click segment are similar to those in the peri-click segment in all pairs. The neutral click stimulus does not induce desynchronization, there is no indication of a disintegrating mechanism.

If we compute the cumulated correlation averages (averages of all pair-correlations) we find a trend demonstrating that the average correlation in the peri-tone segment is lower than any other average (pre-tone, pre-click and peri-click). These results suggest that there is indeed a mechanism that desynchronizes all participating areas after the occurrence of the conditioned (tone) stimulus, and does not react to the neutral (click) stimulus in the same manner.

The second phase of the experiment was the extinction where neither the conditioned, nor the neutral stimulus was followed by a food reward. The calculation of correlation pairs reveal a change in the values. The opposite effect can be observed, this time almost all peri-tone segments lose the significant desynchronization pattern, and an increased variation appeared that might have shifted the values. The conditioning phase was a learning process, but in the extinction phase expectancy does not meet real outcome, which might induce increased but gradually degrading concentration and expectation. The neutral (click) stimuli does not show differences in the paired correlations, meaning that the above depicted phenomenon can indeed be attributed to the conditioned (tone) stimulus and the lack of food reward.

Cumulated averages appear to reinforce this notion, as the peri-tone correlation is remarkably higher than it was for the conditioning phase. Pre-tone, pre-click and peri-click correlations do not show notable differences.

The third phase of the experiment was the reacquisition which, again show immensely exciting results. Correlations, once again, have lower values following the conditioned stimulus for all site-pairs, meaning that the reappearance of the food reward resulted in decreased synchrony of the peri-tone period while pre-tone segments remained elevated. The neutral (click) stimulus induces no changes in the correlation values, the trend of synchrony remains unaltered in both pre-click and peri-click segments.

These results suggest the existence of a mechanism that is able to modulate synchronous activity in the bilateral prefrontal areas and central nuclei of the amygdala driven by a conditioned stimulus that most supposedly affects the functioning of the reward circuitry. Measuring how correlation and synchrony changes in time, can give us more detailed information about a supposedly existing learning curve, that gradually develops the conditioned response and

imprints the relation between the conditioned stimulus and the food reward (Gallistel, Fairhurst et al. 2004).

Frequencies constituting the signal

To further examine these exciting phenomena it is important to evaluate spectral characteristics of the tone-centred epochs, comparing the spontaneous (pre-stimulus) and tone-related (peri-stimulus) epoch segments. A recent study by the Buzsáki Lab (Fujisawa and Buzsáki 2011) demonstrated the existence of a 4 Hz oscillation in rats that coordinates task-related neuronal activity in the medial prefrontal cortex, hippocampus, and the ventral tegmental area. They also found that the increase of power of the 4 Hz oscillation in the prefrontal cortex and the ventral tegmental area modulated gamma power in both structures. In our experiments, spectral analyses show the clear presence of a 4 Hz activity and an oscillation that is within the limits of the theta range. It is interesting however, how other frequency ranges do not seem to participate or contribute significantly in this paradigm.

No obvious patterns are observable on the spectrograms, as a direct and consistent evoked response would be visible on these maps, if it were regularly linked to the stimulus onset.

Integrated power of the 4Hz activity shows observable changes though, starting at a low baseline on Conditioning Day 1 with no statistically significant difference, but by the second conditioning day we can see significant difference between pre- and peri-stimulus intervals in the 4Hz power. There is a significant trend of increase until Conditioning Day 5, where it loses significance (end of learning process?) and it holds until Extinction Day 1 (on which the conditions changed radically, but there is still expectancy from the animal's point of view). From Extinction Day 2 there is a significant descent in power, compared to spontaneous interval until the following day (E3), when it starts to ascend again up to the fourth extinction day (E4). Reacquisition Day 1 turns the trend around into descent once again (conditions for the animal changed radically again) and the significant difference is lost. We do not expect the reacquisition phase to be predictable though, as studies found that the amygdala does not play a vital role in the reacquisition (Kim and Davis 1993, Kim and Davis 1993). What we expected though is that this phase appears faster than the original acquisition (Napier, Macrae et al. 1992, Leung, Bailey et al. 2007).

The theta oscillation is somewhat similar in nature as there is a trend of decreased power in the peri-stimulus segment, but its consistency is reduced as well as the significance. The trend is similar, so it may share some characteristical features as it is also thought to play a role in learning processes. Amygdala also plays a crucial role in reward learning, consequently it has to have a regulating/modulating part as well in the learning/memory-related processes (Seidenbecher, Laxmi et al. 2003, Pape, Narayanan et al. 2005, Narayanan, Seidenbecher et al. 2007, Tye, Cone et al. 2010, Tye, Tye et al. 2010, Lesting, Narayanan et al. 2011, Klavir, Genud-Gabai et al. 2013, Lesting, Daldrup et al. 2013, Likhtik and Gordon 2013). It also needs mentioning how human reward processes regulated by reward structures largely overlap with those demonstrated in animal studies, including the regions of the prefrontal cortex and the amygdala (Aharon, Etcoff N Fau - Ariely et al. 2001, Gottfried, O'Doherty et al. 2003, O'Doherty, Dayan et al. 2003, Aron, Fisher et al. 2005, Hampton, Adolphs et al. 2007, Francois, Huxter et al. 2014).

However, when comparing spectral data with existing fear conditioning results (Lesting, Narayanan et al. 2011), remarkable differences can be observed. Lesting et al. showed an increase in the theta correlation during the fear conditioning phase, which was then followed by a drop or even loss of correlation throughout the extinction. The reacquisition showed locational specificity in the rebound of theta correlation. These results are somewhat the opposite compared to our findings, as we saw a general desynchronization through the reward conditioning, that disappeared in the extinction phase, and returned in the reacquisition. We need to note though, that they did not report a 4 Hz activity as they concentrated only on the theta waves. Our results showed inconsistent theta power, as the occurrence of significant spectral differences in the theta range between spontaneous and peri-tone sections was almost randomized compared to the much more consistent 4 Hz activity. This can be explained by the differences in the paradigm and the underlying mechanisms (fear vs. reward conditioning), and by the targeting of different structures (basolateral vs. central amygdala).

Distribution characteristics of 4Hz and theta oscillations

Knowing that there are two dominant frequencies that are present in most of the epochs during all experimental phases, raises the question: what is the distribution of their occurrence and can they be regarded as evoked potentials – is there a direct relation between the stimulus onset and the instances of the activity? Does the stimulus change the general performance of either of the oscillations?

Distribution analyses showed a significant drop in the occurrence of both 4Hz and theta oscillations after the stimulus onset. This suggests the existence of a coordinating mechanism, that suppresses (active process?) or disfacilitates (passive process?) the presence of these activities. This mechanism does not induce organisation of these processes (judging by the huge variability of inter-peak intervals), neither in spontaneous, nor in stimulus-related settings. Additionally, this mechanism does not lock these activities to the stimulus onset, and yet, with the appearance of the stimulus conditions change radically. Can this be explained with changes in the attention focus as suggested by literature (Kahn, Ward et al. 2012, Funderud, Lovstad et al. 2013, Peers, Simons et al. 2013, Squire, Noudoost et al. 2013)? Can it be regulated by the prefrontal cortex?

Phasic characteristics of the 4Hz activity and the theta oscillation

Based on the results provided by phase histograms the answer is yes, it can be regulated by the prefrontal cortex, suggested by a distinct shift only in the 4Hz activity phase. This 74 degree negative shift in the phase suggests that 1) the 4Hz activity of the amygdala is phase locked to that of the prefrontal cortex, 2) the shift in the angular properties implies that in this particular case the prefrontal cortex is coordinating the amygdala. In Fujisawa's experiment (Fujisawa and Buzsáki 2011) there is a 4Hz activity present until about halfway of the maze, where a decision is made (to turn left – one odour, or right – another odour). During this stage there is an elevated coherence in the 4Hz range between the prefrontal cortex and the ventral tegmental area, which disappears after the decision is made. In our experiments we have a spontaneous interval before the stimulation, with elevated presence of the 4Hz activity, which might either belong to a recurring speculation or to some background stimulus expectation based on memory processes.

The theta phase relationship shows phase locking at 360 degrees, which is the cycle onset. This means that the occurrence of the theta rhythm is synchronous across prefrontal and amygdalar regions. Buzsáki and colleagues found, that the prefrontal 4Hz activity is phase locked to CA1 theta oscillation in the hippocampus. They hypothesized that these physiological mechanisms temporally regulate populations of neurons across prefrontal, limbic and basal ganglia systems (Hyman, Zilli Ea Fau - Paley et al. 2005, Jones and Wilson 2005, Siapas, Lubenov et al. 2005, Benchenane, Peyrache et al. 2010, Fujisawa and Buzsáki 2011). They argue that theta phase-locked PFC neurons can, in theory, transport the theta rhythm to the VTA GABAergic neurons (Carr and Sesack 2000, Carr and Sesack 2000).

Theta and 4Hz activities however, do not appear to be phase-locked in the prefrontal-amygdalar circuitry, based on our findings. This can be explained by the angular shift in the 4Hz activity (~74 degrees), that is caused by a regulatory precedence of prefrontal 4Hz activity – rendering these two distinct oscillations, with complementary roles, to fall out of synchrony.

The amygdala may not play a role in the 4Hz – theta synchronization anyway. The general 4Hz – theta relationship is also considered to originate in the existence of a power increase in the theta band along the frontal midline region of the scalp, which is thought to be a dominant LFP pattern in various cognitive tasks in humans as the "frontal midline theta" (Gevins, Smith et al. 1997, Sarnthein, Petsche et al. 1998, Klimesch, Doppelmayr et al. 2001, Onton, Delorme et al. 2005). Human studies have also suggested that this rhythm is coordinated by hippocampal theta oscillations (Jensen and Tesche 2002), but this new finding with the characterization of a 4Hz activity served as an alternative theory, as it is possibly more related to the 4Hz activity. This is also supported by a study in primates, suggesting that attention and stimulus selection are related with an activity in the low LFP band (Lakatos, Karmos et al. 2008, Schroeder and Lakatos 2009). Thus, knowing that memories and planning are served by hippocampal-prefrontal circuits, as well as the fact that there is a functional binding across various structures of the limbic system carried out by theta oscillations (Buzsaki 2002), it can be logical to find a place for the amygdala in this system, too.

Cross power spectral characteristics

Coherent spectral connections were revealed and identified by CPSD analyses. The finding, that a 4Hz activity dominates the cross-spectral domains exposes some special spectral power attributes directly modulated by the phase of the reward conditioning paradigm. Firstly, the consistent and significant decrease evoked by the conditioned stimulus. Whether it is an active process (down-regulation as suggested by the angular shift in the 4Hz activity between the prefrontal cortex and the amygdala) or a passive process (disfacilitation caused by a change in the attention focus), memory processes must also play an important role in this setting. This is best supported by how CPSD properties of the 4Hz activity change in the extinction phase, where the animal relies on memories from the previous sessions, that still lead them to the food bowl as they still expect the reward to appear. This effect disappears by the third day of this phase, correlating with the changes in the CPSD values. Finally, the speedy reacquisition – as it is often suggested to be a faster process than the original conditioning (Napier, Macrae et al. 1992, Kim and Davis 1993, Kim and Davis 1993, Leung, Bailey et al. 2007) – also relies on memory processes and is aided by reactivation of memory traces. There is no difference in the CPSD values in this session, but it is not necessarily expected anyway, partly because the amygdala does not play a role in the reacquisition (Kim and Davis 1993), and partly because this session may rely on memory processes more than any other phases of the experiment.
Again, when compared with fear conditioning data, we have quite the opposite results here. We have a largely consistent (8 out of 10 sessions) drop in the CPSD power in the peri-stimulus segment, but only in the band of the 4 Hz activity, as the cross-spectral power of the theta wave was not statistically significant. Even though recording sites similar (mPFC vs basolateral and central amygdala), the behavioural paradigm (fear vs. reward conditioning), and necessarily the underlying mechanisms rendered the results completely different.

Conclusion

We have successfully conducted the classical Pavlovian reward conditioning experiments including all conditioning, extinction and reacquisition phases. All participating animals performed in a desired manner, none of the participants failed to go through the training procedures and none of them showed deviations compared to the group average. We managed to measure distinctive differences in the correlation analysis that showed consistent CS-related drop in the wideband synchrony during the conditioning, which then turned around and elicited an increased correlation during the extinction phase, and finally, in the reacquisition phase returned to a significant drop in the level of synchrony, following the tone stimulus.

Spectral analyses revealed two distinct, rhythmical activities, one around 4Hz and another in the theta range of 5-9 Hz. These oscillations were consistently present across all epochs, with increased power when compared to other frequency bands. The 4Hz activity showed a more consistent spectral power centred on the middle of the training phases (suggesting a relation with some learning / memory processes), while theta power showed less consistency.

The distribution of oscillation peaks revealed significant drop in the stimulus-related epoch segments, which supported the primary correlation results. This technique did not reveal a direct link between the oscillation peaks and the stimulus onset, either for the 4Hz or for the theta oscillation.

Phase histograms resulted in a significant difference in the phase-locking mechanism – while the 4Hz activity showed negative angular shift of about 74 degrees, the theta was mostly locked to the cycle onset. There was no phase-locking between the 4Hz activity and the theta oscillation.

Cross power spectral density analysis revealed consistent presence in the 4Hz domain, and the distribution of power values suggested a relation with ongoing memory processes driven by a mechanism from outside the prefrontal-amygdalar circuitry.

The results described here suggest that the amygdala is also affected by a 4Hz activity that was shown to synchronize multiple brain regions during behaviour, and also that it fits into a previously unknown gap in the circuitry coordinated by this 4Hz activity.

Furthermore, the development of an ultrasmall microdrive (described in the Appendices) will allow for the simultaneous observation of multiple regions, therefore enabling to extend the limitations of this study, ultimately leading to the assessment of multiple, interacting animals.

Appendices

OA Neurosciences
Open Access

Methodology

Recent Advances

Development of a miniature microdrive recording system for multisite multichannel recording from rodent brains

A Magony*, A Sik

Abstract

Introduction

Assessing the electrical performance of cell populations can reveal their functions only partially. To discover the underlying mechanisms it is important to examine how they communicate with other brain regions, which can be achieved by implanting multiple recording devices to all possible cooperating areas. Multisite implantations are limited by available space in small animals, thus the need for a miniaturised yet reliable microdrive that allows for increased implantation counts in a single animal is of utmost importance. Here we describe a miniature microdrive unit that can be used in various experimental settings.

Methodology

Based on a previously used design, but by substituting parts with miniature modelling components, we managed to build a reduced size microdrive which is reliable, biocompatible and customisable. The new device is fully compatible with existing recording solutions but it can be implanted in increased amounts into a single animal, where connector size becomes the only technical limitation.

Discussion

The theoretical number of implantThe theoretical number of implantable microdrives is 10 in mice (up to 320 recording channels), 24 in rats (up to 768 recording channels), and is now primarily limited by the connector size. The low profile also allows the use of wireless telemetry to replace the cable and provide unrestricted exploration for the animal as well as interacting animals concurrently, opening the floor to social–behavioural studies.

Conclusion

We successfully modified the concept of the original microdrive and constructed a miniature device that allows the mechanical manipulation of electrode depth in the brain in chronic experiments without the need to anaesthetise the animal. By using the new microdrive, cortical and deep brain structures can be targeted. Although due to the reduced size handling and implantation can be more challenging, the increased number of implantable units makes up for the difficulties and allows the simultaneous examination of multiple brain regions with high accuracy and reliability.

* Corresponding author
Email: a.magony@bham.ac.uk

Neuronal Networks Group, School of Clinical and Experimental Medicine, College of Medical and Dental Sciences, University of Birmingham, Birmingham, B15 2TT, UK

Introduction

An approach to assessing the real-time performance of an area or cell population is the registration of local bioelectrical activity generated by interacting neurons. Although the generating mechanism of the electrophysiological signals still has not yet been revealed entirely, it is considered to reflect the summed electrical activity of several thousand neurons, situated in close vicinity. Due to signal attenuation the activity of deeper brain structures cannot be recorded from the head surface, hence the need for invasive recording techniques enabling to reach deeper cortical layers or subcortical areas. With respect to gradual alterations in brain bioelectrical signals it is believed that subthreshold postsynaptic potential changes on the dendrites of pyramidal cells are responsible for the signal generation, as well as fast, all-or-nothing-like action potentials (units), which are also integral part of the cerebral bioelectrical activity, though their magnitude in the total mass is significantly smaller. Therefore, the development of sophisticated recording equipment capable of registering and separating brain activity is of utmost importance. Deeper brain structures often with nuclear nature require the use of stereotrode or tetrode electrodes, the advantages of which have been widely acknowledged in the separation of unit activity[1,2]. These techniques allow for the assessment of electrical activity in subcortical structures, but they do not provide information about the network structure of concurrent or cooperating regions in the brain when used on their own. Simultaneous observation of multiple, anatomically related structures is essential for understanding how cerebral networks function under various conditions, as synchronisation and de-synchronisation of spatially distant areas play vital roles in learning and memory processes, including behaviour, and numerous other mechanisms of the nervous system[3]. Our aim was to provide a novel tool for accessing multiple brain structures at the same time and further increase the number of implantable devices by miniaturising microdrives that enable the fine tuning of electrode positioning in the brain. Our new microdrive design reduces size without compromising reliability and usability, while supporting the simultaneous examination of electrical activity in spatially distant or close regions.

Licensee OA Publishing London 2014. Creative Commons Attribution License (CC-BY)

FOR CITATION PURPOSES: *Magony A, Sik A.* Development of a miniature microdrive recording system for multisite multichannel recording from rodent brain. OA Neurosciences 2014 Feb 25;2(1):4.

Competing interests: none declared. Conflict of interests: none declared.
All authors contributed to conception and design, manuscript preparation, read and approved the final manuscript.
All authors abide by the Association for Medical Ethics (AME) ethical rules of disclosure.

OA Neurosciences
Open Access

There are fundamentally two types of microdrives used today: single electrode microdrives[4] (nDrive, Neuronexus, Michigan, USA) that allow the vertical adjustment of one electrode, and multi-electrode microdrives[5–7] that can be loaded with multiple electrodes and each one's cerebral depth can be fine-tuned, but these constructions are relatively large in size and weight. Another disadvantage is that all electrodes need to be implanted in a spatially close region preventing recording from spatially distant brain areas.

Methodology

Electrode fabrication

Multisite, tetrode recording electrodes were constructed manually similar to already existing descriptions in the literature[1,8]. Teflon-coated tungsten wires with a diameter of 12 µm (California Fine Wire Company, Grover Beach, USA) were cut to 30 cm segments, then looped twice, fixed to a holder bar and spun on a magnetic spinner with a weight keeping the wires straight until the top of the plate approached the holder bar to about 15 mm. Wires were then allowed to twist backwards for a few turns to release tension. Using a heat gun the insulation was slightly melted to fix the posture and to strengthen the structure of the tetrode. The magnetic weight was then cut down and the electrode was released from the holder bar. Non-twisted wires were cut to have four freely moving wires at the end of the tetrode. The coating was removed about 1 mm from wire tips on all four wires with a flame using a lighter. Each exposed wire was then soldered to dismantled connector pins (A9941-001, Omnetics, Minneapolis, Minnesota, USA) and adjoining surfaces were insulated with non-conductive paint. Contacts and conductance were tested with an electrical stimulator in 0.9% saline solution where bubbles emerged after stimulation. Tetrodes were then stored in a box separately for later use. Prior to usage pins were inserted carefully into the connector (A9942-001, Omnetics, Minneapolis, Minnesota, USA) and sealed with epoxy. Tetrodes were then put in a protective cannula (34G, Cooper's Needle Works, Birmingham, UK) and cut to desired size with sharp surgical scissors. Impedance values were measured and lowered to ~300 kΩ (measured at 1 kHz), using electroplating with gold solution and NanoZ impedance measuring device (Neuralyx Inc., Montana, USA).

Microdrive fabrication using the original design

Commercially available 'C'-profile brass shaft with a height of 6 mm and a depth of 3 mm was used to produce the frame of the traditional microdrive. Two millimetres wide sections were cut with a professional cutter (Proxxon-KS230, Föhren, Germany), and then a hole with a diameter of 1 mm was drilled through the base and the top. A brass screw (245 µm vertical movement/turn, Precision Technology Supplies, East Grinstead, UK) was placed through the holes and in the middle of a small plastic bit (moving part) that pressed against the inner side of the C-frame and allowed a 5 mm vertical repositioning of the electrode. A nut was wound around the screw from the bottom of the frame to prevent vertical movement of the screw itself. The end of the screw was then cut and sanded to size just to fill the nut, and was glued to the nut using superglue. A spacer shaft was attached to the back side of the microdrive towards the 'imaginary' skull to provide an initial fixing to the bone. Prior to implantation the protective cannula (34G, Cooper's Needle Works, Birmingham, UK) of the tetrode was glued to the moving plastic part and the connector was attached to the back side of the microdrive (Figure 1(b)).

New microdrive design

We fabricated the ultra microdrive by using a brass C-profile shaft with a height of 1.5 mm and a depth of 1 mm (Scale Hardware, Ft Lauderdale, Florida, USA). One millimetre wide sections of the C-profile shaft were cut with a professional cutter (Proxxon-KS230, Föhren, Germany), and then a hole with a diameter of 0.6 mm was drilled through the base and the top. A brass screw (125 µm vertical movement/turn, THRB-05-B, Scale Hardware, Ft Lauderdale, FL, USA) with a diameter of 0.5 mm was placed through the holes and in the middle of a small (0.3 mm thick) plastic bit (moving part) pressing against the inner side of the C-frame, and enabling the attached cannula with the electrode inside to move vertically 0.6 mm. A nut was fixed on the screw outside the frame to prevent vertical movement, cut into size and then a spacer shaft was attached to the back side of the microdrive as described above. As an alternative solution, the drive was placed and glued into a pipette tip that served as protection. Prior to surgery the protective cannula of the tetrode was glued to the moving plastic part and the connector was attached to the back side of the microdrive (Figure 1(a), (c) and (d)).

Implantation and recordings

Thirteen male Sprague-Dawley rats (Charles-River, Margate, UK) weighing between 300 and 350 g were used for implanting chronic recording devices. All procedures conformed to the UK Animals (Scientific Procedures) Act 1986. Implantation surgeries were performed in designated surgical theatres of the Biomedical Services Unit, University of Birmingham, Birmingham, UK, with sterile tools and equipment. The anaesthesia of the animals was induced in an anaesthetic chamber with isoflurane vaporised in oxygen (3% isoflurane and 100% oxygen). The heads of the rats were shaved and were then fixed

Licensee OA Publishing London 2014. Creative Commons Attribution License (CC-BY)

FOR CITATION PURPOSES: *Magony A, Sik A.* Development of a miniature microdrive recording system for multisite multichannel recording from rodent brain. OA Neurosciences 2014 Feb 25;2(1):4.

Competing interests: none declared. Conflict of interests: none declared.
All authors contributed to conception and design, manuscript preparation, read and approved the final manuscript.
All authors abide by the Association for Medical Ethics (AME) ethical rules of disclosure.

OA Neurosciences
Open Access

Methodology

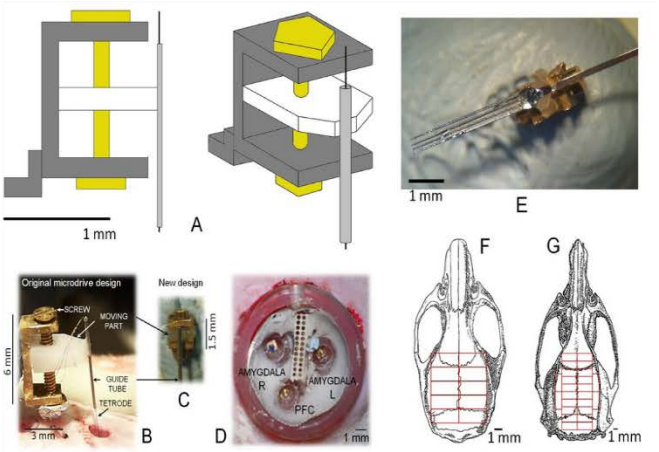

Figure 1: (a) Schematic views of the microdrive. Parallel sides of the brass C-frame are drilled through to fit a screw across the frame. A plastic moving part is placed between the sides, to which the protective cannula with the tetrode inside is glued, so that by turning the screw the vertical position of the electrode can be tuned. (b) Construction of original microdrive (6 × 3 × 3 mm). The tetrode is inside a guide tube which is attached to a plastic bit bored through by a screw. The turn of the screw moves the tube up or down so that the cerebral depth of the electrode can be fine-tuned. (c) In the new design we managed to reduce the size of the microdrive significantly (to 1.5 × 1 × 1 mm), thus we can increase the number of implantable electrodes without spatial restriction allowing us to record from several distinct brain regions simultaneously. (d) Example of three implanted microdrives (left amygdala, right amygdala and PFC) with a 16 channel connector in the middle. (e) Example of commercial silicon probe attached to the microdrive. Estimation on the number of implantable microdrives in mice (f) and rats (g). Red rectangles indicate the area required by the microdrive and the electrode secured to the scull. PFC, prefrontal cortex.

in a stereotactic frame where a low (1.5%) isoflurane anaesthesia was provided via a nose mask. The pinch reflex was checked regularly to assess the depth of anaesthesia. Heart rate, breathing pattern and body temperature were monitored constantly. Body temperature was controlled by a heating pad and maintained at 37°C. Eyes were covered with moisturising agent, ear canals were lubricated with EMLA cream (25 mg lidocaine and 25 mg prilocaine/g) to reduce possible inconvenience caused by the ear bars. After cutting the skin, cleaning and leaving the skull surface to dry, four holes were drilled for anchoring screws to achieve better fixation of dental cement. Small craniotomies were drilled above the targeted regions (coordinates relative to the Bregma were obtained from the Rat Brain Atlas[9]). The dura was carefully removed and then four tetrodes attached to microdrives were inserted into the craniotomies: two electrodes were lowered to the prefrontal cortex (PFC) on both sides (anterior–posterior (AP): +3.2 mm, medial–lateral (ML): ±0.8 mm, dorsal–ventral (DV): 3 mm), and two electrodes to the amygdalae on both sides (AP: −2.5 mm, ML: ±4 mm, DV: 7.8 mm). Reference and ground electrodes were connected and placed under one of the posterior anchoring screws. Moving parts (screw, nut and cannula) were embedded in wax to allow the vertical adjustment of the electrodes, whereas microdrive frames, all wires and the connector in the middle were embedded in dental cement. The skin was then stitched with sterile sutures, and following analgesia (Temgesic, 1 mL/kg was administered intraperitoneally) the animal was removed from the stereotactic frame and transported to the recovery room and placed in a container above a heating pad, where sucrose fluid was injected subcutaneously to compensate possible dehydration. Animals recovered and were fed *ad libitum* for 1 week before recordings commenced. A Tucker–Davis Technologies (TDT, Alachua, FL, USA) PZ2 preamplifier was used to collect signals from the brain and the amplified signals were then fed through optical fibre to a TDT RZ2 Z-Series base station. Data were transported through optical fibre to a Windows PC for storage and processing. The original TDT software was used to control the recording and to store the data with the following parameters: 16 channels, 24 kHz sampling rate with a 0.5 Hz–12 kHz band-pass filter and 16-bit signal resolution. At the end of the experiment animals were perfused to perform histology. Recorded files were converted to Matlab (Mathworks, Natick, USA) format after the experiment to feed all data into our custom-made software toolbox.

Results

All microdrives with attached tetrodes were implanted successfully. Although the difficulty as well as the time required for the implantation procedure increased noticeably due to the challenge in handling the much smaller sized microdrives, the signal quality did not change compared with the signal with the original design. Thus, reduction in the

Licensee OA Publishing London 2014. Creative Commons Attribution License (CC-BY)

FOR CITATION PURPOSES: *Magony A, Sik A.* Development of a miniature microdrive recording system for multisite multichannel recording from rodent brain. OA Neurosciences 2014 Feb 25;2(1):4.

Competing interests: none declared. Conflict of interests: none declared.
All authors contributed to conception and design, manuscript preparation, read and approved the final manuscript.
All authors abide by the Association for Medical Ethics (AME) ethical rules of disclosure.

OA Neurosciences
Open Access

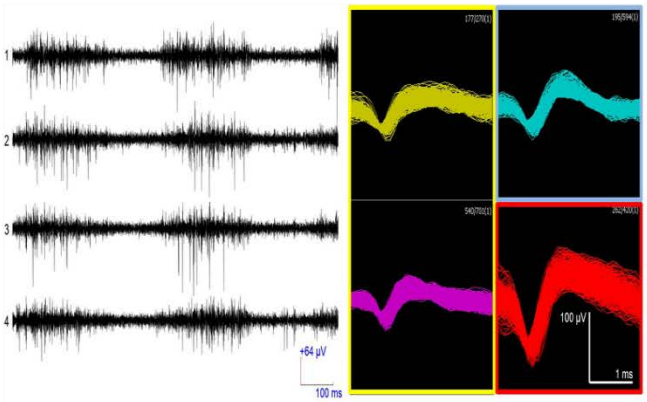

Figure 2: Example of filtered unit recording (left) and clustered spike waveforms (right) registered in the rat PFC during anaesthesia using a tetrode. Action potentials can be classified into three clusters (1 and 3, 2, 4) containing three cells' activity from one single position of the tetrode. PFC, prefrontal cortex.

drive size had no negative effect on signal reliability, the factor which is absolutely essential. Importantly, the noise level showed the same characteristics both with original and new designs and was satisfactory in the new miniaturised device even without any electrical shielding or other protection. Signal quality was maintained for weeks, although we had recurring problems with keeping the Omnetics connectors clean as the freely moving rats managed to get rid of protecting covers and so allowing dust and dirt into the connector holes, which was prevented by using dummy connectors in the sockets. The screw in the microdrive that is responsible for moving the electrode vertically was marked with a marker pen, so that it was easier to follow its accurate location while turning to move the electrode. The working distance of the microdrive (around 600 µm) was satisfactory to position the electrodes so that multiple neurons' unit activity was detected, but it might be challenging in larger animals or brain areas if the initial position is not determined adequately. Beyond the size reduction, the weight of the microdrive also radically decreased from 0.192 g (original design) to 0.026 g (new design).

The endurance of the microdrive was verified by physical tests and thanks to the rigid construction, none of the drives was disassembled by a reasonable amount a force. Similarly, no unwanted movements were detected in the implanted devices even when turning the screws.

Although mostly tetrodes were used for acquiring local field potential and unit recordings, multishank silicon probes were also attached to the drive for testing purposes (Figure 1(e)). Physical tests showed no differences in endurance or reliability when compared with tetrodes. Thus, this mechanical device can also be used for the fine positioning of silicon probes.

In most cases we were able to obtain clean, noiseless and artefact-free signals from which we could register field potential signal as well as single unit activity. To examine action potentials first we filtered the wide band signal with a zero phase-shift band-pass filter between 500 Hz and 5 kHz. Then, after threshold detection we applied principal component analysis for feature extraction, and expectation maximisation algorithm for sorting spiking activity. Results show reliable local field potential signals as well as detectable and separable single and multiunit activity in the range of 50–150 microvolt range (Figure 2). Recordings typically yielded two to six separable cells per tetrode in one single position of the electrode. Local field potential during sleep showed characteristic features of the slow sleep oscillation – up and down states – in the PFC.

Discussion

The development of a microdrive that serves the same mechanical functions but at about 1/20th of the size of the original microdrive design is important for reaching deeper structures and recording single cell, multiple unit activity and field potential signals, and also has prominent importance in the neurophysiological examination of behaviour. Rat experiments showed that the new, radically miniaturised design proved to be reliable in terms of the integrity of the components and the achievable signal quality. However, new challenges appeared during implantation. In the absence of a holder equipment that allowed the secure yet gentle grip of the miniature microdrive, we fabricated a screw-controlled precision holder, using pointed scalpel blades, a spring and epoxy to hold parts together. We also realised that physics seem to have different attributes when such small-sized devices are to be handled: even the smallest drops of wax and dental cement were hard to control as they started spreading immediately after touching the surface, which was quite disadvantageous because of the miniature size of the microdrive. Therefore, extra care and caution

Licensee OA Publishing London 2014. Creative Commons Attribution License (CC-BY)

FOR CITATION PURPOSES: *Magony A, Sik A.* Development of a miniature microdrive recording system for multisite multichannel recording from rodent brain. OA Neurosciences 2014 Feb 25;2(1):4.

Competing interests: none declared. Conflict of interests: none declared.
All authors contributed to conception and design, manuscript preparation, read and approved the final manuscript.
All authors abide by the Association for Medical Ethics (AME) ethical rules of disclosure.

OA Neurosciences
Open Access

had to be applied throughout surgical implantations. Due to the size, the implantation procedure is relatively more complicated and needs more concentration and time, but the increased number of implantable devices enables the simultaneous registration of the activity from more brain regions, which is not feasible with the original design. The theoretical limit in the number of implantable microdrives is around 10 in a mouse (Figure 1(f)), 20 in a rat (Figure 1(g)), and is now primarily limited by the size of the connector that also has to be positioned on the skull. A solution to this problem could be the use of connectors with vertical contacts instead of a horizontal socket, in a tall but narrow construction, or alternatively, placing the connector on the neck. It is also worth mentioning that the tight connection of the Omnetics connector requires the experimenter to undergo a training process with the animal as connecting the cable needs an increased amount of force which can be uncomfortable for the animal. Discomfort can also be avoided by slightly anaesthetising the animal for the duration of securely connecting the recording cable, but this procedure is only viable using inhalational anaesthetics. Due to the size of the drive we could use very short cables without any copper shielding that would add more weight to the head of the animal.

The low profile of the microdrives also allows the use of wireless telemetry to replace the cable and thus permit unrestricted exploration for the animal. There are existing commercially available low weight wireless transmitters supporting the simultaneous sampling of up to 64 channels (Triangle Biosystems, Durham, NC, USA) at high sampling rates required by single unit separation, as well as dual wireless systems that make it possible to record the activity of two (or three, one with a cable) interacting animals concurrently, opening the floor to social–behavioural studies.

Conclusion

Besides the fact that our new microdrives have extremely reduced size and weight, based on our experiments they support the reliable recording of both field potential and single unit signals. Implantation tests also revealed they are remarkably biocompatible as no infection or inflammation appeared even months after the implantation, thus they can be used in various experimental settings. Our primary aim was miniaturisation and recording unit activity for several hours that we have achieved. Experiments can require long-term stable recordings (weeks, months) that we have not tested; however, we see no reason why tall and weighty drives could be more stable than our miniature construction. On the contrary, low profile drives where the top of the drive is close to the pivot point (skull) are likely less fragile and more stable. Estimations on the number of implantable devices suggest up to 10 microdrives in mice and 24 in rats based on the surface area required. These calculations suggest that altogether 10 tetrodes (40 channels) or silicon probes (up to 320 channels) can be implanted in mice, whereas 24 tetrodes (96 channels) or silicon probes (up to 768 channels) in rats, which could be a huge advance over currently existing solutions, mostly if the number of simultaneously examined brain regions is taken into account.

Abbreviations list

AP, anterior–posterior; DV, dorsal–ventral; ML, medial–lateral; PFC, prefrontal cortex.

Acknowledgement

This work was financially supported by Medical Research Council G1001235.

References

1. Jog MS, Connolly CI, Kubota Y, Iyengar DR, Garrido L, Harlan R, Graybiel AM. Tetrode technology: advances in implantable hardware, neuroimaging, and data analysis techniques. J Neurosci Methods. 2002 Jun;117(2):141–52.
2. Buzsaki G. Large-scale recording of neuronal ensembles. Nat Neurosci. 2004 May;7(5):446–51.
3. Fujisawa S, Buzsaki G. A 4 Hz oscillation adaptively synchronizes prefrontal, VTA, and hippocampal activities. Neuron. 2011 Oct;72(1):153–65.
4. Bilkey DK, Muir GM. A low cost, high precision subminiature microdrive for extracellular unit recording in behaving animals. J Neurosci Methods. 1999 Oct;92(1–2):87–90.
5. Keating JG, Gerstein GL. A chronic multi-electrode microdrive for small animals. J Neurosci Methods. 2002 Jun;117(2):p. 201–6.
6. Kloosterman F, Davidson TJ, Gomperts SN, Layton SP, Hale G, Nguyen DP, Wilson MA. Micro-drive array for chronic in vivo recording: drive fabrication. J Vis Exp. 2009 Apr;1094(26).
7. Battaglia FP, Kalenscher T, Cabral H, Winkel J, Bos J, Manuputy R, et al. The Lantern: an ultra-light micro-drive for multi-tetrode recordings in mice and other small animals. J Neurosci Methods. 2009 Apr;178(2):291–300.
8. Nguyen DP, Layton SP, Hale G, Gomperts SN, Davidson TJ, Kloosterman F, Wilson MA. Micro-drive array for chronic in vivo recording: tetrode assembly. J Vis Exp. 2009 Apr;1098(26).
9. Paxinos G, Watson C. The rat brain in stereotaxic coordinates, 6 ed. New York: Academic Press; 2007.

Licensee OA Publishing London 2014. Creative Commons Attribution License (CC-BY)

FOR CITATION PURPOSES: *Magony A, Sik A.* Development of a miniature microdrive recording system for multisite multichannel recording from rodent brain. OA Neurosciences 2014 Feb 25;2(1):4.

Competing interests: none declared. Conflict of interests: none declared.
All authors contributed to conception and design, manuscript preparation, read and approved the final manuscript.
All authors abide by the Association for Medical Ethics (AME) ethical rules of disclosure.

A2. WaveSolution: A novel analytical toolbox for electrophysiological signal processing and analysis

Introduction

In view of the fact that the mechanisms of brain functions are so diverse and obscure, the demand for efficient data processing software is of utmost importance. Since we can draw conclusions based only on precise results, the significance of the correct application of methods is primary. In order to gain appropriate and reliable outcome, a new software toolbox has been developed in partial collaboration with Dr. Richard Csercsa (Institute for Psychology, Hungarian Academy of Sciences, Budapest, Hungary).

Methods

The development process of an analytical software is always different from that of other software products. Since all conclusions drawn from experimental results depend on the method of analysis, the accuracy and reliability of such analytical methods are crucial. Through the course of software development we applied three methods to comply with the criteria:

"Extreme programming (XP)" – a modern, so called Agile programming technique that was designed for trustworthy programming (Beck 2001). This kind of development involves the presence (on-sight or online) of two programming engineers, one for coding and the other for inspecting (the roles change regularly). This involves the fact that due to this joint programming method it is difficult to designate single parts or functions of the toolbox to one person, thus in my thesis I will concentrate on including the features that were designed by myself. One can suppose that programming in pairs makes the process of implementation easier and faster, but it can also slow down the progress and can often generate disagreement between the engineers. Every coder has their own programming style to which they prefer to cling, nevertheless joint work is still very beneficial and efficient for the sake of quality, reliability, reparability and amendability as well as cost effectiveness.

"Formal specification" – the analytical methods are formally specified before the coding process. This involves mathematical, logical or information theoretical representation of the

problem with thorough verification of all state transition functions leading from input to the output (Monin and Hinchey 2003). The importance of formal specification and formal methods lies in the fact that it can contribute to the robustness and reliability of a system.

"Dedicated testing" – all functions of the complete analytical software are validated and verified through pre-designed testing, in which the tools are tested with both simulated, real and extreme (out of limits) data. This phase ensures that the correct output is generated in every case, for every input, and it also allows for a fail-safe system to be implemented, all substantial parts of software quality control.

With the use of these practices the possibility of failures can be minimized, while high level of reliability can be guaranteed (Veto 2005).

Results

The result is an approximately 15 000 code-line long software toolbox running in Matlab with an easy to use, clear and user-friendly graphical user interface. All functions are accessible in menus familiar from classical Windows and Mac programs (figure 53). All features have default parameters which are calculated and recommended based on actual circumstances detected by the software, but those who want to have greater control can also find and modify all possible parameters. Outputs of the toolbox can easily be exported in various formats supported by Matlab and by many commercially available products. For advanced users who want to implement their own functions and include it in the software, the interface and the structure of plug-ins is available for customized development. Also, those familiar with Matlab commands and formulae can execute manual calculations within the software, therefore all supported Matlab functions can be used (Hanselman and Littlefield 2004, Pratap 2005).

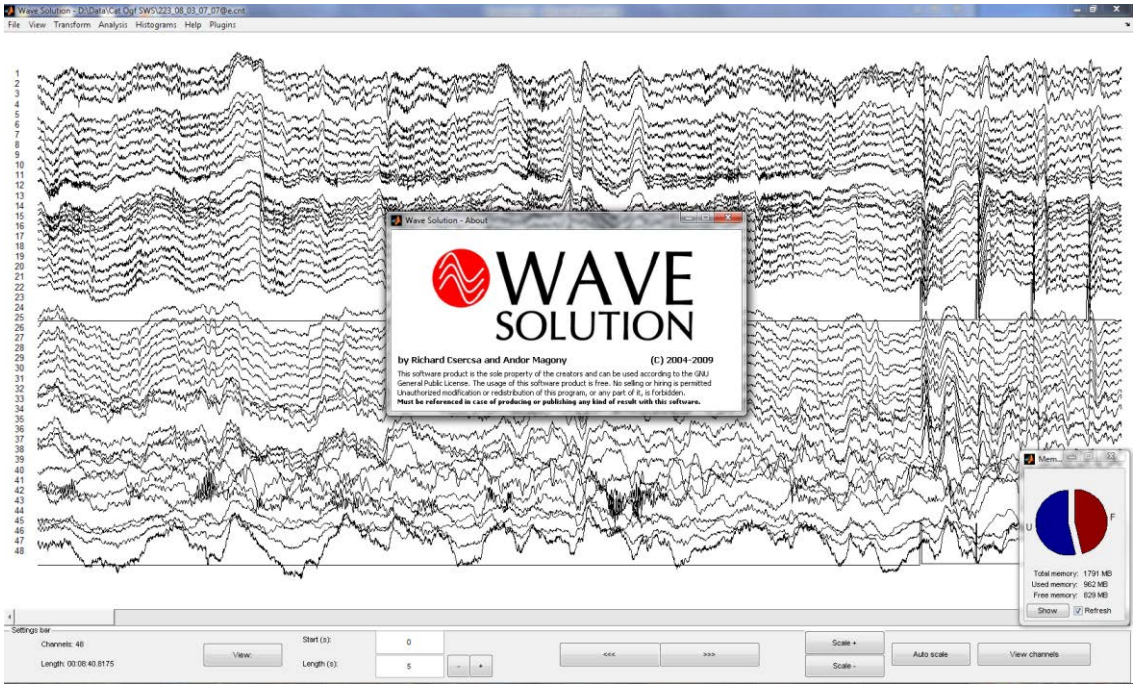

Figure 53: The main window of WaveSolution.

Wave Solution is a multichannel data processing system running an intuitive graphical user interface with built-in computation and evaluation procedures, equipped with the following major analytical functions:

- Support of various file formats: CNT, EEG, AVG, MAT and EDF.
- MapView: 2D and 3D representations of multichannel waveforms where colours represent amplitude.
- Voltage threshold: manual and semi-automatic (using SD coefficient) threshold function with built in peak detection.
- Histograms: Peri-event time histogram, population histogram, and phase histogram.
- Epoch processing: transformation of continuous signals into epochs by using stimulus time codes.
- Spike sorting: semi-automatic spike sorting using Principal Component Analysis for feature extraction, Expectation Maximization and K-means algorithms for clusterization.
- Hilbert transform: computation of angular characteristics of a signal. Also used for phase histograms.
- Current Source Density maps: calculates the summated value of a neuron population's trans-membrane currents in a given region.

- Correlation maps: computes the correlation value of all possible channel-pairs resulting in an N x N dimensional matrix.
- Coherence maps: This function discovers the magnitude squared coherence estimate Cxy for the input signals.
- Fast Fourier Transform: it transforms the signal into the frequency domain and displays it in the desired frequency range.
- Zero phase shift filter: a finite impulse response filter, using a special, two-way filtering method to avoid shifting in the signal.
- Spectrogram: it computes the short-time Fourier transform (STFT) to obtain the frequency components that constitute a signal in time (time-frequency map).

Discussion

Wave Solution, a novel analytical toolbox for electrophysiological signal processing and analysis has been successfully developed. The built-in analytical and comparative, mathematical, information theoretical and signal processing functions make it possible to compute and evaluate the outcomes of even more complex studies including behavioural and event related experiments. Due to the thorough design and the Agile implementation, as well as the formal specification, systematic testing and quality management of all functions the produced results are robust and reliable. Thanks to a special data architecture its processing speed is comparable to commercially available products despite the fact that it is not natively run but within the Matlab framework. Its design also allows for easy modifications and supplementation due to the modular construction and hierarchy, which is an important factor knowing that these are the most expensive phases of software architecture and maintenance.

With the support of spike sorting, numerous options for signal comparison and advanced epoch features including ERP (event-related potentials) processing it is a great tool for a wide scale of experimental settings. This software product is open source, freely available, and can be freely developed with the implementation of plug-ins, to suit one's own needs.

References

Adams, W., S. Kusljic and M. van den Buuse (2008). "Serotonin depletion in the dorsal and ventral hippocampus: effects on locomotor hyperactivity, prepulse inhibition and learning and memory." Neuropharmacology **55**(6): 1048-1055.

Aggleton, J. P. (2000). The amygdala : a functional analysis. Oxford, OX; New York, Oxford University Press.

Aharon, I., D. Etcoff N Fau - Ariely, C. F. Ariely D Fau - Chabris, E. Chabris Cf Fau - O'Connor, H. C. O'Connor E Fau - Breiter and H. C. Breiter (2001). "Beautiful faces have variable reward value: fMRI and behavioral evidence." Neuron **32**(0896-6273 (Print)): 537-551.

Aron, A., H. Fisher, D. J. Mashek, G. Strong, H. Li and L. L. Brown (2005). "Reward, motivation, and emotion systems associated with early-stage intense romantic love." J Neurophysiol **94**(1): 327-337.

Bassareo, V., M. A. De Luca and G. Di Chiara (2007). "Differential impact of pavlovian drug conditioned stimuli on in vivo dopamine transmission in the rat accumbens shell and core and in the prefrontal cortex." Psychopharmacology (Berl) **191**(3): 689-703.

Battaglia, F. P., T. Kalenscher, H. Cabral, J. Winkel, J. Bos, R. Manuputy, T. van Lieshout, F. Pinkse, H. Beukers and C. Pennartz (2009). "The Lantern: an ultra-light micro-drive for multi-tetrode recordings in mice and other small animals." J Neurosci Methods **178**(2): 291-300.

Baxter, M. G. and E. A. Murray (2002). "The amygdala and reward." Nat Rev Neurosci **3**(7): 563-573.

Beck, K. (2001). "Manifesto for Agile Software Development." Agile Alliance **1**(1).

Benchenane, K., A. Peyrache, M. Khamassi, P. L. Tierney, Y. Gioanni, F. P. Battaglia and S. I. Wiener (2010). "Coherent theta oscillations and reorganization of spike timing in the hippocampal- prefrontal network upon learning." Neuron **66**(6): 921-936.

Bennett-Levy J, Butler G, Fennell M, Hackmann A, Mueller M, Westbrook D and R. K (2004). Oxford Guide to Behavioural Experiments in Cognitive Therapy, Oxford University Press.

Bilkey, D. K. and G. M. Muir (1999). "A low cost, high precision subminiature microdrive for extracellular unit recording in behaving animals." J Neurosci Methods **92**(1-2): 87-90.

Bouton, M. E. (2007). Learning and behavior : a contemporary synthesis. Sunderland, Mass., Sinauer Associates, Publishers.

Buzsaki, G. (2002). "Theta oscillations in the hippocampus." Neuron **33**(3): 325-340.

Buzsaki, G. (2004). "Large-scale recording of neuronal ensembles." Nat Neurosci **7**(5): 446-451.

Buzsaki, G., C. A. Anastassiou and C. Koch (2012). "The origin of extracellular fields and currents--EEG, ECoG, LFP and spikes." Nat Rev Neurosci **13**(6): 407-420.

Cardinal, R. N., J. A. Parkinson, J. Hall and B. J. Everitt (2002). "Emotion and motivation: the role of the amygdala, ventral striatum, and prefrontal cortex." Neurosci Biobehav Rev **26**(3): 321-352.

Carr, D. B. and S. R. Sesack (2000). "GABA-containing neurons in the rat ventral tegmental area project to the prefrontal cortex." Synapse **38**(2): 114-123.

Carr, D. B. and S. R. Sesack (2000). "Projections from the rat prefrontal cortex to the ventral tegmental area: target specificity in the synaptic associations with mesoaccumbens and mesocortical neurons." J Neurosci **20**(10): 3864-3873.

Corsi-Cabrera, M., E. Perez-Garci, Y. Del Rio-Portilla, E. Ugalde and M. A. Guevara (2001). "EEG bands during wakefulness, slow-wave, and paradoxical sleep as a result of principal component analysis in the rat." Sleep **24**(4): 374-380.

Dumont, E. C., M. Martina, R. D. Samson, G. Drolet and D. Pare (2002). "Physiological properties of central amygdala neurons: species differences." Eur J Neurosci **15**(3): 545-552.

Elston, G. N. (2003). "Cortex, cognition and the cell: new insights into the pyramidal neuron and prefrontal function." Cereb Cortex **13**(11): 1124-1138.

Everitt, B., R. N. Cardinal, J. A. Parkinson and T. W. Robbins (2003). "Appetitive behavior: impact of amygdala-dependent mechanisms of emotional learning." Ann N Y Acad Sci **985**(0077-8923 (Print)): 233-250.

Francois, J., J. Huxter, M. W. Conway, J. P. Lowry, M. D. Tricklebank and G. Gilmour (2014). "Differential contributions of infralimbic prefrontal cortex and nucleus accumbens during reward-based learning and extinction." J Neurosci **34**(2): 596-607.

Fujisawa, S. and G. Buzsáki (2011). "A 4 Hz oscillation adaptively synchronizes prefrontal, VTA, and hippocampal activities." Neuron **72**(1097-4199 (Electronic)): 153-165.

Funderud, I., M. Lovstad, M. Lindgren, T. Endestad, P. Due-Tonnessen, T. R. Meling, R. T. Knight and A. K. Solbakk (2013). "Preparatory attention after lesions to the lateral or orbital prefrontal cortex--an event-related potentials study." Brain Res **1527**: 174-188.

Fuster, J. M. (2008). The prefrontal cortex. Amsterdam; Boston, Academic Press/Elsevier.

Gallagher, M., P. Graham and P. Holland (1990). "The amygdala central nucleus and appetitive Pavlovian conditioning: lesions impair one class of conditioned behavior." Journal of Neuroscience **10**(0270-6474 (Print)): 1906-1911.

Gallistel, C. R., S. Fairhurst and P. Balsam (2004). "The learning curve: implications of a quantitative analysis." Proc Natl Acad Sci U S A **101**(36): 13124-13131.

Gevins, A., M. E. Smith, L. McEvoy and D. Yu (1997). "High-resolution EEG mapping of cortical activation related to working memory: effects of task difficulty, type of processing, and practice." Cereb Cortex **7**(4): 374-385.

Glascher, J., R. Adolphs, H. Damasio, A. Bechara, D. Rudrauf, M. Calamia, L. K. Paul and D. Tranel (2012). "Lesion mapping of cognitive control and value-based decision making in the prefrontal cortex." Proc Natl Acad Sci U S A **109**(36): 14681-14686.

Goodfellow, N. M., M. Benekareddy, V. A. Vaidya and E. K. Lambe (2009). "Layer II/III of the prefrontal cortex: Inhibition by the serotonin 5-HT1A receptor in development and stress." J Neurosci **29**(32): 10094-10103.

Gottfried, J. A., J. O'Doherty and R. J. Dolan (2003). "Encoding predictive reward value in human amygdala and orbitofrontal cortex." Science **301**(5636): 1104-1107.

Hampton, A. N., R. Adolphs, M. J. Tyszka and J. P. O'Doherty (2007). "Contributions of the amygdala to reward expectancy and choice signals in human prefrontal cortex." Neuron **55**(4): 545-555.

Hanselman and Littlefield (2004). Mastering Matlab 7, Prentice Hall.

Heimer, L. (2003). "A new anatomical framework for neuropsychiatric disorders and drug abuse." Am J Psychiatry **160**(10): 1726-1739.

Hitchcott, P. K., C. M. Bonardi and G. D. Phillips (1997). "Enhanced stimulus-reward learning by intra-amygdala administration of a D3 dopamine receptor agonist." Psychopharmacology (Berl) **133**(3): 240-248.

Holland, P. C. and M. Gallagher (2004). "Amygdala-frontal interactions and reward expectancy." Curr Opin Neurobiol **14**(2): 148-155.

Hyman, J. M., A. M. Zilli Ea Fau - Paley, M. E. Paley Am Fau - Hasselmo and M. E. Hasselmo (2005). "Medial prefrontal cortex cells show dynamic modulation with the hippocampal theta rhythm dependent on behavior." Hippocampus(1050-9631 (Print)).

Ikemoto, S. (2010). "Brain reward circuitry beyond the mesolimbic dopamine system: a neurobiological theory." Neurosci Biobehav Rev **35**(2): 129-150.

Jensen, O. and C. D. Tesche (2002). "Frontal theta activity in humans increases with memory load in a working memory task." Eur J Neurosci **15**(8): 1395-1399.

Jog, M. S., C. I. Connolly, Y. Kubota, D. R. Iyengar, L. Garrido, R. Harlan and A. M. Graybiel (2002). "Tetrode technology: advances in implantable hardware, neuroimaging, and data analysis techniques." J Neurosci Methods **117**(2): 141-152.

Jones, M. W. and M. A. Wilson (2005). "Theta rhythms coordinate hippocampal-prefrontal interactions in a spatial memory task." PLoS Biol **3**(12): e402.

Kahn, J. B., R. D. Ward, L. W. Kahn, N. M. Rudy, E. R. Kandel, P. D. Balsam and E. H. Simpson (2012). "Medial prefrontal lesions in mice impair sustained attention but spare maintenance of information in working memory." Learn Mem **19**(11): 513-517.

Kandel E. R., Schwartz J. H. and Jessell T. H. (2000). Principles of Neural Science. New York, McGraw-Hill.

Keating, J. G. and G. L. Gerstein (2002). "A chronic multi-electrode microdrive for small animals." J Neurosci Methods **117**(2): 201-206.

Kim, M. and M. Davis (1993). "Electrolytic lesions of the amygdala block acquisition and expression of fear-potentiated startle even with extensive training but do not prevent reacquisition." Behav Neurosci **107**(4): 580-595.

Kim, M. and M. Davis (1993). "Lack of a temporal gradient of retrograde amnesia in rats with amygdala lesions assessed with the fear-potentiated startle paradigm." Behav Neurosci **107**(6): 1088-1092.

Kita, J. M., B. M. Kile, L. E. Parker and R. M. Wightman (2009). "In vivo measurement of somatodendritic release of dopamine in the ventral tegmental area." Synapse **63**(11): 951-960.

Klavir, O., R. Genud-Gabai and R. Paz (2013). "Functional connectivity between amygdala and cingulate cortex for adaptive aversive learning." Neuron **80**(5): 1290-1300.

Klimesch, W., M. Doppelmayr, A. Yonelinas, N. E. Kroll, M. Lazzara, D. Rohm and W. Gruber (2001). "Theta synchronization during episodic retrieval: neural correlates of conscious awareness." Brain Res Cogn Brain Res **12**(1): 33-38.

Kloosterman, F., T. J. Davidson, S. N. Gomperts, S. P. Layton, G. Hale, D. P. Nguyen and M. A. Wilson (2009). "Micro-drive array for chronic in vivo recording: drive fabrication." J Vis Exp(26).

Lakatos, P., G. Karmos, A. D. Mehta, I. Ulbert and C. E. Schroeder (2008). "Entrainment of neuronal oscillations as a mechanism of attentional selection." Science **320**(5872): 110-113.

Lechin, F., B. van der Dijs and G. Hernandez-Adrian (2006). "Dorsal raphe vs. median raphe serotonergic antagonism. Anatomical, physiological, behavioral, neuroendocrinological, neuropharmacological and clinical evidences: relevance for neuropharmacological therapy." Prog Neuropsychopharmacol Biol Psychiatry **30**(4): 565-585.

Lesting, J., T. Daldrup, V. Narayanan, C. Himpe, T. Seidenbecher and H. C. Pape (2013). "Directional theta coherence in prefrontal cortical to amygdalo-hippocampal pathways signals fear extinction." PLoS One **8**(10): e77707.

Lesting, J., R. T. Narayanan, C. Kluge, S. Sangha, T. Seidenbecher and H. C. Pape (2011). "Patterns of coupled theta activity in amygdala-hippocampal-prefrontal cortical circuits during fear extinction." PLoS One **6**(6): e21714.

Leung, H. T., G. K. Bailey, V. Laurent and R. F. Westbrook (2007). "Rapid reacquisition of fear to a completely extinguished context is replaced by transient impairment with additional extinction training." J Exp Psychol Anim Behav Process **33**(3): 299-313.

Likhtik, E. and J. A. Gordon (2013). "A surprised amygdala looks to the cortex for meaning." Neuron **80**(5): 1109-1111.

Lopez de Armentia, M. and P. Sah (2004). "Firing properties and connectivity of neurons in the rat lateral central nucleus of the amygdala." J Neurophysiol **92**(3): 1285-1294.

Lupien, S., B. S. McEwen, M. R. Gunnar and C. Heim (2009). "Effects of stress throughout the lifespan on the brain, behaviour and cognition." Nat Rev Neurosci(1471-0048 (Electronic)).

Mackintosh, N. (1975). "A theory of attention: Variations in the associability of stimulus with reinforcement." Psychol. Rev. **82**: 276-298.

Miller, E. K. and J. D. Cohen (2001). "An integrative theory of prefrontal cortex function." Annu Rev Neurosci **24**: 167-202.

Miller, E. K., D. J. Freedman and J. D. Wallis (2002). "The prefrontal cortex: categories, concepts and cognition." Philos Trans R Soc Lond B Biol Sci **357**(1424): 1123-1136.

Monin, J. and M. Hinchey (2003). Understanding formal methods, Springer.

Morris, J. S. and R. J. Dolan (2001). "Involvement of human amygdala and orbitofrontal cortex in hunger-enhanced memory for food stimuli." J Neurosci **21**(14): 5304-5310.

Naiman, J. (2008). How Societies Work: Class, Power and Change. Toronto, Fernwood Publishing Co Ltd.

Napier, R. M., M. Macrae and E. J. Kehoe (1992). "Rapid reaquisition in conditioning of the rabbit's nictitating membrane response." J Exp Psychol Anim Behav Process **18**(2): 182-192.

Narayanan, R. T., T. Seidenbecher, C. Kluge, J. Bergado, O. Stork and H. C. Pape (2007). "Dissociated theta phase synchronization in amygdalo- hippocampal circuits during various stages of fear memory." Eur J Neurosci **25**(6): 1823-1831.

Nguyen, D. P., S. P. Layton, G. Hale, S. N. Gomperts, T. J. Davidson, F. Kloosterman and M. A. Wilson (2009). "Micro-drive array for chronic in vivo recording: tetrode assembly." J Vis Exp(26).

Niedermeyer, E. (2004). "The electrocerebellogram." Clin EEG Neurosci **35**(2): 112-115.

O'Doherty, J. P., P. Dayan, K. Friston, H. Critchley and R. J. Dolan (2003). "Temporal difference models and reward-related learning in the human brain." Neuron **38**(2): 329-337.

Onton, J., A. Delorme and S. Makeig (2005). "Frontal midline EEG dynamics during working memory." Neuroimage **27**(2): 341-356.

Otani, S. (2004). Prefrontal cortex: from synaptic plasticity to cognition, Kluwer Academic Publishers.

Pape, H. C., R. T. Narayanan, J. Smid, O. Stork and T. Seidenbecher (2005). "Theta activity in neurons and networks of the amygdala related to long-term fear memory." Hippocampus **15**(7): 874-880.

Pavlov, I. P. and G. V. Anrep (1927). Conditioned reflexes; an investigation of the physiological activity of the cerebral cortex. New York, Dover Publications.

Paxinos, G. and C. Watson (1986). The rat brain in stereotaxic coordinates. Sydney; Orlando, Academic Press.

Pearce, J. and G. Hall (1980). "A model for Pavlovian conditioning: variations in the effectiveness of conditioned but not of unconditioned stimuli." Psychol. Rev. **87**: 532-552.

Peers, P. V., J. S. Simons and A. D. Lawrence (2013). "Prefrontal control of attention to threat." Front Hum Neurosci **7**: 24.

Pratap, R. (2005). Getting Started with MATLAB 7, Oxford University Press.

Quirk, G. J. and D. Mueller (2008). "Neural mechanisms of extinction learning and retrieval." Neuropsychopharmacology **33**(1): 56-72.

Rescorla, R. (1987). "A Pavlovian analysis of goal-directed behavior." American Psychology **42**: 119-129.

Rescorla, R. A., A. W. Wagner, A. H. Black and W. F. Prokasy (1972). A theory of Pavlovian conditioning: Variations in the effectiveness of reinforcement and nonreinforcement. Classical Conditioning II: Current Research and Theory, Appleton-Century-Crofts**:** 64-99.

Rodgers, J. L. and W. A. Nicewander (1988). "Thirteen ways to look at the correlation coefficient." The American Statistician **42**(1): 59-66.

Sarnthein, J., H. Petsche, P. Rappelsberger, G. L. Shaw and A. von Stein (1998). "Synchronization between prefrontal and posterior association cortex during human working memory." Proc Natl Acad Sci U S A **95**(12): 7092-7096.

Satoru, T., K. Mitsuyasu and I. Shunsuke (2004). "Network of transcription factors for biological functions." Tanpakushitsu Kakusan Koso **49**(17 Suppl): 2955-2960.

Schiess, M. C., P. M. Callahan and H. Zheng (1999). "Characterization of the electrophysiological and morphological properties of rat central amygdala neurons in vitro." J Neurosci Res **58**(5): 663-673.

Schroeder, C. E. and P. Lakatos (2009). "Low-frequency neuronal oscillations as instruments of sensory selection." Trends Neurosci **32**(1): 9-18.

Seamans, J. K. and C. R. Yang (2004). "The principal features and mechanisms of dopamine modulation in the prefrontal cortex." Prog Neurobiol **74**(1): 1-58.

Seidenbecher, T., T. R. Laxmi, O. Stork and H. C. Pape (2003). "Amygdalar and hippocampal theta rhythm synchronization during fear memory retrieval." Science **301**(5634): 846-850.

Shinnick-Gallagher, P. (2003). The amygdala in brain function : basic and clinical approaches, New York, N.Y., New York Academy of Sciences.

Siapas, A. G., E. V. Lubenov and M. A. Wilson (2005). "Prefrontal phase locking to hippocampal theta oscillations." Neuron **46**(1): 141-151.

Song, D., R. H. M. Opris I Fau - Chan, V. Z. Chan Rh Fau - Marmarelis, R. E. Marmarelis Vz Fau - Hampson, S. A. Hampson Re Fau - Deadwyler, T. W. Deadwyler Sa Fau - Berger and T. W. Berger (2012). "Functional connectivity between Layer 2/3 and Layer 5 neurons in prefrontal cortex of

nonhuman primates during a delayed match-to-sample task." IEEE Medical Biological Proceedings(1557-170X (Print)).

Squire, R. F., B. Noudoost, R. J. Schafer and T. Moore (2013). "Prefrontal contributions to visual selective attention." Annu Rev Neurosci **36**: 451-466.

Swanson, L. and G. Petrovich (1998). "What is the amygdala?" Trends Neurosci **8**(0166-2236 (Print)): 323-331.

Tye, K. M., J. J. Cone, W. W. Schairer and P. H. Janak (2010). "Amygdala neural encoding of the absence of reward during extinction." J Neurosci **30**(1): 116-125.

Tye, K. M. and P. H. Janak (2007). "Amygdala neurons differentially encode motivation and reinforcement." J Neurosci **27**(15): 3937-3945.

Tye, K. M., L. D. Tye, J. J. Cone, E. F. Hekkelman, P. H. Janak and A. Bonci (2010). "Methylphenidate facilitates learning-induced amygdala plasticity." Nat Neurosci **13**(4): 475-481.

Vertes, R. P. (2004). "Differential projections of the infralimbic and prelimbic cortex in the rat." Synapse **51**(1): 32-58.

Veto, I. (2005). Software technology. Budapest, Pázmány University.

Weiskrantz, L. (1964). "Neurological Studies and Animal Behaviour." Br Med Bull **20**: 49-53.

Whishaw, I. Q. and B. Kolb (2004). The Behavior of the Laboratory Rat: A Handbook with Tests, Oxford University Press, USA.

Wiley, R. H. (2003). "Is there an ideal behavioural experiment?" Animal Behaviour **66**(3): 585-588.

Wise, R. A. (2000). "Interactions between medial prefrontal cortex and meso-limbic components of brain reward circuitry." Prog Brain Res **126**(0079-6123 (Print)): 255-262.

Wise, R. A. (2002). "Brain reward circuitry: insights from unsensed incentives." Neuron **36**(2): 229-240.

Yang, C. R., J. K. Seamans and N. Gorelova (1996). "Electrophysiological and morphological properties of layers V-VI principal pyramidal cells in rat prefrontal cortex in vitro." J Neurosci **16**(5): 1904-1921.